Nonperturbative aspects of gravity and field theory

Philipp Burda

A Thesis presented for the degree of
Doctor of Philosophy

Centre for Particle Theory
Department of Mathematical Sciences
University of Durham
England

October 2015

Nonperturbative aspects of gravity and field theory

Philipp Burda

Submitted for the degree of Doctor of Philosophy
October 2015

Abstract

In this thesis we investigate unusual and non-trivial interplays between gravity and field theory. We concentrate on two examples, one related to holography and the other to the physics of false vacuum decay. In the first chapter we overview basic concepts and techniques from both these examples.

In chapter 2 we construct solutions describing flows between AdS and Lifshitz spacetimes in IIB supergravity. We find that flows from AdS_5 can approach either AdS_3 or $\mathrm{Lifshitz}_3$ in the IR depending on the values of the deformation from AdS_5. Surprisingly, the choice between AdS and Lifshitz in the IR depends only on the value of the deformation, not on its character; the breaking of the Lorentz symmetry in the flows with a Lifshitz IR is spontaneous. We find that the values of the deformation which lead to flows to Lifshitz make the UV field theory dual to the AdS_5 geometry unstable, so that these flows do not offer an approach to defining the field theory dual to the Lifshitz spacetime.

In chapter 3 we consider the possibility that small black holes can act as nucleation seeds for the decay of a metastable vacuum. Using a thin-wall bubble approximation for the nucleation process, we show that black holes can stimulate vacuum decay.

In chapter 4 we apply this technique to the particular example of the Higgs potential with generic quantum gravity corrections. We show how small black holes can act as seeds for vacuum decay, spontaneously nucleating a new Higgs phase centred on the black hole with a lifetime measured in millions of Planck times rather than billions of years. The constraints on the parameter space of corrections to the

Higgs potential are outlined. We demonstrate that for suitable parameter ranges, the vacuum decay process dominates over the Hawking evaporation process. We also comment on the application of these results to vacuum decay seeded by black holes produced in particle collisions. By relaxing the conditions for the thin-wall approximation and proceeding to the numerical calculations an expansion of the range of the parameter space is proposed.

Declaration

The work in this thesis is based on research carried out at the Centre for Particle Theory, the Department of Mathematical Sciences, England. No part of this thesis has been submitted elsewhere for any other degree or qualification and it is all my own work unless referenced to the contrary in the text. The work is based substantially on the following papers [31, 69, 70, 134] where parts have been reproduced with the permission of the respective authors.

Acknowledgements

First of all I would like to thank my supervisor Ruth Gregory for her wise guidance throughout these 3 years. She showed me an outstanding example of a modern theoretical physicist and will always be a role-model in science for me. I also would like to thank my collaborators during my graduate studies in Durham, Simon Ross and Ian Moss, for a very interesting and inspiring scientific discussion. I hope I have learned a lot from them.

From a personal perspective, I would like to thank my parents for their endless love and support. It is only because of them I have an opportunity to do science, the most interesting thing in the world! I hope that I will be able to support all their dreams in future.

I'm especially grateful to my partner Lina for her love, help and patience. I know sometimes it is difficult, but I believe that we will succeed in everything moving through life together!

In addition, I would like to thank my housemates and colleagues, Reza and Ragu. Thank you guys for the great discussions during long night hours, sometimes even with a white-board in our living room. It was fun!

And the last, but not least, I would like to thank my Master thesis advisor Emil Akhmedov for introducing to me the world of theoretical physics and helping me to understand a lot of things there.

My research was supported by an EPSRC International Doctoral Scholarship.

Contents

List of Figures

List of Tables

Chapter 1

Introduction

This year we celebrate the centenary of the General Theory of Relativity discovered by Einstein in 1915 [1]. It is now extremely well verified, at least locally in our solar system, and has found a practical application in GPS [2]; thus any fundamental description of Nature should include General Relativity, at least in some limit.

There are several ways that the fundamental theory of gravity could manifest itself in Nature. For example, the very successful Standard Cosmological Model requires an initial state. Other examples are the information loss puzzle of black holes [3] and the question of understanding their entropy [4]. In this latter problem string theory may have provided some genuine insight [5]. Although there are several approaches to Quantum Gravity that have been proposed: String Theory [6], Loop Quantum Gravity [7], Casual Sets [8], Casual Dynamical Triangulations [9]; it is probably fair to say that String Theory is a much better developed theory. String Theory uses the same logic as quantum field theory (QFT), applying the same basic rules to extended objects, namely strings. Low energy effective actions of String Theory are very well understood, and therefore provide us with a beautiful example of the appearance of gravity in a fundamental theory.

In the present thesis we will consider two examples of non-trivial interplay between gravity and field theory. In one of them, gravity (in this case, supergravity theory) provides a useful tool for investigating a strong coupling regime of particular quantum field theories. In the other, gravity combines with the field theory to give new insight into non-perturbative quantum processes.

In the first example, the tool is usually called holography and was triggered by the first example of a correspondence between the classical limit of Type IIB superstring theory on an Anti de Sitter (AdS) background and $\mathcal{N} = 4$ Super Yang-Mills (SYM) theory in Minkowski spacetime in the strong coupling regime [10]. We will review this correspondence along with some directions for generalizations in the next section. In this basic example only the case of superconformal relativistic field theory was considered, but from the perspective of exploring real physical systems by means of a bulk gravitational theory, it is important to figure out how far we can push this correspondence. In particular, what amount of symmetry could we break or modify? We will concentrate on the breaking of relativistic invariance and investigate the possibility of exploring non-relativistic theories with Lifshitz scaling [11] through holography in Chapter 2.

Our second example concerns the non-trivial inclusion of gravity into the physics of false vacuum decay. The canonical description of this process was set out by Coleman in 1976 [12, 13] and originally did not include gravity. Subsequently, with de Luccia, gravity was included [14] but only in the context of homogeneous solutions. We will review the basics of such phase transitions below. However, in order to truly appreciate the role of gravity in such cosmological phase transitions it is important to consider non-homogeneous seeds which can possibly trigger vacuum decay. Such inhomogeneities in gravitational theories are most naturally realised by black holes, therefore we will consider mutual effects of black holes on the probabilities of vacuum decay in Chapter 3. Moreover, due to the fact that the Standard Model Electroweak Higgs vacuum could became unstable if we take into account higher energy corrections [15, 16, 18, 85], we will discuss the effect of the presence of black holes in this very important cosmological example in Chapter 4.

1.1 Overview of Holography

In this section we introduce a very powerful tool for studying strongly coupled regimes and various non-perturbative aspects of particular field theories. This tool originates from string theory and is usually called the AdS/CFT correspondence,

holography or, more generally, gauge/gravity duality [19]. Basically, this is a correspondence between string theory on specific curved backgrounds and some quantum field theories in flat spacetime. Below we will briefly review open/closed string duality, which lies at the core of this proposed tool, along with a basic textbook example of AdS/CFT correspondence.

1.1.1 Open/Closed String Duality and D-branes

Any process in string theory can be seen from both the open and closed string perspective. This suggests the existence of two equivalent descriptions of any object in string theory, known as an open/closed string duality.

D-branes will serve us as the main example of the power and usefulness of such dual pictures because it is exactly the comparison of two equivalent low-energy descriptions of stacks of D-branes that led Maldacena to the idea of the AdS/CFT correspondence [10]. Initially D-branes were introduced in string theory as extended hypersurfaces on which open strings could end [20, 21]. The 'D' in the name stands for the Dirichlet, as is is usually assumed that the endpoints of the strings have Dirichlet boundary conditions in the directions transverse to the brane. It was then realized that D-branes are another type of fundamental object in string theory in addition to strings, with their own dynamics described by the DBI action [22] in the low energy limit. The DBI action properly takes into account the gauge degrees of freedom associated with the open strings and in a weak field strength limit reduces to the gauge field theory action. On the other hand, by virtue of an open/closed string duality the worldsheet of an open string moving along a closed trajectory on a brane could be seen as a worldsheet of a closed string emitted by the brane. Hence, D-branes could be viewed also as a source of closed strings which have a graviton (massless spin-2 field) in their spectrum. This suggests an existence of gravitational description of D-branes. Such a description was found by Polchinski [23], when he showed that in the low energy limit, D-branes could be alternatively described as extremal black p-brane solutions first found by Horowitz and Strominger [24]. We will now examine both these pictures for a particular example of a stack of N parallel coincident D3-branes embedded in a 10-dimensional spacetime of Type IIB string

theory and will see how the correspondence emerges.

Before we proceed to the detailed analysis it is worth describing the low energy limit which we will use in the derivation. In the context of string theory, low energies means that we will consider energies much smaller than the energy scale associated with the string length l_s, $E \ll l_s^{-1}$. A convenient way to apply this limit is to keep all energies bounded and take the $l_s \to 0$ limit. Since $l_s \sim \sqrt{\alpha'}$, this is equivalent to the $\alpha' \to 0$ limit, which is exactly what is usually implied as the low energy limit in string theory. Due to the fact that masses of string excitations are proportional to $1/\sqrt{\alpha'}$, all the massive modes decouple at low energies. Further simplifying limits will be discussed below.

Open string picture

From the point of view of an open string at low energies one can naturally decompose an effective action for the brane into three parts [25]

$$S_{open} = S_{DBI} + S_{bulk} + S_{int} \tag{1.1.1}$$

where S_{DBI} corresponds to the worldvolume action of massless excitations sitting on a brane. The second term S_{bulk} describes bulk degrees of freedom living far from the brane, i.e. strings in flat 10-dimensional spacetime, that are closed even in the open string picture, because far from the brane there is no surface on which strings could end. Moreover, in the low energy limit, closed strings reduce to free supergravity theory living on a flat 10-dimensional spacetime [25]. The last term S_{int} describes an interaction between bulk and brane degrees of freedom, and because the strength of the interactions is proportional to the positive powers of α' bulk and brane degrees of freedom decouple from each other. Therefore, the only non-trivial part is the low energy limit of the DBI action for the stack of D3-branes. In order to deal with this limit properly, we will first consider an example of a single D-brane, then comment on the system with multiple branes.

From the basic requirements of Lorentz and reparametrization invariance, one can realize that the action for a single Dp-brane should be some sort of higher dimensional generalization of the Nambu-Goto action [22]. An action which properly

takes into account all massless degrees of freedom living on a brane is

$$S_{Dp} = -T_p \int d^{p+1}\zeta \; e^{-\Phi} \sqrt{\det\left[\gamma_{AB} + \mathtt{F}_{AB}\right]} \tag{1.1.2}$$

here $\{\zeta^A,\, A = 0 \dots p\}$ are the intrinsic coordinates on the brane worldvolume, T_p is the tension of the brane, and γ_{AB} is the pullback of the metric to the worldvolume of the brane

$$\gamma_{AB} = \frac{\partial X^\mu}{\partial \zeta^A} \frac{\partial X^\nu}{\partial \zeta^B} g_{\mu\nu} \tag{1.1.3}$$

The exponential factor in (1.1.2) contains the dilaton field Φ. It is convenient to extract a constant part of the dilaton Φ_0, which determines the asymptotic value of the string coupling constant, $g_s = e^{\Phi_0}$, responsible for the strength of string interactions and loop quantum corrections. $\mathtt{F}_{AB} = B_{AB} + 2\pi\alpha' F_{AB}$ is a proper gauge invariant combination of the pullback of 2-form field $B_{\mu\nu}$ and an abelian worldvolume gauge field F_{AB}.

All the embedding coordinates $X^\mu(\zeta_A)$ in (1.1.3) naively represent new dynamical fields, however by using reparametrization invariance and choosing a static gauge

$$X^A = \zeta^A, \quad A = 0, \dots, p \tag{1.1.4}$$

we can remove all the longitudinal fluctuations of the brane and the pullback of the metric will depend only on the transverse fluctuations X^I, which after rescaling we will identify with scalar fields $\phi^I = X^I / 2\pi\alpha'$ living on a brane. Taking this into account we can simplify the lagrangian in (1.1.2) in the low energy limit for a flat background with the B-field switched off

$$\begin{aligned} \sqrt{\det\left[\gamma_{AB} + \mathtt{F}_{AB}\right]} &= \sqrt{\det\left[\eta_{AB} + (2\pi\alpha')^2 \sum_i \partial_A \phi_i \partial_B \phi_i + 2\pi\alpha' F_{AB}\right]} = \\ &= 1 + \frac{1}{2}(2\pi\alpha')^2 \left(F_{AB}F^{AB} + \sum_i \partial_A \phi^i \partial_B \phi_i \right) + \left(\alpha'^4\right), \quad \alpha' \to 0 \end{aligned} \tag{1.1.5}$$

One can see that we get the lagrangian for an abelian gauge field theory with 6 additional scalar fields. If we expand the number of D-branes and consider a stack of N coincident branes, then open strings in the picture will have an opportunity to end on different branes, hence all the fields in (1.1.5) will get additional indices identifying branes between which the string is stretched. Overall for each field there

are N^2 options, hence this component can naturally be packed into $N \times N$ matrix. All this gives us a hint that the $U(1)$ gauge theory for a single brane will be promoted to the $U(N) = U(1) \times SU(N)$ gauge theory[1]. The detailed derivation of the low energy action for the stack of N D3-branes is technically involved, so we present here only the final result (a potential term for the scalar fields, which now transform in the adjoint of $SU(N)$ has appeared after an action of T-duality)

$$S_{DBI} = -\frac{1}{g_{YM}^2} \int d^{p+1}\zeta \ \mathrm{Tr} \left(\frac{1}{4} F_{AB} F^{AB} + \frac{1}{2} \sum_i \mathcal{D}_A \phi^i \mathcal{D}_B \phi_i - \frac{1}{4} \sum_{i \neq j} [\phi_i, \phi_j]^2 \right) \tag{1.1.6}$$

This is the bosonic part of an action for $\mathcal{N} = 4$ Super Yang-Mills theory with $SU(N)$ gauge group in 4 dimensions. Hence, the overall low energy action (1.1.1) in an open string picture is reduced to the sum of an action for $\mathcal{N} = 4$ Super Yang-Mills theory in 4 dimensions and free supergravity theory in 10 dimensions.

Closed string picture

In the closed string picture, as we described above, it is natural to present D-branes as a source of closed strings, hence in the low-energy limit far from the brane we again will have free supergravity theory in flat spacetime but now in the near brane region we use the gravitational description, which was put forward by Polchinski.

As was shown by Horowitz and Strominger [24], a stack of N coincident D3-branes of Type IIB string theory has an equivalent gravitational description in terms of an extremal 3-brane solution of the corresponding supergravity theory

$$ds^2 = H(r)^{-\frac{1}{2}} \left(dt^2 - d\vec{x}^2 \right) - H(r)^{\frac{1}{2}} \left(dr^2 + r^2 d\Omega_5^2 \right) \tag{1.1.7}$$

where the warp factor $H(r) = 1 + L^4/r^4$ with $L^4 = 4\pi g_s N l_s^4$. In the region near the brane $r \ll L$, and $H(r) \to L^4/r^4$ and the metric (1.1.7) reduces to an $AdS_5 \times S^5$ spacetime with radius of curvature L. The spacetime is curved near the branes, hence even in the low energy limit modes with arbitrary energy are allowed in this

[1] An overall $U(1)$ factor in the $U(N)$ case corresponds to a "centre of mass" degree of freedom, hence it can be ignored.

region, because their energy, measured at infinity, will be red-shifted. In other words, we will have full Type IIB string theory in $AdS_5 \times S^5$ spacetime.

1.1.2 AdS/CFT correspondence

We have described a system of N coincident D3-branes from both the open and closed string perspective and each time, in the low energy limit the effective action reduces to the decoupled sum of a free supergravity theory in 10 dimensional flat spacetime and some non-trivial theory in the near brane region. In one case this non-trivial theory is an $SU(N)$ $\mathcal{N} = 4$ SYM theory in 4 dimensional Minkowski spacetime and in the other case Type IIB string theory in $AdS_5 \times S^5$ spacetime. Since we have described the same system twice and the trivial part in both cases was the same, these theories should be equivalent! This is the so-called strong version of Maldacena's conjecture. In order to put this correspondence to practical use, it will be helpful to take some further limits in order to make at least one side of the correspondence simple.

On the gauge theory side one can consider the 't Hooft limit, when $N \to \infty$ while the combination $\lambda = N g_{YM}^2$ is kept fixed. Only planar diagrams survive in this limit and due to the fact that $g_{YM}^2 = 4\pi g_s$ all the quantum gravity corrections on the string theory side will be suppressed as well. If we further take the limit of large λ (keeping g_{YM} small) we can reduce the string theory side to classical supergravity on AdS_5, since the curvature length scale will be much bigger than the string length scale

$$\left(\frac{L}{l_s}\right)^4 = 4\pi g_s N = g_{YM}^2 N = \lambda \tag{1.1.8}$$

After these limits we arrive to the most famous and well-understood form of the correspondence, namely, the conjectured equivalence of the strongly coupled regime of planar $\mathcal{N} = 4$ $SU(N)$ SYM theory in a 4 dimensional Minkowski spacetime and the classical Type IIB supergravity theory in a 5 dimensional AdS spacetime, which we will refer as the AdS/CFT correspondence.

Modern point of view

We have presented a sketch of the original 'derivation' of the AdS/CFT correspondence, following mostly Maldacena's logic. It is already almost twenty years since this was proposed and people have studied and tested this correspondence in various ways, each time confirming that it holds. All this, along with a very unexpected form of the correspondence (higher dimensional gravitation theory equivalent to a lower-dimensional non-gravitational quantum field theory) pushed people to think more generally about the nature of gauge/gravity duality. Below we will present a more recent point of view on the gauge/gravity duality, which does not rely on string theory per se. We will mostly follow the logic of recent reviews ([26, 27]).

According to the proposed duality, a specific gauge theory should contain information about a gravitational theory within itself. If we look at this from the matter content perspective, the spin-2 graviton should somehow arise from gauge theory degrees of freedom. An immediate proposal, that the emergent graviton could be composed from the two spin-1 gauge bosons has an obvious obstacle in terms of Weinberg-Witten theorem [28], but this obstruction can be avoided if the graviton lives in a different spacetime. This is exactly what happens in holography, when gravity lives in a spacetime with one additional dimension. The next question is how this extra dimension can occur from a gauge theory point of view. In other words, we need to find some quantity in quantum field theory which is changing, and more importantly the physics should behave locally with respect to this quantity. A good candidate would be the energy scale, because the RG equation, describing the flow of the coupling constants in the theory with respect to the energy scale, is a local differential equation. Additionally, because it is obvious that only the strongly coupled regime of gauge theory could reproduce quantum gravity, it is important that we would have a long range of energies where the coupling remains strong. Ideally, this range should be infinite in order to allow an infinite bulk direction. This is the case in a conformal field theory where the couplings do not run with energy.

In order to justify that the gauge theory can also describe additional excitations of various energies propagating as well in the bulk direction, the number of degrees of freedom in a theory should be big enough. An easy way to organize this is to

consider the 't Hooft limit of the gauge theory, i.e. take $N \to \infty$ in the rank of gauge group $SU(N)$, while keeping the coupling $\lambda = g_{YM}^2 N$ finite, but large as well.

Coming back to properties of conformal field theory, let us recall that the theory formulated on Minkowski spacetime is invariant under the rescaling $x^\mu \to \alpha x^\mu$, if we simultaneously rescale the energy $E \to E/\alpha$. Hence, if we identify the inverse energy scale with a coordinate along an extra dimension $z \sim 1/E$, we will naturally arrive to an AdS metric

$$ds^2 = \frac{\ell^2}{z^2}\left(\eta_{\mu\nu}dx^\mu dx^\nu + dz^2\right) \tag{1.1.9}$$

Finally, it is very convenient to promote both sides of the correspondence to supersymmetric configurations, because on the gauge theory side, supersymmetry helps hold strongly coupled field theory under control by excluding most of the possible instabilities, and on the gravity side supersymmetry dictates an extension to the full supergravity, which is formulated in 10 dimensions and has an $AdS_5 \times S^5$ solution. All these speculations have been intensively explored and clarified in past years, so now we are in the position that it would be much more peculiar were the AdS/CFT correspondence not true.

Despite the fact that this modern 'derivation' of AdS/CFT is not very technical, it clearly shows the importance of different concepts like relativistic invariance, conformal invariance and supersymmetry for the correspondence to exist, and indicates the difficulties which one may encounter trying to generalize the correspondence to theories without these symmetries.

1.1.3 Exploring AdS/CFT

In this section we present evidence of validity of the correspondence and some examples of concrete calculations within AdS/CFT.

The first and immediate check of the proposed equivalence between two different theories is the relation between the symmetries of the theories. On one side we have an $\mathcal{N} = 4$ SYM in 4 dimensions which is a conformal theory with supersymmetry, hence the global symmetries of the theory are a product of conformal group in four dimensions $SO(4,2)$ and R-symmetry group $SU(4)_R \simeq SO(6)_R$. On the other side

we have Type IIB SUGRA in $AdS_5 \times S_5$, hence an isometry group of the spacetime is a product of isometry group of 5 dimensional AdS spacetime $SO(4,2)$ and the group of symmetries of a 5-sphere $SO(6)$. Hence the global bosonic symmetries on the field theory side are identical to the group of isometries of the spacetime on the gravity side.

This matching of global symmetries is just the first step in a series of tests of the correspondence that has been performed over the years. We will now proceed to the discussion of some more practical consequences of the correspondence along with a recipe on how to apply it.

An important feature of AdS/CFT, from a practical point of view, is a correspondence between the observables of both theories, hence between supergravity fields in AdS and local gauge invariant operators of $\mathcal{N} = 4$ SYM. A general strategy was proposed by Witten in [29]. The central relation is an equality of the partition function of Type IIB string theory on an AdS background with specific boundary conditions for a particular field, and a generating functional for correlators of the corresponding operator in a dual quantum field theory, sourced by these boundary conditions

$$\mathcal{Z}_{string}\left[\phi_0\right] = \left\langle \exp\left(-\mathrm{i}\int d^4x\ \phi_0 \mathcal{O}\right)\right\rangle_{QFT} \tag{1.1.10}$$

An operator $\mathcal{O}$ of the gauge theory has to lie in the same representation of the symmetry group as the field ϕ.

This expression, conjectured to hold in the general case, could be put to a practical use for the weak form of the correspondence, because at strong coupling together with the large N limit, the string theory side reduces to the classical supergravity theory and we can use a saddle point approximation for the partition function on the left

$$\mathcal{Z}_{string}\left[\phi_0\right] \to \mathcal{Z}_{SUGRA}\left[\phi_0\right] \simeq e^{S_{cl}[\phi_0]} \tag{1.1.11}$$

At the same time, on the right hand side we have a deep quantum limit of field theory with large coupling, where it is very hard to perform any direct calculation. Hence, the relation (1.1.10) provides us with a concrete realization of the practical application of the correspondence, when on-shell gravitational calculations are used in order to obtain results in an off-shell strongly coupled gauge theory. In particular,

because from the field theory side we have a generating function for the correlators of operator $\mathcal{O}$, all of them could be obtained from the classical supergravity solutions

$$\langle \mathcal{O}_1 \dots \mathcal{O}_n \rangle = \frac{1}{Z_{SUGRA}} \frac{\delta^n}{\delta \phi_0} Z_{SUGRA}\left[\phi_0\right]\Big|_{\phi_0=0} \tag{1.1.12}$$

We now proceed to a basic example of such a calculation. We will consider the simplest case of a scalar field in AdS and will comment on the 1-point correlation function, or the vacuum expectation value (the VEV), of the corresponding operator. This exercise will help us to clarify the relation between properties of the bulk fields and operators of the field theory on the boundary, which we will use a lot in the following sections.

Consider a massless scalar field in $AdS_5 \times S_5$ spacetime. Performing a Kaluza-Klein reduction we can expand it in spherical harmonics on S^5

$$\phi(x, y) = \sum_l \phi_l(x) Y_l(y) \tag{1.1.13}$$

Substituting this expansion into the equation of motion $\Box_{10}\phi = 0$, we get a system of massive scalar fields in a 5-dimensional AdS spacetime with the masses inherited from the corresponding spherical harmonics. Hence, it is sufficient to consider an example of a single scalar field with unspecified mass

$$\left(\Box_5 + m^2\right)\phi = 0 \tag{1.1.14}$$

Choosing coordinates on AdS_5

$$ds^2 = \frac{r^2}{L^2}\left(dt^2 - d\vec{x}^2\right) - \frac{L^2}{r^2} dr^2 \tag{1.1.15}$$

and assuming a power law fall-off of the field near the boundary,

$$\phi \to r^{\Delta-4}\phi_0, \quad \text{as} \quad r \to \infty \tag{1.1.16}$$

we arrive to the following equation at leading order in the $r \to \infty$ limit

$$\left(\Delta^2 - 4\Delta - m^2 L^2\right)\phi_0 = 0 \tag{1.1.17}$$

Hence we have two solutions $\Delta_\pm = 2 \pm \sqrt{4 + L^2 m^2}$, which are both real for $m^2 L^2 \geq -4$; this is known as the Breitenlohner-Freedman bound of stability for scalar fields

in AdS_5 [30]. Denoting the bigger solution Δ_+ as Δ without the subscript, we get the following form of the near boundary behaviour of the field ϕ

$$\phi \sim r^{\Delta-4}\phi_0 + r^{-\Delta}\phi_1 \tag{1.1.18}$$

Naively, ϕ_0 and ϕ_1 are related to the two linearly independent solutions of the second order equation (1.1.14) and could be chosen arbitrarily. However, the condition of regularity of the fields at $r = 0$ provides a relation between these coefficients, so eventually only a single boundary condition at $r \to \infty$ is needed. Usually, the mode related to ϕ_0 is non-normalizable and the coefficient ϕ_0 is precisely what we have used as the boundary condition for the field in AdS and the coupling of a corresponding operator in (1.1.10).

Now we will show that the scaling dimension of an operator $\mathcal{O}$ corresponding to the scalar field in consideration is equal to Δ. The metric (1.1.15) is invariant under the following rescaling

$$\{t, \vec{x}, r\} \to \{t', \vec{x}', r'\} = \left\{\lambda t, \lambda\vec{x}, \lambda^{-1}r\right\} \tag{1.1.19}$$

Then from the fact that scalar field is also invariant under these transformations $\phi'(r', \vec{x}') = \phi(r, \vec{x})$ we derive how its boundary value should scale

$$\phi_0' = \lambda^{\Delta-4}\phi_0 \tag{1.1.20}$$

Hence, taking into account the definition of the dimension of an operator, $\mathcal{O}' = \lambda^{-[\mathcal{O}]}\mathcal{O}$, and the invariance of the coupling term in the conformal theory on a boundary

$$\int d^4x'\ \phi_0'\mathcal{O}' = \int d^4x\ \phi_0\mathcal{O} \tag{1.1.21}$$

we can derive that in order to preserve conformal invariance we should have $[\mathcal{O}] = \Delta$.

As we have discussed above, due to regularity conditions, the mode ϕ_1 in (1.1.18) is not an independent solution, mathematically it is a functional of the boundary value ϕ_0. The physical meaning of ϕ_1 could be revealed from calculating the VEV of the corresponding operator through the general procedure (1.1.12). After some simplifications we get

$$\langle\mathcal{O}\rangle = \left.\frac{\delta S_{cl}}{\delta\phi_0}\right|_{\phi_0=0} = \phi_1|_{\phi_0=0} \tag{1.1.22}$$

So if a non-normalizable mode in the expansion (1.1.18) is a source of an operator in a dual field theory, the normalizable mode corresponds to the VEV of this operator. Note, that in order to preserve conformal symmetry the 1-point function of an operator with non-zero dimension should vanish, in other words ϕ_1 should be proportional to ϕ_0. However, this is not the case if we study non-conformal deformations of the original conformal theory through AdS/CFT.

The ability of an operator to drive the flow from the original conformal fixed point to some new one (maybe without conformal symmetry) in the UV or IR depends on the way the coupling of an operator is changing with energy scale. If the coupling is increasing under the RG flow from UV to IR, then the operator is called relevant and it could drive an the flow to the new fixed point in IR; if the coupling is decreasing under the lowering of energy scale then the operator is called irrelevant and it can not drive the flow to a lower energies; if the coupling does not change then the operator is called marginal. From the scaling transformation (1.1.19) we see that the new length-scale $x' = \lambda^{-1}x$ will be bigger for a transformation with $\lambda < 1$, hence such transformation will lower the energy scale. From (1.1.20) we can deduce that for $\Delta < 4$ the coupling will be bigger at the lower energies, so the operator is relevant; for $\Delta > 4$ the coupling will decrease and in this case an operator will be irrelevant; and for $\Delta = 4$ an operator will be marginal. We will use these observations a lot in the following sections.

1.2 Introduction to false vacuum decay

In this section we will discuss a non-perturbative process in quantum theory related to the tunnelling from one local minimum of the potential to another. In quantum field theory it is usually called false vacuum decay. We will start from the basic setup of the problem in quantum mechanics, which we will address as generally as possible and hence will be able to introduce all the useful technical notations and concepts. After that, we will proceed to the field theory example, where aspects of infinite amount of degrees of freedom will have to be taken into account, and finally we will add gravity to the mixture and examine the influence of spacetime curvature

on the probability of false vacuum decay.

1.2.1 Quantum mechanical invitation

There are two equivalent formulations of quantum theory. One in terms of states and operators and the other one in terms of paths (trajectories) via the path integral. As it was in the example with an open/closed string duality, having two equivalent descriptions sometimes helps to find an alternative approach to the hard problem via the dual description; a difficult question on one side is sometimes related to a straightforward calculation on the other side. This is the case for the example of the ground state in quantum theory, especially when there are non-trivial configurations of the minima.

Let us start with the general expression for the transition amplitude in quantum theory between the state $|x_i\rangle$ at $t = -t_0/2$ and $\langle x_f|$ at $t = t_0/2$, written in two equivalent formulations

$$\left\langle x_f \left| e^{-\mathrm{i}Ht_0} \right| x_i \right\rangle = \int \mathcal{D}x \; e^{\mathrm{i}S[x(t)]} \tag{1.2.23}$$

here H is a Hamiltonian of the system, $S\left[x(t)\right]$ is an action, evaluated on a trajectory between points $(x_i, -t_0/2)$ and $(x_f, t_0/2)$, $\mathcal{D}x$ is a proper measure for the integration over paths together with a normalization factor. Performing an expansion over the energy eigenstates, for the left hand side we get

$$\left\langle x_f \left| e^{-\mathrm{i}Ht_0} \right| x_i \right\rangle = \sum_n e^{-\mathrm{i}E_n t_0} \psi_n\left(x_f\right) \psi_n^*\left(x_i\right) \tag{1.2.24}$$

From this sum it is obvious that if we want to study the ground state of the theory, it is convenient to perform a Wick rotation, i.e. transform to an imaginary time $\tau = \mathrm{i}t$. Then, the oscillating exponent in every term of the sum becomes an exponentially decreasing one, and in the large (imaginary) time limit $\tau \to \infty$, only the term with the lowest energy E_0 hence the wave function of the ground state will survive

$$\sum_n e^{-\mathrm{i}E_n t_0} \psi_n\left(x_f\right) \psi_n^*\left(x_i\right) \xrightarrow[\tau_0 \,(=\mathrm{i}t_0) \to \infty]{} e^{-E_0 \tau_0} \psi_0\left(x_f\right) \psi_0^*\left(x_i\right) \tag{1.2.25}$$

Now let us examine what happens with the right hand side of (1.2.23) in this limit. First of all, after the transition to the imaginary time every path now will be weighted

with the exponent of an Euclidean action

$$S = \int_{-t_0/2}^{t_0/2} \left[\frac{1}{2}\dot{x}^2 - V(x)\right] dt \xrightarrow[\tau=\mathrm{i}t]{} \mathrm{i}S_E = \mathrm{i}\int_{-\tau_0/2}^{\tau_0/2} \left[\frac{1}{2}\dot{x}^2 + V(x)\right] d\tau \tag{1.2.26}$$

Substituting this into the exponent in the path integral we get a decreasing exponential weight for every trajectory, hence, according to the method of steepest descent, the major contribution to the integral will come from the path that is a solution of Euclidean equations of motion.

$$\int \mathcal{D}x\, e^{\mathrm{i}S[x(t)]} \xrightarrow[\tau=\mathrm{i}t]{} \int \mathcal{D}x\, e^{-S_E[x(\tau)]} \simeq e^{-S_E[x_{cl}]} \tag{1.2.27}$$

here $x_{cl}(\tau)$ is a solution of $\delta S_E = 0$, which is equivalent to the equation of motion $\ddot{x} = V'(x)$ for a particle in a inverted potential "$-V(x)$". It is important to note that the expression for the energy, which is a constant of the motion, due to the inversion of the potential will look like this:

$$E = \frac{1}{2}\dot{x}^2 - V(x) = const \tag{1.2.28}$$

If the potential has only one single minimum at some point x_0, then the only solution of the Euclidean equation of motion with a finite action is $x(\tau) = x_0 = const$. Then by considering Gaussian fluctuations around the classical solution one can fix the value of the pre-factor of the exponential in (1.2.27), and treat even a simple U-shaped potential accurately.

The situation becomes much more interesting if we consider the double-well potential

$$V(x) = \lambda\left(x^2 - \eta^2\right)^2 \tag{1.2.29}$$

In this case the ground state becomes non-trivial, because we have two minima at $x = \pm\eta$, and one could in principle consider the situation of a system initially in the state $x = -\eta$ but eventually finding itself at the state $x = \eta$. Note that classically, such a process is forbidden, but for the inverted potential we can find a solution where the particle starts almost at rest from $x = -\eta$, travels through the valley and then climbs back up and reach $x = \eta$ state when $\tau \to \infty$.

Using the fact that the energy (1.2.28) is equal to zero throughout all the motion one can simplify the expression for the action

$$\int_{-\infty}^{\infty} \left(\frac{1}{2}\dot{x}_{cl}^2 + V\left(x_{cl}\right)\right) d\tau = \int_{-\infty}^{\infty} \dot{x}_{cl}^2 d\tau = \int_{-\eta}^{\eta} \dot{x} dx = \int_{-\eta}^{\eta} \sqrt{2V(x)} dx \tag{1.2.30}$$

and get the following answer for the amplitude of the process

$$\lim_{\tau\to\infty} \langle\eta|\, e^{-H\tau}\, |-\eta\rangle \simeq e^{-S[x_{cl}]} = \exp\left[-\int_{-\eta}^{\eta} \sqrt{2V}dx\right] = \exp\left[-\frac{\omega^3}{12\lambda}\right] \qquad (1.2.31)$$

where ω is a characteristic of the potential around each minimum, $\omega^2 = V''(\pm\eta) = 8\lambda\eta^2$.

It is worth discussing each part of this relation. In the first, the approximate equality provides us with a strategy of addressing the question of vacuum decay: one solves the Euclidean equations of motion together with proper boundary conditions and substitutes this solution to the Euclidean action. The second equality relates this transition to the under-barrier tunnelling in quantum mechanics (recall the general expression for the transmission coefficient in a WKB-approximation, $T = \exp\left[-2\sqrt{2(V-E)}\right]$). Finally, the answer and its dependence on the coupling constant λ indicates that such a vacuum transition is a non-perturbative process.

1.2.2 Tunnelling in quantum field theory via bubbles

The next step in understanding the fate of a ground state is to proceed to the system with many, or infinite, numbers of degrees of freedom, namely quantum field theory. For the sake of brevity and simplicity we will consider only the example of a real scalar field theory ϕ and will start by specifying the form of the potential, which will serve as the main example for the problem under consideration. We consider a double well potential with an extra term which breaks the symmetry between the two minima rendering only one of them an absolute energy minimum. Let us assume that this absolute minimum (which we will call the true vacuum) is at $\phi = \phi_T$, while the other minimum with bigger value of the potential energy (which we will call the false vacuum) is at $\phi = \phi_F$.

Initially the system is in the false vacuum state, i.e. $\phi = \phi_F$, everywhere in space. Classically, such an initial state would be absolutely stable because there is a potential barrier between the false and the true vacuum, however in a quantum theory, as we reviewed in a previous section, the question about the ground state in a multiple minima potential is not so trivial due to the under-barrier penetration phenomenon. However, the case of quantum field theory is special, because this is a

quantum mechanical system with an infinite number of degrees of freedom. In order to tunnel to the new vacuum state one might think each degree of freedom should tunnel and the probability for all them to tunnel simultaneously is obviously equal to zero. Therefore, naively, under-barrier penetration is not possible in a quantum field theory and the initial false vacuum state should be stable. This is of course not the case and tunnelling in quantum field theory is possible, and below we discuss the way to deal with an an issue of infinite number of degrees of freedom. Let us assume that at some moment of time the degrees of freedom associated with some finite spherical region of space simultaneously tunnel through the potential barrier to the true vacuum state, the probability of such process is not zero because only a finite amount of degrees of freedom are involved. There is an energy difference between the true and false vacuum states, hence we gained some energy during this transition. There is also a border of the region where the transition occurred and the field performs a rapid uplift from the true to the false value on this border and this costs some energy. The balance of energy will determine what will then happen with this bubble of the true vacuum. The gain in energy is proportional to the volume of a sphere and scales like R^3 with the radius of the true vacuum bubble. The cost is related to the surface area of the bubble and scales like R^2. Therefore there always exists a critical size of the bubble R_c, such that if the bubble with critical or bigger radius is formed it will start to grow boundlessly and eventually will cover all the space, and the entire system will transit to the true vacuum state. This is very schematic description of a tunnelling process in quantum field theory, below we will show how this picture emerges from a technical derivation based on approach which we derived in a previous section.

According to the results of the previous section the probability of a vacuum transition is proportional to the exponent of an Euclidean action evaluated on a solution of the equations of motion with proper boundary conditions. An important and very natural assumption we would like to make is that a dominant contribution to such a phase transition is coming from the solution with four dimensional Euclidean rotational invariance. Below we will demonstrate that for the shape of the potential specified above there is always such an $O(4)$-invariant solution, hence we can limit

ourselves to the case, when the field ϕ is a function of a four-dimensional euclidean distance $\rho = (\tau^2 + \vec{x}^2)^{1/2}$ only. In this limit an expression for the Euclidean action is

$$S_E = 2\pi^2 \int d\rho\, \rho^3 \left[\frac{1}{2} \left(\frac{d\phi}{d\rho} \right)^2 + V(\phi) \right] \tag{1.2.32}$$

and the equations of motion simplifies to

$$\frac{d^2\phi}{d\rho^2} + \frac{3}{\rho} \frac{d\phi}{d\rho} = \frac{dV}{d\phi} \tag{1.2.33}$$

In order to avoid issues with background subtraction, it is easier to assume that the energy of a false vacuum, in which the system was initially, is equal to zero, $V(\phi_F) = 0$. If gravity is not included such shifts of energy will not change the physics. However, when gravity is taken into account one will need to be more careful because the value of the potential energy at the minimum will determine a spacetime geometry. We will discuss the impact of gravity in detail in the next section.

First, the boundary conditions for equation (1.2.33) follow partially from the assumption that initially the system was in the false vacuum state:

$$\lim_{\tau=-\infty} \phi(\tau, \vec{x}) = \phi_F \tag{1.2.34}$$

and also from the fact that the field ϕ should relax to the false vacuum value at large distances

$$\lim_{|\vec{x}|\to\infty} \phi(\tau, \vec{x}) = \phi_F \tag{1.2.35}$$

in order to guarantee finiteness of the action. Recalling time reflection symmetry of the theory both these conditions could be translated to the following boundary condition in terms of the four-dimensional distance

$$\lim_{\rho\to\infty} \phi(\rho) = \phi_F \tag{1.2.36}$$

Using time translation symmetry of the problem, we can assume that the bubble of the true vacuum emerges at rest at $\tau = 0$, hence

$$\frac{\partial}{\partial\tau} \phi(\tau, \vec{x}) \bigg|_{\tau=0} = 0 \tag{1.2.37}$$

this gives the second boundary condition for the equation (1.2.33):

$$\left.\frac{d\phi\left(\rho\right)}{d\rho}\right|_{\rho=0}=0 \tag{1.2.38}$$

which is also necessary in order to avoid a singularity at $\rho = 0$.

In order to demonstrate that the equation (1.2.33) with the boundary conditions (1.2.36, 1.2.38) always has a solution we will use a mechanical analogy. This system describes a classical particle, which is moving in a potential '$-V$' and experiences a friction force proportional to the 'velocity' $d\phi/d\rho$ and inversely proportional to the 'time' ρ. From the boundary conditions it follows that initially the particle was at rest in the vicinity of the top of the potential, $\phi \approx \phi_T$, then rolls down towards the second maximum of the potential at $\phi = \phi_F$, which it should reach at an infinite future $\rho = \infty$. Due to the friction, if the particle were initially too far from the ϕ_T-maximum then it would not have enough energy in order to even reach the ϕ_F-maximum. However, if the particle were initially very close to the ϕ_T-top of the potential, it will stay there for too long, and because the friction force is inversely proportional to time this force will become too small and the particle will pass through the false vacuum hill in a finite amount of time and after that will run away to infinity. From this picture it is obvious that there is always a critical initial position of the particle, for which it will approach the false vacuum in the infinite future. The time that particle stays near the true vacuum in the beginning is equal to the radius of the bubble.

The mechanical analogy we have used above suggests a limit in which the problem simplifies and we can get an answer for the probability of the false vacuum decay in a closed form. If the energy difference between the false and true vacuum $\epsilon = V\left(\phi_F\right) - V\left(\phi_T\right)$ is small, then the friction force should also be very small during the motion. In other words, the particle should spend quite a long time at rest near the point $\phi = \phi_T$; when the friction force becomes small enough the particle quickly rolls down almost to the point $\phi = \phi_F$ and will stay there forever. This is called a *thin-wall* limit, because transition from one vacuum to another happens very quickly, or in other words happens at almost constant ρ.

The calculation of the Euclidean action simplifies in this limit, because we can naturally divide the integration in (1.2.32) into three parts. When ρ is less than

some critical radius ρ_b (radius of the bubble), the field ϕ, or our 'particle', stays very close to the true vacuum and we can ignore any derivative terms in this region

$$S_b = 2\pi^2 \int_0^{\rho_b} d\rho\ \rho^3 V\left(\phi_T\right) = -\frac{1}{2}\pi^2 \rho_b^4 \epsilon \tag{1.2.39}$$

The next region is where the transition from one vacuum to another happens. As we discussed, in a thin-wall limit, the transition to the false vacuum occurs almost at a constant value of $\rho = \rho_b$, and it is convenient to introduce a notion of the bubble wall: a 3-dimensional surface with a tension that divides regions with different vacua. Using an obvious field theory analogue of (1.2.31), for the region corresponding to the bubble wall we get

$$S_w = 2\pi^2 \int_{\rho_b-\delta}^{\rho_b+\delta} d\rho\ \rho^3 \left[\frac{1}{2}\left(\frac{d\phi}{d\rho}\right)^2 + V(\phi)\right] = 2\pi^2 \rho_b^3 \int_{\phi_T}^{\phi_F} \sqrt{2V(\phi)} d\phi = 2\pi^2 \rho_b^3\ \sigma \tag{1.2.40}$$

where we have introduced the surface tension of the wall, σ. After the wall, the field ϕ has relaxed to the false vacuum value and is not changing, the action is equal to zero in this third region. Overall, for the action we get

$$S_E = S_b + S_w = -\frac{1}{2}\pi^2 \rho_b^4 \epsilon + 2\pi^2 \rho_b^3\ \sigma \tag{1.2.41}$$

An actual value of the bubble radius corresponds to the solution of the equations of motion in the thin-wall limit, hence it delivers an extremum to the action. Therefore, by differentiation of the expression above with respect to the ρ_b we can find its proper value:

$$\frac{\partial S_E}{\partial \rho_b} = 0\ \Rightarrow\ \rho_b = \frac{3\sigma}{\epsilon} \tag{1.2.42}$$

Substituting it back we find the final answer for the Euclidean action in a thin-wall limit

$$S_E = \frac{27\pi^2 \sigma^4}{2\epsilon^3} \tag{1.2.43}$$

After the bubble of a true vacuum emerges it starts to expand very rapidly and eats up all the space, one could see this by returning to the Minkowskian time t in which constant four dimensional Euclidean distance corresponds to the expanding in time three dimensional surface

$$\rho^2 = \tau^2 + \vec{x}^2 = \vec{x}^2 - t^2 \tag{1.2.44}$$

where the wall is a hyperboloid in spacetime, expanding ever more rapidly and asymptoting to a lightcone.

1.2.3 Tunnelling in quantum field theory with gravity

As we advertised in the introduction, a description of any fundamental process in nature should include gravity. The decay of the false vacuum in a field theory is no exception. In the present section we overview an initial attempt to take into account the effects of gravitation on false vacuum decay due to Coleman and de Luccia [14].

From a general perspective, if we want to take into account gravitation we use the following action

$$S = \int \sqrt{-g} \left(\frac{1}{2} \partial_\mu \phi \partial^\mu \phi + V(\phi) - \frac{1}{2\kappa} \mathcal{R} \right) \tag{1.2.45}$$

Immediately, the problem about the ground state becomes much harder, as we in principle get ten additional unknown functions (independent components of the metric). However, if we limit ourself to the most obvious and simple appearance of gravity, namely the vacuum solutions, them it is again very natural to assume that gravity will not break spherical symmetry, at least to leading order, i.e. for the semi-classical consideration in which we are interested in. The assumption of $O(4)$ symmetry immediately reduces the amount of new unknowns to a single function in the ansatz for the metric

$$ds^2 = d\xi^2 + \rho\left(\xi\right)^2 d\Omega_3^2 \tag{1.2.46}$$

where $d\Omega_3^2$ is a line element on a unit three-sphere, representing the orbits of the $O(4)$ symmetry, ρ is the radius of these spheres, and ξ is a radial coordinate which is orthogonal to all the angular coordinates on the spheres, hence it moves us from one orbit to another.

The only non-trivial Einstein equation for such a metric is reduced to

$$\rho'^2 = 1 + \frac{1}{3}\kappa\rho^2 \left(\frac{1}{2}\phi'^2 - V \right) \tag{1.2.47}$$

here and throughout this section the primes denote differentiation with respect to ξ.

The equation of motion for the scalar field, where we assume that field ϕ depends only on ξ, is

$$\phi'' + \frac{3\rho'}{\rho}\phi' = \frac{dV}{d\phi} \tag{1.2.48}$$

The metric (1.2.46) is invariant under a constant shift of ξ and we can use this symmetry to choose $\rho(0) = 0$, hence from the second term in (1.2.47) it follows that $\phi'(0) = 0$ as well. Finally, $\phi(\infty) = \phi_F$, because the field ϕ should relax to the false vacuum value outside of the bubble[2].

The equation (1.2.48) differs from its analogue for the field theory without gravity, (1.2.33), only by the coefficient in front of the ϕ' term. However, as we discussed above, we neglect this term in a thin-wall approximation, therefore we can solve the equation for ϕ in an analogous way. Having the solution for $\phi(\xi)$ in hand, one can integrate the equation (1.2.47) straightforwardly. Hence the whole system of equations of motions can be solved in a thin-wall approximation.

The next question is a computation of the action in this limit. It is important to note that in this case one has to be careful with shifting the energy of a false vacuum state because when gravity is included, energy gravitates, and the value of the potential at each minimum will have a physical meaning since it will curve the spacetime in one way or another. Therefore, in order to have a finite decay rate, we need to perform a background subtraction, and the answer for the probability of false vacuum decay will be determined by the difference between the Euclidean action for the bubble solution and the Euclidean action for the false vacuum

$$B = S_E\left[\phi_b\right] - S_E\left[\phi_F\right]. \tag{1.2.49}$$

The expression for the Euclidean action itself is also will be different due to the Einstein-Hilbert term. The Ricci curvature of the metric (1.2.46) is

$$\mathcal{R} = \frac{6}{\rho^2}\left(1 - \rho\rho'' - \rho'^2\right). \tag{1.2.50}$$

Substituting this into (1.2.45), we integrate by parts in order to get rid of the second

[2]If there is some $\xi = \xi_{end} > 0$ at which $\rho(\xi_{end}) = 0$, then the last boundary condition is replaced by $\phi'(\xi_{end}) = 0$ and spacetime will have the topology of a four-sphere

derivative term, and use (1.2.47) to get rid of ρ', and finally we get:

$$S_E = 4\pi^2 \int d\xi \ \left(\rho^3 V - \frac{3\rho}{\kappa}\right) \tag{1.2.51}$$

As before in the thin-wall limit we can divide the integration into three parts. Outside the bubble, $\phi = \phi_F$ and due to background subtraction we get

$$B_{outside} = 0. \tag{1.2.52}$$

in the transition region, i.e. at the wall of the bubble, ρ is constant and equal to the radius of the bubble, hence using (1.2.51) we get

$$B_{wall} = S_E\left[\phi, \rho_b\right] - S_E\left[\phi_F, \rho_b\right] = 4\pi^2\rho_b^3 \int d\xi \ \left[V(\phi) - V(\phi_F)\right] = 2\pi^2\rho_b^3\sigma. \tag{1.2.53}$$

For the region inside the bubble $\phi = \phi_T$, hence from (1.2.47) we can derive

$$d\xi = \frac{d\rho}{\sqrt{1 - \frac{1}{3}\kappa\rho^2 V}}. \tag{1.2.54}$$

Substituting this in (1.2.51) and integrating gives

$$S_{Einside}\left[\phi_T\right] = \frac{12\pi^2}{\kappa^2 V(\phi_T)} \left(\left[1 - \frac{1}{3}\kappa\rho_b^2 V(\phi_T)\right]^{3/2} - 1\right) \tag{1.2.55}$$

Now we must subtract the background contribution from the false vacuum, which finally yields

$$B_{inside} = S_{Einside}\left[\phi_T\right] - S_{Einside}\left[\phi_F\right] \tag{1.2.56}$$

We can derive the general expression for B in a thin-wall approximation with gravity in terms of the energies of the true and false vacuum states, however, in order to appreciate the influence of gravity on the probability of false vacuum decay, it is better to consider two illustrative examples that show how important the inclusion of gravity could be.

The first example is when we have positive false vacuum energy $V(\phi_F) = \epsilon > 0$, and a zero true vacuum energy $V(\phi_T) = 0$, hence the tunnelling is from de Sitter to Minkowski spacetime. Substituting this in (1.2.56) after some simplifications we get

$$B = B_{wall} + B_{inside} = 2\pi^2\rho_b^3\sigma - \frac{6\pi^2}{\kappa}\rho_b^2 - \frac{12\pi^2}{\kappa^2\epsilon}\left(\left[1 - \frac{1}{3}\kappa\rho_b^2\epsilon\right]^{3/2} - 1\right) \tag{1.2.57}$$

By differentiation it is easy to find an actual radius of the bubble for which B will be stationary

$$\rho_b = \frac{12\sigma}{4\epsilon + 3\kappa\sigma^2} = \frac{\rho_0}{1 + (\rho_0/2\ell)^2} \tag{1.2.58}$$

here ρ_0 is the bubble radius without gravity given by (1.2.42), and $\ell = \sqrt{3/\kappa\epsilon}$ is the radius of de Sitter spacetime, which is outside of the bubble. Substituting (1.2.58) back into (1.2.57) we get an expression for the tunnelling exponent

$$B = \frac{B_0}{\left[1 + (\rho_0/2\ell)^2\right]^2} \tag{1.2.59}$$

here B_0 is the action without gravity, given by (1.2.43). As one can see, in this case gravity enhances the decay rate by reducing the action.

The second example is tunnelling from flat Minkowski spacetime to an Anti de Sitter spacetime with negative vacuum energy, hence $V(\phi_F) = 0$ and $V(\phi_T) = -\epsilon < 0$. Performing an analogous calculation for the tunnelling exponent in this case we get

$$B = \frac{B_0}{\left[1 - (\rho_0/2\ell)^2\right]^2} \tag{1.2.60}$$

Note the sign difference in the denominator, therefore for the second example gravity will make the probability of decay smaller and, in principle, could even completely stabilize the false Minkowski vacuum.

Chapter 2

Lifshitz holography

2.1 Introduction

In this chapter, based on [31], we will describe a particular top-down approach to the extension of holography to non-relativistic field theories. This is interesting both for the potential application of these theories in condensed matter physics and for its potential to enlarge our understanding of holographic dualities (for reviews see e.g. [32–34]). Such theories have a symmetry under the generalized scaling $t \to \lambda^z t$, $\vec{x} \to \lambda \vec{x}$. Comparing this to the scaling symmetry of AdS spacetime (1.1.19), which is dual to relativistic field theories, it was realized in [11] that a holographic dual to the Lifshitz field theory could be constructed by considering spacetimes with a metric

$$ds^2 = r^{2z} dt^2 - r^2 d\vec{x}^2 - \frac{dr^2}{r^2}, \tag{2.1.1}$$

which have an isometry under $t \to \lambda^z t$, $\vec{x} \to \lambda \vec{x}$, $r \to \lambda^{-1} r$. In [11, 35] simple "bottom-up" models admitting such solutions were proposed. They have since been realized as solutions in "top-down" models obtained from string theory: the case $z = 2$ proves to be the simplest to realize [36–39], but a construction allowing for general values of z was given in [40]. Some other particular values of z were also realized in [41–43].

An interesting goal in such top-down constructions is to get a better understanding of the non-relativistic field theories dual to such Lifshitz solutions. It is particularly interesting to understand these holographic theories, as no examples of

interacting theories with Lifshitz symmetries are known. In [44], holographic RG flows relating the Lifshitz and AdS solutions in the context of the massive IIA setup in [40] were constructed, and it was noted that the RG flows offered a potential approach to understanding the field theory dual to Lifshitz, as one could consider the flow from an AdS solution with a known dual to Lifshitz. Related work on such flows and their applications includes [45–53]. A dynamical interpolation was studied in [54]. A different approach to relating AdS to Lifshitz is [55, 56].

In this chapter, we extend the work of [44] by considering flows involving the type IIB Lifshitz solutions in [40]. We start with five-dimensional gauged supergravity obtained by compactifying IIB on an S^5, and consider further compactifying two spatial directions on a compact hyperbolic space, with certain gauge fluxes turned on on this space. There are asymptotically AdS_5 solutions, where the proper size of the compact hyperbolic space grows near the boundary, and AdS_3 and 3-dimensional Lifshitz (denoted Li_3) solutions where it has constant size. As in [44], we consider flows relating all these solutions. We focus particularly on the flows from AdS_5, and analyze these in detail, identifying the deformation of AdS_5 which sources the flow and discussing its dual field theory description.

Working in the IIB context has two advantages: the field theory dual to the asymptotically AdS_5 solution is the familiar $\mathcal{N} = 4$ SYM, and the deformation we are interested in includes as a special case a supersymmetric twist which has been previously studied in [57]. In the supersymmetric flow, [57] showed that the twist involves not only turning on a flux Q but also adding a source λ for a scalar operator transforming in the **20** of the $SU(4)$ R-symmetry. We will see that the flows to non-supersymmetric AdS_3 and Lifshitz geometries involve changing the values of Q and λ in a coordinated way: the flow reaches an IR fixed point on one-dimensional subspaces in the space of $\{Q, \lambda\}$ deformations.

Surprisingly, we do not need to turn on a source which breaks Lorentz symmetry explicitly in the UV to realize flows to Lifshitz: this Lorentz symmetry breaking will emerge spontaneously for appropriate values of $\{Q, \lambda\}$.

In [57], the deformation by $\{Q, \lambda\}$ was related to a change in the scalar Lagrangian in the $\mathcal{N} = 4$ SYM theory, and it was shown to lead to flat directions for

certain scalars in the supersymmetric case. We analyze this field theory Lagrangian deformation for our non-supersymmetric cases and find that there is a finite range of non-supersymmetric flows to AdS_3 where the flat directions get lifted and the field theory scalars in the deformed field theory will be stable in the UV. Disappointingly, for the flows to Li_3, the field theory deformation always leads to some runaway directions in the scalar space. These runaways correspond to brane nucleation instabilities in the bulk geometry (discussed for example in [58, 59]), as we show explicitly by a probe brane calculation. Thus, for the flows to Lifshitz, the UV field theory is unstable, and this flow does not offer us a way to define the IR theory dual to the Lifshitz geometry. As in [44], we also find that for some values of z the Lifshitz geometries have linearized modes which appear to violate the generalization of the Breitenlohner-Freedman bound [30]. These two types of instabilities do not appear to be related.

In section 2.2, we review the Romans 5D gauged SUGRA model [60] and review the Lifshitz solutions in this model [40], as well as discussing the families of AdS_3 solutions. We then discuss the flows in section 2.3, first performing a linearized analysis about each of the solutions to determine the qualitative character of the flows and then numerically constructing the various flows. In section 2.4, we analyze the deformation away from AdS_5 in the UV and discuss the dual field theory.

2.2 Lifshitz and AdS solutions in 5-dimensional gauged supergravity

We consider a consistent truncation of the $\mathcal{N} = 4$ five-dimensional gauged supergravity theory obtained by reduction of the ten-dimensional type IIB supergravity on S^5, where we keep an $SU(2) \times U(1)$ subgroup of the $SU(4)$ gauge group, and a single scalar ϕ [60]. This theory is a consistent truncation of the full higher dimensional theory, in the sense that any solutions in the 5D theory can be uplifted to Type IIB supergravity solutions in ten dimensions (see [61] for explicit detail).

The field content of the theory consists of the metric $g_{\mu\nu}$, 5D dilaton field ϕ, $SU(2)$ gauge field $A^{(i)}_\mu$, $U(1)$ gauge field $\mathcal{A}_\mu$ and two antisymmetric tensor fields

$B^{\alpha}_{\mu\nu}$. The bosonic part of the Lagrangian is

$$\begin{aligned}\mathcal{L} =& -\frac{R}{4}+\frac{1}{2}\partial_\mu\phi\partial^\mu\phi-\frac{1}{4}\xi^{-4}\mathcal{F}_{\mu\nu}\mathcal{F}^{\mu\nu}-\frac{1}{4}\xi^2\left(F^{(i)}_{\mu\nu}F^{\mu\nu(i)}+B^{\mu\nu\alpha}B^{\alpha}_{\mu\nu}\right)\\&+\frac{1}{4}\epsilon^{\mu\nu\rho\sigma\lambda}\left(\frac{1}{g_1}\epsilon_{\alpha\beta}B^{\alpha}_{\mu\nu}D_\rho B^{\beta}_{\sigma\lambda}-F^{(i)}_{\mu\nu}F^{(i)}_{\rho\sigma}\mathcal{A}_\lambda\right)+P(\phi),\end{aligned} \tag{2.2.2}$$

where $\xi=e^{\sqrt{\frac{2}{3}}\phi}$, the scalar field potential is

$$P(\phi)=\frac{g_2}{8}\left(g_2\xi^{-2}+2\sqrt{2}g_1\xi\right), \tag{2.2.3}$$

and field strengths are

$$\begin{aligned}\mathcal{F}_{\mu\nu}&=\partial_\mu\mathcal{A}_\nu-\partial_\nu\mathcal{A}_\mu,\\F^{(i)}_{\mu\nu}&=\partial_\mu A^{(i)}_\nu-\partial_\nu A^{(i)}_\mu+g_2\epsilon^{ijk}A^{(j)}_\mu A^{(k)}_\nu.\end{aligned} \tag{2.2.4}$$

The $U(1)$ gauge coupling g_1 and $SU(2)$ gauge coupling g_2 are two independent parameters of the theory. It was shown in [60] that these parameters can be eliminated by field redefinitions so that there are only three physically different theories, the $\mathcal{N}=4^+$ theory, when $g_1g_2>0$, the $\mathcal{N}=4^0$ theory, when $g_2=0$, and the $\mathcal{N}=4^-$ theory, when $g_1g_2<0$. We will consider here only the $\mathcal{N}=4^+$ theory, i.e. we assume $g_1g_2>0$. We also set $B^{\alpha}_{\mu\nu}=0$ identically for all solutions and flows considered here.

The equations of motion for the rest of the fields are then

$$\begin{aligned}R_{\mu\nu}&=2\partial_\mu\phi\partial_\nu\phi+\frac{4}{3}g_{\mu\nu}P(\phi)-\xi^{-4}\left(2\mathcal{F}_{\mu\rho}\mathcal{F}^{\rho}_{\nu}-\frac{1}{3}g_{\mu\nu}\mathcal{F}_{\rho\sigma}\mathcal{F}^{\rho\sigma}\right)\\&\quad-\xi^2\left(2F^{(i)}_{\mu\rho}F^{\rho(i)}_{\nu}-\frac{1}{3}g_{\mu\nu}F^{(i)}_{\rho\sigma}F^{\rho\sigma(i)}\right),\\\Box\phi&=\frac{\partial P}{\partial\phi}+\sqrt{\frac{2}{3}}\xi^{-4}\mathcal{F}_{\mu\nu}\mathcal{F}^{\mu\nu}-\sqrt{\frac{1}{6}}\xi^2F^{(i)}_{\rho\sigma}F^{(i)\rho\sigma},\\D_\nu\left(\xi^{-4}\mathcal{F}^{\nu\mu}\right)&=\frac{1}{4}\epsilon^{\mu\nu\rho\sigma\tau}F^{(i)}_{\nu\rho}F^{(i)}_{\sigma\tau},\\D_\nu\left(\xi^2F^{\nu\mu(i)}\right)&=\frac{1}{2}\epsilon^{\mu\nu\rho\sigma\tau}F^{(i)}_{\nu\rho}\mathcal{F}_{\sigma\tau}.\end{aligned} \tag{2.2.5}$$

2.2.1 Ansatz for solutions and flows

To construct flows, we only need to consider radial dependence of the bulk fields; we assume the holographic RG flow geometries we consider will preserve the translational invariance in the t and x directions, and will have the topological flux through

the compact hyperbolic space. The most general ansatz we will need to consider is thus

$$ds^2 = e^{2F(r)}dt^2 - r^2dx^2 - e^{2d(r)}\frac{dr^2}{r^2} - e^{2h(r)}\frac{dy_1^2+dy_2^2}{y_2^2}, \tag{2.2.6}$$

the 5D dilaton ϕ is also only a function of r, and we assume the gauge fields have at most nonzero $r-t$ or $r-x$ components. It is convenient to parametrize the fields in such a way as to eliminate geometric factors:

$$\begin{aligned} F^{(3)}_{rt} &= \frac{\tilde{A}(r)}{\xi r}e^{F+D}\,, \qquad F^{(3)}_{rx} = \frac{B(r)}{\xi}e^{D}\,, \qquad F^{(3)}_{y_1y_2} = \frac{Q}{g_2y_2^2}\,, \\ \mathcal{F}_{rt} &= \frac{A(r)\xi^2}{r}e^{F+D}\,, \qquad \mathcal{F}_{rx} = \tilde{B}(r)\xi^2e^{D}\,, \end{aligned} \tag{2.2.7}$$

where we have also introduced shifted and rescaled variables in order to eliminate g_1 and g_2 from all expressions:

$$\begin{aligned} D(r) &= d(r) + \frac{1}{3}\ln\left(g_1g_2^2\right), \\ H(r) &= h(r) + \frac{1}{3}\ln\left(g_1g_2^2\right), \\ \varphi(r) &= \xi^3(r)g_1g_2^{-1}, \end{aligned} \tag{2.2.8}$$

Substituting all this into the equations (2.2.5) and introducing the new variable $\rho = \ln r$ we get

$$\begin{aligned} \frac{R^t_t}{g_1^{\frac{2}{3}}g_2^{\frac{4}{3}}} &= e^{-2D}\left[F' - F'D' + F'^2 + F'' + 2H'F'\right] \\ &= \frac{1}{6}\left(\varphi^{-\frac{2}{3}} + 2\sqrt{2}\varphi^{\frac{1}{3}}\right) + \frac{4}{3}\left(A^2+\tilde{A}^2\right) + \frac{2}{3}\left(\tilde{B}^2+B^2\right) + \frac{2}{3}\varphi^{\frac{2}{3}}Q^2e^{-4H} \\ \frac{R^x_x}{g_1^{\frac{2}{3}}g_2^{\frac{4}{3}}} &= e^{-2D}\left[F' - D' + 1 + 2H'\right] \\ &= \frac{1}{6}\left(\varphi^{-\frac{2}{3}} + 2\sqrt{2}\varphi^{\frac{1}{3}}\right) - \frac{2}{3}\left(A^2+\tilde{A}^2\right) - \frac{4}{3}\left(\tilde{B}^2+B^2\right) + \frac{2}{3}\varphi^{\frac{2}{3}}Q^2e^{-4H} \\ \frac{R^r_r}{g_1^{\frac{2}{3}}g_2^{\frac{4}{3}}} &= e^{-2D}\left[F'' + F'^2 - F'D' - D' + 1 - 2H'D' + 2H'^2 + 2H''\right] \\ &= \frac{-\varphi'^2}{3\varphi^2e^{2D}} + \frac{1}{6}\left(\varphi^{-\frac{2}{3}} + 2^{\frac{3}{2}}\varphi^{\frac{1}{3}}\right) + \frac{4}{3}\left(A^2+\tilde{A}^2-\tilde{B}^2-B^2\right) + \frac{2}{3}\varphi^{\frac{2}{3}}Q^2e^{-4H} \\ \frac{R^{y_1}_{y_1}}{g_1^{\frac{2}{3}}g_2^{\frac{4}{3}}} &= e^{-2H} + e^{-2D}\left[H'' + 2H'^2 + H'F' + H' - H'D'\right] \\ &= \frac{1}{6}\left(\varphi^{-\frac{2}{3}} + 2\sqrt{2}\varphi^{\frac{1}{3}}\right) - \frac{2}{3}\left(A^2+\tilde{A}^2\right) + \frac{2}{3}\left(\tilde{B}^2+B^2\right) - \frac{4}{3}\varphi^{\frac{2}{3}}Q^2e^{-4H} \end{aligned} \tag{2.2.9}$$

for the Einstein equations, where a prime now denotes ∂_ρ, and

$$\begin{aligned}\Box \ln\varphi &= -e^{-2D}\partial_\rho^2 \ln\varphi - e^{-2D}\partial_\rho \ln\varphi\,(1+F'-D'+2H') \\ &= \frac{1}{2}\left(-\varphi^{-\frac{2}{3}}+\sqrt{2}\varphi^{\frac{1}{3}}\right) + 4\left(\tilde{B}^2-A^2\right) - 2\left(B^2-\tilde{A}^2\right) - 2\varphi^{\frac{2}{3}}Q^2e^{-4H}\end{aligned} \tag{2.2.10}$$

$$\begin{aligned}\partial_\rho\left(\varphi^{-\frac{2}{3}}rAe^{2H}\right) &= 2\varphi^{-\frac{1}{3}}rBQe^{D}\,; \qquad \partial_\rho\left(\varphi^{\frac{1}{3}}Be^{F+2H}\right) = 2\varphi^{\frac{2}{3}}AQe^{F+D} \\ \partial_\rho\left(\varphi^{\frac{1}{3}}r\widetilde{A}e^{2H}\right) &= 2\varphi^{\frac{2}{3}}r\widetilde{B}Qe^{D}\,; \qquad \partial_\rho\left(\varphi^{-\frac{2}{3}}\widetilde{B}e^{F+2H}\right) = 2\varphi^{-\frac{1}{3}}\widetilde{A}Qe^{F+D}\end{aligned} \tag{2.2.11}$$

$$A\widetilde{B}+\widetilde{A}B=0 \tag{2.2.12}$$

for the 5D dilaton and gauge equations.

This system appears to involve eight unknown functions, but we see that in the Lifshitz solutions, one of the two sets of fluxes must be zero to satisfy (2.2.12), and therefore at most we turn on either the tilded or the untilded fluxes but never both. Thus, in a given flow we will have six unknown functions. These will be subject to seven equations: (2.2.9, 2.2.10), and two equations from (2.2.11). As usual, one of the equations in (2.2.9) is redundant because of the Bianchi identity.

2.2.2 AdS_5 asymptotic solution

In the ansatz (2.2.6), we have sliced our five dimensional space-time with two dimensional hyperbolic slices and $2+1$ dimensional planar slices. As such therefore, there is no solution for F, D, and H which is globally AdS_5, however, there are solutions which asymptote to AdS_5 at large r, where the curvature of the hyperbolic space is effectively suppressed. These solutions will have

$$F\sim\rho\,, \quad D\sim D_0\,, \quad H\sim H_0+\rho \tag{2.2.13}$$

as $\rho\to\infty$, and will have a constant 5D dilaton, $\varphi\sim\varphi_0$, and vanishing gauge fluxes, $A\sim B\sim\widetilde{A}\sim\widetilde{B}\sim 0$ to leading order. Substituting this in (2.2.9, 2.2.10, 2.2.11), the leading order equations fix

$$\begin{aligned}4e^{-2D_0} &= \frac{1}{6}\left(\varphi_0^{-\frac{2}{3}}+2\sqrt{2}\varphi_0^{\frac{1}{3}}\right), \\ 0 &= \frac{1}{2}\left(-\varphi_0^{-\frac{2}{3}}+\sqrt{2}\varphi_0^{\frac{1}{3}}\right),\end{aligned} \tag{2.2.14}$$

which can easily be solved to find

$$\varphi_0 = \frac{1}{\sqrt{2}} \quad D_0 = \frac{4}{3}\ln 2. \tag{2.2.15}$$

These asymptotically AdS_5 solutions exist for any values of H_0 and the topological charge Q.

2.2.3 $AdS_3 \times \mathcal{H}_2$ solution

In [57], a supersymmetric $AdS_3 \times \mathcal{H}^2$ solution was considered. Here we regard this as part of a one-parameter family of $AdS_3 \times \mathcal{H}^2$ solutions in the ansatz (2.2.6). In principle, it is possible to consider a more general two-parameter family of AdS_3 solutions by turning on two fluxes.

We will get an $AdS_3 \times \mathcal{H}_2$ spacetime from the metric (2.2.6) by taking constant values for $H = H_0$ and D_0, and setting $F(\rho) = \rho$. It is easy to check that the system has such a solution for constant 5D dilaton field φ_0 and vanishing bulk gauge fluxes $A = \widetilde{A} = B = \widetilde{B} = 0$ if

$$e^{-2D_0} = \frac{\varphi_0^{\frac{1}{3}}}{2\sqrt{2}}\,, \quad e^{-2H_0} = \frac{1}{2\varphi_0^{\frac{2}{3}}}\,, \quad Q^2 = \varphi_0\sqrt{2} - 1. \tag{2.2.16}$$

Therefore, we have a family of AdS_3 solutions, parametrized by the value of 5D dilaton field φ_0, which should be in the range $\varphi_0 \in [\frac{1}{\sqrt{2}}, \infty)$. These solutions are illustrated by a grey line in figure 2.1.

2.2.4 $Li_3 \times \mathcal{H}_2$ solution

We now review the Lifshitz solutions obtained in [40]. As noted above, such solutions are obtained by taking either the tilded or untilded fluxes to vanish. The solutions are obtained from our ansatz by setting $F(\rho) = z\rho$, and taking constant functions $H = H_0$ and $D = D_0$ as in the AdS_3 solutions.

Tilded Lifshitz solution $z \geq 1$

If we turn on a *tilded* pair of gauge fluxes $\widetilde{A} = \widetilde{A}_0$, $\widetilde{B} = \widetilde{B}_0$ for some constant values $\widetilde{A}_0$ and $\widetilde{B}_0$, ($A = B \equiv 0$) then (2.2.9, 2.2.10, 2.2.11) are satisfied if

$$\begin{aligned} \varphi_0 &= \frac{\sqrt{2}(z+1)}{2z^2+3z-2}, & \widetilde{A}_0^2 &= \frac{z(z-1)}{2}e^{-2D_0}, \\ e^{-2D_0} &= \left[2(z+1)^2(2z^2+3z-2)\right]^{-\frac{1}{3}}, & \widetilde{B}_0^2 &= \frac{z-1}{2}e^{-2D_0}, \\ e^{-2H_0} &= \frac{3}{2}ze^{-2D_0}, & Q^2 &= \frac{2z^2+3z-2}{9z}. \end{aligned} \tag{2.2.17}$$

This family of solutions is parametrized by the value of the dynamical exponent z, which in this case should be greater than one, and is shown in figure 2.1 as a blue line.

Untilded Lifshitz solution $1 \leq z \leq 2$

If we turn on the other pair of fluxes, i.e. *untilded* gauge fluxes $A = A_0$, $B = B_0$ for some constant values A_0 and B_0, ($\widetilde{A} = \widetilde{B} \equiv 0$) then (2.2.9, 2.2.10, 2.2.11) are satisfied if

$$\begin{aligned} \varphi_0 &= \frac{\sqrt{2}z(z+1)}{-2z^2+3z+2}, & A_0^2 &= \frac{z(z-1)}{2}e^{-2D_0}, \\ e^{-2D_0} &= \left[2z^2(z+1)^2(-2z^2+3z+2)\right]^{-\frac{1}{3}}, & B_0^2 &= \frac{z-1}{2}e^{-2D_0}, \\ e^{-2H_0} &= \frac{3}{2}ze^{-2D_0}, & Q^2 &= \frac{-2z^2+3z+2}{9z}. \end{aligned} \tag{2.2.18}$$

This second family of solutions is again parametrized by z, but this must now lie in the range $1 \leq z \leq 2$ which gives positive Q^2. These solutions are shown as a red line in the (Q^2, φ_0) plane in Figure 2.1.

2.3 RG flow solutions

We now turn to the construction of flows interpolating between the solutions reviewed in the previous section. Such interpolating solutions correspond to RG flows in the dual field theory, with the solution at small r corresponding to the IR limit of the RG flow, and the solution at large r corresponding the the UV limit of the RG flow. The study of such holographic flows was initiated in [62, 63].

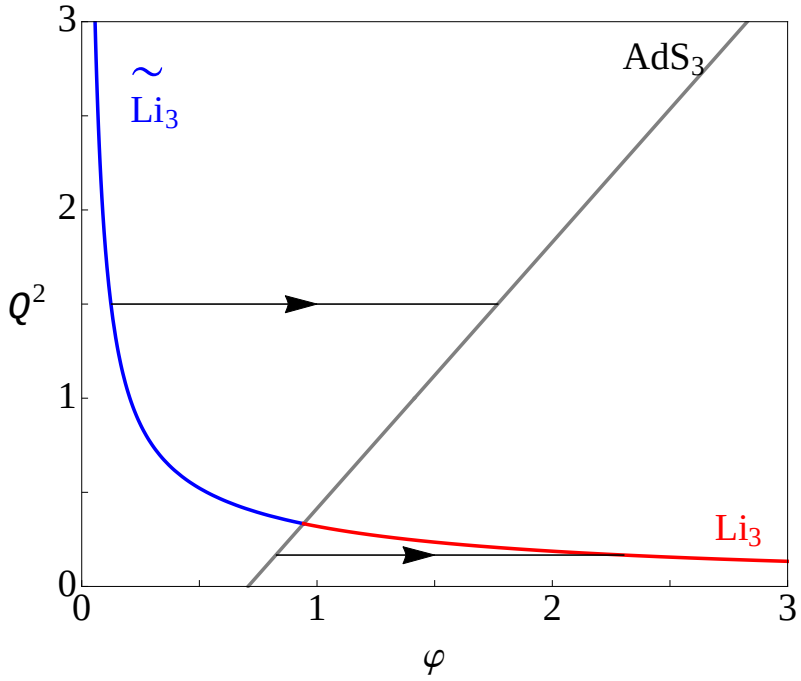

Figure 2.1: The values of Q, φ_0 for the AdS_3, $\widetilde{Li_3}$ and Li_3 solutions. The AdS_3 family is parametrized by φ_0, which determines $Q^2 = \sqrt{2}\varphi_0 - 1$. The Lifshitz families are parametrized by z, which determines Q and φ_0. Also shown are flows between the solutions, which must occur at constant Q, with an arrow depicting the direction of the flow.

Analogous flows were previously constructed for the Type IIA theory in [44]. As in that case, the charge Q will be conserved along the flows; flows will move horizontally in figure 2.1. Therefore the solutions that can be related by flows are the $\widetilde{\text{Li}}_3$ and AdS_3 for large enough values of Q, and AdS_3 and Li_3 for smaller values of Q. There is also the possibility of having flows which start from the asymptotically AdS_5 solution in the UV, which exists for any value of the charge Q, and approach any of these AdS_3 or Lifshitz solutions in the IR.

2.3.1 Linearized analysis

Before we proceed to the construction of the actual flows, we will perform a linearized perturbation analysis around each of the fixed-point solutions, to determine which direction we would expect the flows to go in (that is, which solution should be in the IR and which in the UV). This corresponds to computing the dimensions of the

deforming operators in the dual field theories. We then construct the interpolating solutions numerically.

Linearisation around AdS_5

The expansion around the asymptotically AdS_5 solution is a little more conceptually involved than the others, because AdS_5 is not an exact solution of the equations of motion, but only an asymptotic solution. We can avoid these subtleties by imagining that we take the radius of curvature of the compact hyperbolic space to zero by taking $h_0 \to \infty$, and neglecting terms in the equations of motion involving e^{-2h_0}. This will give us the linearized form of the equations of motion around the pure AdS_5 solution which will allow us to read off the scaling of the linearized solutions. These scalings will remain valid for the linearized modes in the asymptotically AdS_5 solution with finite h_0 to leading order at large r, as the physical volume of the compact hyperbolic space diverges as $r \to \infty$.

We write the solution as

$$\begin{aligned} &\partial_\rho F = 1 + y_0(\rho), && D = D_0 + y_1(\rho), && A = y_8(\rho), \\ &H = \rho + H_0 + y_2(\rho), && \partial_\rho H = 1 + y_4(\rho), && B = y_9(\rho), \\ &\varphi = \varphi_0 + y_3(\rho), && \partial_\rho \varphi = 0 + y_5(\rho), \end{aligned} \tag{2.3.19}$$

and linearize in the y_i, taking $H_0 \to \infty$. At linear order we will not see the constraint (2.2.12), but we recall that we will only consider solutions with either (y_6, y_7) or (y_8, y_9), but not all four at the same time. The other equations in (2.2.9, 2.2.10, 2.2.11) then give us a system of first-order equations,

$$\begin{aligned} &\dot{y}_0 = -4y_0, && \dot{y}_1 = y_0 - 8y_1 + 2y_4, && \dot{y}_2 = y_4, \\ &\dot{y}_3 = y_5, && \dot{y}_4 = -4y_4, && \dot{y}_5 = -4y_3 - 4y_5, \\ &\dot{y}_6 = -3y_6, && \dot{y}_7 = -3y_7, && \dot{y}_8 = -3y_8, && \dot{y}_9 = -3y_9, \end{aligned} \tag{2.3.20}$$

and a constraint equation,

$$y_1 = \frac{y_0 + 2y_4}{4}. \tag{2.3.21}$$

We can easily verify that this constraint is consistent with the first-order system. Imposing the constraint, and keeping one of the two pairs of gauge fluxes, we will

have a seven-dimensional space of linearized solutions. For example, for the case where we keep (y_8, y_9), the linearized solutions are

$$\begin{aligned} \partial_\rho F &= 1 + C_0 e^{-4\rho}, & \varphi &= \varphi_0 + \lambda\rho e^{-2\rho} + \eta e^{-2\rho}, \\ D &= D_0 + \frac{1}{4}(C_0 + 2C_4)e^{-4\rho}, & A &= C_8 e^{-3\rho}, \\ H &= \rho + H_0 + C_2 - \frac{1}{4}C_4 e^{-4\rho}, & B &= C_9 e^{-3\rho}. \end{aligned} \tag{2.3.22}$$

These solutions correspond to infinitesimal VEVs and sources for corresponding operators. The constants C_0, C_4 are the energy density and an anisotropic pressure; the corresponding sources are deformations of the boundary metric. These are C_2 and a constant F_0 in F, which we can freely add since the equations of motion only involve $\partial_\rho F$. Both C_2 and F_0 are pure gauge degrees of freedom; the former corresponds to shifting the background H_0, and the latter is a pure diffeomorphism. The parameters C_8 and C_9 are charge densities for the gauge fields; the corresponding sources are constant components of the vector potentials, which are pure gauge, and are also absent from our ansatz since we wrote it in terms of the field strengths. Finally λ and η are the source and VEV for the operator corresponding to the 5D dilaton. This operator is particularly interesting to us as we will see that the flows from AdS_5 to the AdS_3 and Lifshitz solutions will involve turning on this source. As this is a relevant deformation, we would expect flows from AdS_5 in the UV, approaching the other solutions in the IR.

Since they do not enter into the equations of motion in our ansatz, the constant part of F and the constant part of the gauge potentials will not play any role in the flows we consider. This is a remarkable fact; it implies that in the flows from AdS_5 to Lifshitz, the only physical source we can find turned on at the AdS_5 end of the flow is λ. This does not break the Lorentz invariance. Thus, when we have a flow to Lifshitz, the breaking of the Lorentz invariance along the flow is spontaneous.

Linearisation around AdS_3 solutions

We expect to have flows relating AdS_3 to both $\widetilde{\text{Li}}_3$ and Li_3 spacetimes, therefore it is interesting to consider perturbations for both tilded and untilded fluxes in this

case. Hence, we have the following linear perturbation from the AdS_3 solution

$$\mathbf{X} = \mathbf{X}_0 + \mathbf{y}, \tag{2.3.23}$$

where $\mathbf{X}_0 = \left(F', D, H, \varphi, H', \varphi', \widetilde{A}, \widetilde{B}, A, B\right) = (1, D_0, H_0, \varphi_0, 0, 0, 0, 0, 0, 0)$ is the fixed point solution corresponding to the $AdS_3 \times \mathcal{H}_2$ spacetime and $\mathbf{y}(\rho)$ is a vector of perturbations. Linearising the equations of motion around the fixed point gives us a linear system

$$\dot{\mathbf{y}} = \mathbb{A}_{AdS_3} \cdot \mathbf{y}, \tag{2.3.24}$$

together with a constraint equation analogous to (2.3.21). The matrix $\mathbb{A}_{AdS_3}$ is a 10×10 matrix dependent on the background field values, however, as with the AdS_5 case, we may only switch on either the tilded or untilded fluxes, which both have exactly the same form of perturbation equations. In addition, the Bianchi identity implies a zero mode, thus our effective perturbations are reduced to a seven-dimensional system

$$\dot{\mathbf{y}}_{\text{red}} = \mathbb{A}_{\text{red}} \cdot \mathbf{y}_{\text{red}}, \tag{2.3.25}$$

where $\mathbf{y}_{\text{red}} = (\delta F', \delta H, \delta\varphi, \delta H', \delta\varphi', \delta A(\delta\widetilde{A}), \delta B(\delta\widetilde{B}))$, and writing $c = \sqrt{2}/\varphi_0$:

$$\mathbb{A}_{\text{red}} = \begin{bmatrix} -2 & 0 & 0 & 0 & 0 & 0 & 0 \\ 0 & 0 & 0 & 1 & 0 & 0 & 0 \\ 0 & 0 & 0 & 0 & 1 & 0 & 0 \\ 0 & \frac{16-2c}{3} & \frac{\sqrt{2}c}{9}(c-2) & -2 & 0 & 0 & 0 \\ 0 & \frac{4\sqrt{2}}{c}(c-2) & \frac{2-4c}{3} & 0 & -2 & 0 & 0 \\ 0 & 0 & 0 & 0 & 0 & -1 & \sqrt{4-2c} \\ 0 & 0 & 0 & 0 & 0 & \sqrt{4-2c} & -1 \end{bmatrix} \tag{2.3.26}$$

In this format we see the perturbation of the flux decouples from the geometry, and the equation for $\delta F'$ also decouples. This matrix has a set of eigenvalues $\{\Delta_i\}$,

$$\Delta_i = -2\,; \quad -1 \pm \sqrt{4 - c \pm \sqrt{9 - 2c + c^2}}\,; \quad -1 \pm \sqrt{4 - 2c}\,, \tag{2.3.27}$$

with corresponding eigenvectors $\{\mathbf{v}_i\}$, thus the solution of the linear system (2.3.25) is

$$\mathbf{y}_{\text{red}} = \sum_i \mathbf{v}_i e^{\Delta_i \rho}. \tag{2.3.28}$$

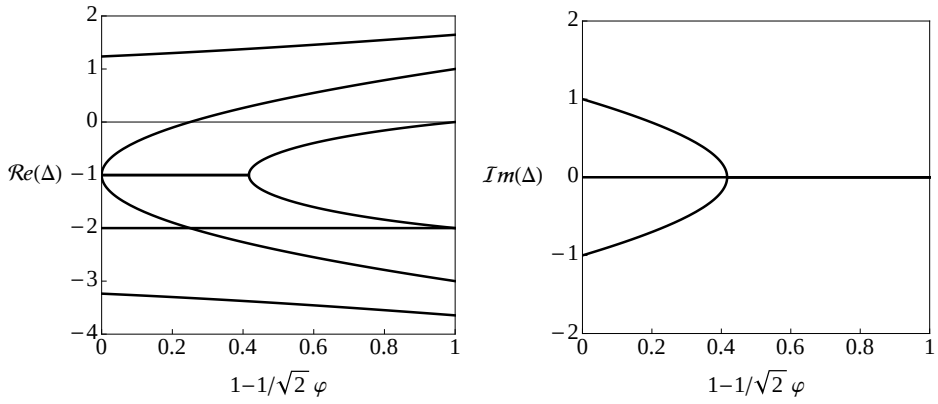

Figure 2.2: Plots of real and imaginary parts of the eigenvalues of the linear perturbations from the AdS_3 solution as functions of the background value of the 5D dilaton field φ_0.

The eigenvalues are plotted in figure 2.2, and we see that as in [44], some of the eigenvalues are complex for some values of φ_0, signalling a potential instability of these solutions. We will return to this issue at the end of our analysis.

Clearly, the $\Delta = -2$ eigenvalue corresponds to a pure geometry fluctuation, and actually corresponds to the fluctuation from a mass. The final pair of eigenvalues $\Delta_\pm = -1 \pm \sqrt{4 - \frac{2\sqrt{2}}{\varphi_0}}$ switch on flux, hence corresponding operators on the field theory side are relevant when $\Delta_+ < 0$, i.e. for $\frac{1}{\sqrt{2}} < \varphi_0 < \frac{2\sqrt{2}}{3}$.

Note that $\varphi_0 = \frac{2\sqrt{2}}{3}$ corresponds exactly to the point where all AdS_3, $\widetilde{\text{Li}}_3$ and Li_3 solutions coincide. Hence, for $\frac{1}{\sqrt{2}} < \varphi_0 < \frac{2\sqrt{2}}{3}$ we will have a relevant operator near AdS_3. If we excite the untilded fluxes, we can then expect a flow from the AdS_3 solution in the UV to the Li_3 solution in the IR. For $\varphi_0 > \frac{2\sqrt{2}}{3}$ we will have an irrelevant operator near AdS_3. So if we excite the tilded fluxes, we can expect to have flows from the $\widetilde{\text{Li}}_3$ spacetime in the UV to the AdS_3 spacetime in IR. These expected flows are presented in Figure 2.1. We will construct these flows numerically below.

In addition to the flux deformations, we see from figure 2.2 that there is one deformation which is always irrelevant. This should correspond to the flow approaching AdS_3 from the asymptotically AdS_5 solution.

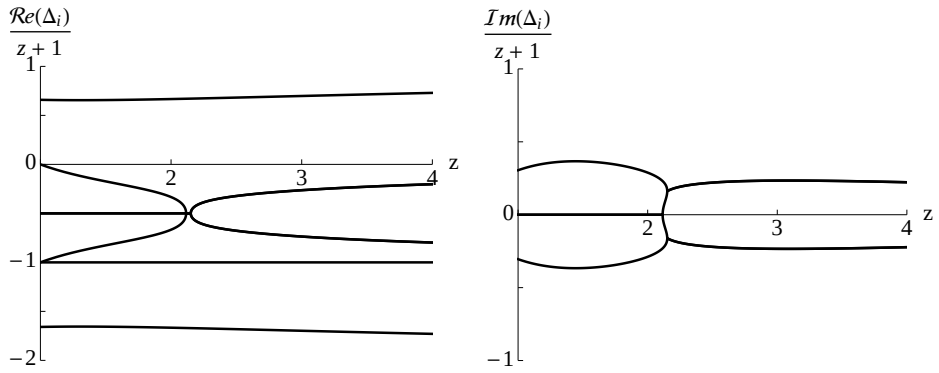

Figure 2.3: Plots of the real and imaginary parts of the eigenvalues of the linear perturbations from the $\widetilde{\text{Li}}_3$ solutions, divided by $z+1$, as functions of the background values of the dynamical exponent z.

Linearisation around $\widetilde{\text{Li}}_3$ solutions

In this case we must set the untilded fluxes to zero identically to satisfy (2.2.12). We write the variables as

$$\mathbf{X} = \mathbf{X}_0 + \mathbf{y}, \tag{2.3.29}$$

where $\mathbf{X}_0 = \left(F', D, H, \varphi, H', \varphi', \widetilde{A}, \widetilde{B}\right) = \left(z, D_0, H_0, \varphi_0, 0, 0, \widetilde{A}_0, \widetilde{B}_0\right)$ are the background values and $\mathbf{y}$ are the linear perturbations. This gives a linear system

$$\dot{\mathbf{y}} = \mathbb{A}_{\widetilde{Li}_3} \cdot \mathbf{y} \tag{2.3.30}$$

together with a constraint equation analogous to (2.3.21). The entries of the matrix $\mathbb{A}_{\widetilde{Li}_3}$ are parametrized by the value of dynamical exponent z, and although the corresponding eigenvalues can be found analytically (in terms of square roots of solutions to a cubic) their form is not particularly illuminating thus we present them only graphically in figure 2.3. The eigenvalues occur in pairs with the sum of each pair equal to $-(z+1)$. We see that we have complex eigenvalues for all values of z along this family. We also note that there is a single irrelevant mode, corresponding to the expected flow approaching this solution from the asymptotically AdS_5 solution.

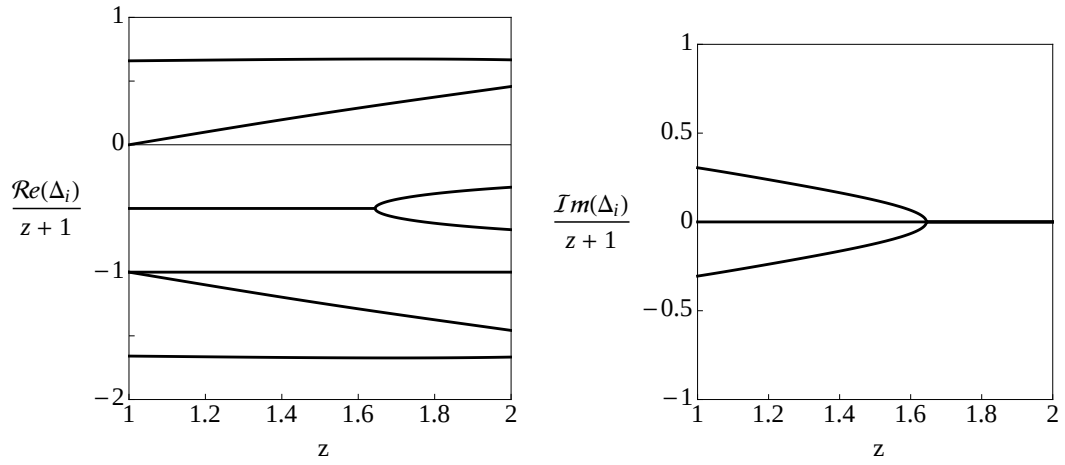

Figure 2.4: Plots of the real and imaginary parts of the eigenvalues of linear perturbations from the Li_3 solutions, divided by $z+1$, as functions of the background values of the dynamical exponent z, in this case $1 \leq z \leq 2$.

Linearisation around $\mathbf{Li}_3$ solutions

This is similar to the previous case, although now it is the tilded fluxes which must be set equal to zero. We again have an 8-dimensional system of linear perturbations, with background values $\mathbf{X}_0 = (F', D, H, \varphi, H', \varphi', A, B) = (z, D_0, H_0, \varphi_0, 0, 0, A_0, B_0)$, and a linear system with a matrix $\mathbb{A}_{Li_3}$ and a constraint. We will again have seven linearly independent modes, with eigenvalues coming in pairs, with the sum of the eigenvalues in each pair equal to $-(z+1)$. The resulting eigenvalues are presented in figure 2.4. Here we see complex eigenvalues for a range of values of z near 1, but there is a range near 2 where all the eigenvalues are real and the solutions may be stable. We also note that there are two irrelevant modes, corresponding to the expected flows approaching this solution from asymptotically AdS_5 and AdS_3 solutions.

2.3.2 Numerical Flows

Here we present the result of numerical solutions of the full non-linear system of equations of motion for the interpolating solutions between different fixed points in UV ($r \to \infty$) and IR ($r \to 0$). We discuss first the flows between AdS_3 and Li_3

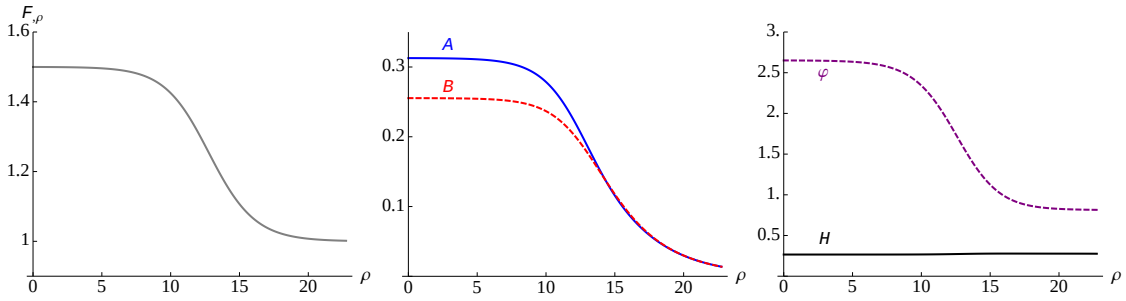

Figure 2.5: Solution interpolating between Li_3 with $z = 3/2$ and AdS_3, with $Q^2 = \frac{4}{27}$.

spacetimes and then consider the flows from the asymptotically AdS_5 solution in the UV.

Flows between AdS_3 and Li_3 spacetimes

From the linearized analysis, we expect flows from AdS_3 in the UV to Li_3 in the IR and flows from $\widetilde{\mathrm{Li}}_3$ in the UV to AdS_3 in the IR, as depicted in figure 2.1. We constructed examples of these flows numerically, using a shooting method. The shooting is carried out starting from the IR fixed point at small r, integrating numerically to larger r. Shooting is required to obtain the flows between AdS_3 and Li_3 because the IR fixed point always has two positive eigenvalues, and the generic flow will go to the asymptotically AdS_5 solution. Hence possible directions of shooting lie in the plane spanned by the two corresponding unstable directions and can be parametrized by the single angle variable, say, ζ. We find the value of ζ giving the desired flow by bisection of an initial interval of values of ζ.

- $Q^2 \in \left[0, \frac{1}{3}\right]$: *Flows from AdS_3 to Li_3*

  We present an example of such a solution in figure 2.5: this case interpolates between the untilded Lifshitz solution with $z = 3/2$ for small r (IR) and the AdS_3 solution for large r (UV) . The plot of F' shows that it starts from the value 3/2 and goes to 1, the other plots show how fluxes of the gauge fields go to zero at large r.

- $Q^2 > \frac{1}{3}$: *Flows from $\widetilde{Li}_3$ to AdS_3*

  We present an example of such a solution in figure 2.6: this case interpolates

between AdS_3 for small r (IR) and the $\widetilde{\text{Li}}_3$ solution with $z = 2$ for large r (UV) . The plot of $\partial_\rho F$ shows that it starts from 1 and goes to the value 2, the other plots show how fluxes of the gauge fields grow, approaching constant values at large r.

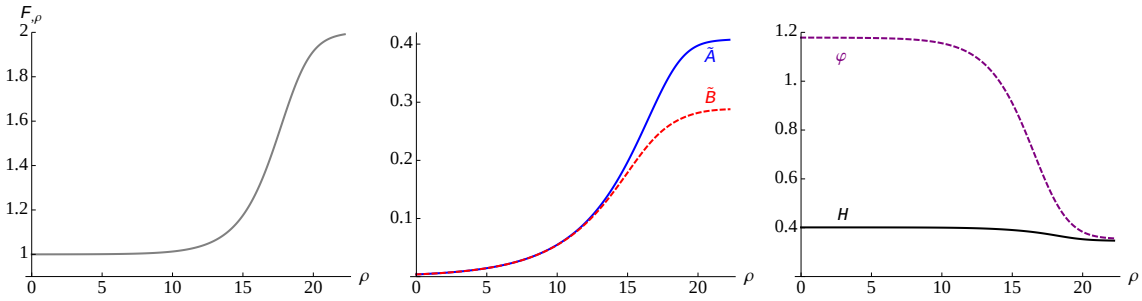

Figure 2.6: Solution interpolating between AdS_3 and $\widetilde{\text{Li}}_3$ with $z = 2$, with $Q^2 = \frac{2}{3}$.

Flows from AdS_5

The flows which approach the asymptotically AdS_5 solution in the UV and end at AdS_3 or Li_3 in IR are easy to construct numerically, integrating outward from the IR. We find that the endpoint of the flow from AdS_5 is uniquely determined by the pair $\{Q, \lambda\}$, where λ is the coefficient in front of the slow fall-off mode in the expansion of the 5D dilaton field near the AdS_5 solution,

$$\varphi = \frac{1}{\sqrt{2}} + \frac{\lambda}{r^2} \ln r + \frac{\eta}{r^2} + \dots . \tag{2.3.31}$$

On the field theory side, λ corresponds to the source of an operator $\mathcal{O}_2$, as discussed in Maldacena and Nunez [57], however, for future reference we note that the deformation parameter used there, $\bar{\lambda}$, is related to our λ via

$$\bar{\lambda} = \frac{\sqrt{2}}{3} e^{2h_0} \lambda \tag{2.3.32}$$

This operator (together with the curvature of the $\mathcal{H}_2$ and the flux Q) induces the RG flow on the field theory side. As noted previously, the fact that these flows only involve turning on a source for this operator implies that the flows to Lifshitz spacetimes break the Lorentz invariance spontaneously.

The values of $\bar{\lambda}$ for which we flow to the different solutions are presented schematically in Figure 2.7. If we move along the AdS_3 (grey) line in the direction of increasing of Q, then the corresponding value of $\bar{\lambda}$ is also increasing. For $Q = 0$ $\bar{\lambda} = 0$,

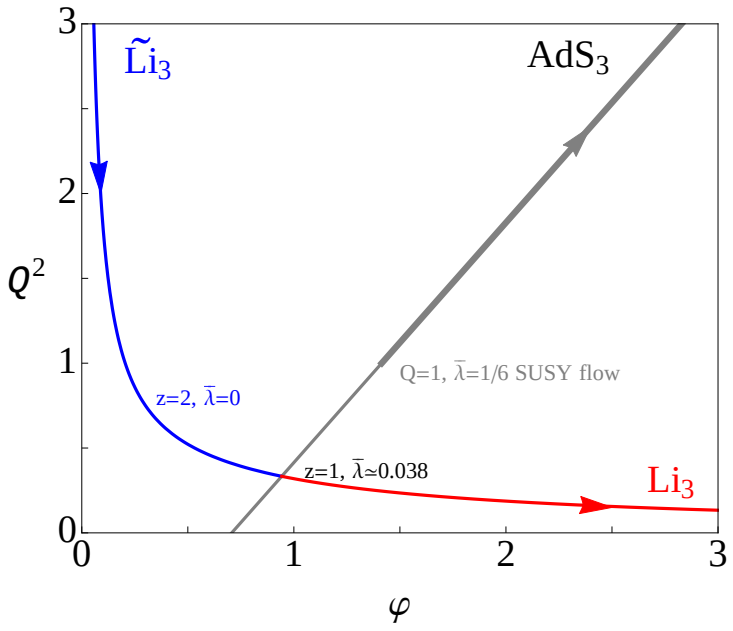

Figure 2.7: Plots of AdS$_3$, $\widetilde{Li_3}$ and Li$_3$ solutions, indicating the corresponding value of $\bar{\lambda}$ in the asymptotically AdS$_5$ UV region in the flow solutions. The arrows indicate the direction of increasing $\bar{\lambda}$.

while for $Q = 1$ $\bar{\lambda} = \frac{1}{6}$; this latter value corresponds to the supersymmetric flow of [57]. If we move along the $\widetilde{Li_3}$ (blue) line up (in the direction of increasing Q and also increasing z), then the corresponding value of $\bar{\lambda}$ is decreasing, in such a way that for $Q = \sqrt{\frac{2}{3}}$ $(z = 2)$ $\bar{\lambda} = 0$.[1] Above this point $\bar{\lambda} < 0$. If we move along the Li$_3$ (red) line down (in the direction of decreasing Q, but increasing z), then the corresponding value of $\bar{\lambda}$ is increasing. Numerically, $\bar{\lambda} \to \frac{1}{6}$ as $z \to 2$ $(Q \to 0)$. We will discuss the field theoretic implications of the values of $\bar{\lambda}$ in the next section, but first comment on stability of the supergravity solutions.

2.3.3 Stability to condensation of supergravity fields

In the analysis of the linearized perturbations, we encountered some complex eigenvalues for some values of parameters, as in the analysis of the IIA case in [44]. For a decoupled scalar, such complex eigenvalues appear when the scalar violates the

[1] This is a numerical result, but it seems very reasonable, because in Lifshitz theories, a theory with $z = 2$ always was a special case.

Breitenlohner-Freedman bound, and there is then an instability to condensation of the scalar. We would expect that there will be a similar instability to condensation of the modes with complex eigenvalues in our case, although we will not attempt to carry out a time-dependent analysis to demonstrate this instability explicitly. Certainly the appearance of the complex eigenvalues obstructs the usual interpretation of the eigenvalue as the dimension of the corresponding operator in the field theory.

Also, it was noted in [64] that purely from a bulk spacetime perspective, when such complex eigenvalues appear for a scalar field there is no boundary condition which preserves the inner product which is invariant under the Lifshitz scaling isometry. Thus, we expect that in the cases with complex eigenvalues, we simply cannot choose boundary conditions such that our bulk solution is dual to an anisotropic scaling invariant field theory with a conserved inner product.

A nice field theory dual description of the fixed points with complex eigenvalues is thus unlikely to exist. This leaves as potentially interesting cases a range of the AdS_3 fixed points and a range of the untilded Li_3 fixed points with z near 2. This is an interesting range of Lifshitz solutions, and an improvement of the IIA case, where the Lifshitz solutions with no complex eigenvalues were at larger values of z.

2.4 The UV field theory

Our interest in studying flows, particularly those from asymptotically AdS_5 spacetimes, is mainly that they might help us to understand the field theories dual to these spacetimes. In this section, we consider some stability issues that can obstruct our ability to learn about the field theory from these flows. For field theory on a flat space, the scalars in the adjoint of $SU(N)$ have flat directions corresponding to the Coulomb branch. However in our class of spacetimes, we are compactifying two of the directions on which the field theory lives on a space of negative curvature. One might therefore expect the curvature coupling of the field theory scalars to produce a runaway instability for the diagonal components of these scalar matrices. From the bulk spacetime point of view, the diagonal components of the scalars are positions of branes, so this runaway would be a brane nucleation instability.

The story is of course more complicated, because in addition to the negative curvature space, we are introducing a flux $F^{(3)}_{y_1 y_2} = q/y_2^2$ on these directions, and also adding a source for the operator dual to the 5D dilaton ϕ. In the supersymmetric case analysed in [57], the effects of these deformations combine to preserve a twisted supersymmetry. The whole RG flow is supersymmetric, so on the field theory side the deformation of $\mathcal{N} = 4$ SYM is preserving some supersymmetry. One would then not expect the field theory to have a scalar instability, and indeed the terms combine to leave us with flat directions for some of the field theory scalars [57]. Similarly, from the bulk perspective, the addition of the flux and deformation of the S^5 (encoded in the 5D dilaton) will modify both the DBI and WZ components of a probe brane action, which could stabilise the brane.

We now present analyses from both points of view – using the Maldacena-Nunez approach to contruct the field theory, then confirming our results by a direct probe brane calculation.

2.4.1 UV field theory analysis

Let us analyze the field theory deformation for our general family of flows. The field theory includes six real scalars, transforming in the vector representation of the $SO(6)$ R-symmetry group and the adjoint of $SU(N)$. The consistent truncation we work with preserves an $SU(2) \times U(1)$ subgroup of $SO(6)$, so it is convenient to organize the scalars into three complex scalar fields $\mathcal{W}_1, \mathcal{W}_2$ and $\mathcal{W}_3$, where $\mathcal{W}_1$ and $\mathcal{W}_2$ transform under the $SU(2)$ and $\mathcal{W}_3$ transforms under the $U(1)$. The bulk 5D dilaton ϕ corresponds to an operator $\mathcal{O}_2$ which is a symmetric traceless combination of the scalars transforming in the **20** of $SO(6)$ [57],

$$\mathcal{O}_2 = Tr\left\{\frac{2}{3}|\mathcal{W}_3|^2 - \frac{1}{3}\left(|\mathcal{W}_1|^2 + |\mathcal{W}_2|^2\right)\right\}. \tag{2.4.33}$$

The deformation we consider has a negative curvature in the y_1, y_2 directions and a flux of the τ^3 component of the $SU(2)$ gauge field through those directions, and a source for $\mathcal{O}_2$ with a coefficient $\bar{\lambda}$. This corresponds to a deformation of the scalar

part of the field theory Lagrangian to

$$S = \int d^4x \left\{ \frac{1}{2} |D_\mu \mathcal{W}_1|^2 + \frac{1}{2} |D_\mu \mathcal{W}_2|^2 + \frac{1}{2} |\partial_\mu \mathcal{W}_3|^2 - \frac{R}{12} \sum_i |\mathcal{W}_i|^2 + \frac{3}{4} \bar{\lambda} R \mathcal{O}_2 \right\}, \tag{2.4.34}$$

where $D_\mu = \partial_\mu + \mathrm{i}A_\mu$ is the gauge-covariant derivative with respect to the component of the $SU(2)$ gauge field we turn on, and R is the Ricci scalar of the two dimensional hyperbolic spacetime (note $R = -|R| < 0$). Substituting in $A_{y_1} = q/y_2$, we have

$$\begin{aligned} S = \int d^4x \Bigg\{ & \frac{1}{2} \sum_i |\partial_\mu \mathcal{W}_i|^2 - |R| \left(\frac{\bar{\lambda}}{2} - \frac{1}{12} \right) |\mathcal{W}_3|^2 \\ & - |R| \left[\frac{Q^2}{8} - \left(\frac{\bar{\lambda}}{4} + \frac{1}{12} \right) \right] \left(|\mathcal{W}_1|^2 + |\mathcal{W}_2|^2 \right) \Bigg\}, \end{aligned} \tag{2.4.35}$$

where the normalization of the Q^2 term and the coefficient of $\bar{\lambda}$ have been fixed by reference to the supersymmetric case, which corresponds to $\bar{\lambda} = \frac{1}{6}$ and $Q = 1$.

2.4.2 Probe brane calculation

We now want to explore this field theory from the bulk perspective. Holographically, R-symmetry scalar fields correspond to inserting a brane with its four infinite dimensions parallel to an r =const. section of the 5D space, and at a given position on the (possibly distorted) S^5. The effective action of such a probe brane is given by the sum of a geometric DBI term, and a topological WZ term:

$$S = -T_3 g_s^{-1} \int e^{-\Phi} \sqrt{-\det[\gamma_{AB} + \mathtt{F}_{AB}]} d^4\zeta + T_3 \int C_4 \tag{2.4.36}$$

where ζ^A are the intrinsic coordinates on the brane worldvolume; γ_{AB} the induced metric; $\mathtt{F}_{AB} = \mathtt{B}_{AB} + 2\pi\alpha' F_{AB}$, the pullback of the 2-form field to the brane (zero in this background) and worldvolume gauge field (which we also set to zero); finally, C_4 is the pullback of the 4-form gauge potential onto the brane.

In order to compute this action, we first need the background geometry. The twisting introduced previously corresponds to a distortion of the S^5 in the reduction of the IIB SUGRA as described in [61][2]. Lifting the 5D solutions of (2.2.6,2.2.7) to

[2]Note that there are some factors of two between the variables used here and those of [61]: $(\phi)_{LPT} = \phi/2$, $(g_i)_{LPT} = g_i/2$, and $A_{LPT} = 2A$, where A stands for either the U(1) or SO(3) gauge field.

10D[3], and writing

$$\begin{aligned} S &= \sin\chi \qquad \Delta = \xi^2 S^2 + \xi^{-1} C^2 \\ C &= \cos\chi \qquad U = \xi S^2 + \xi^{-2} C^2 + \xi \end{aligned} \tag{2.4.37}$$

gives[4] [40]:

$$\begin{aligned} ds^2 = \Delta^{\frac{1}{2}} \left(e^{2F} dt^2 - r^2 dx^2 - e^{2d} \frac{dr^2}{r^2} - e^{2h} \frac{dy_1^2 + dy_2^2}{y_2^2} \right) \\ - \xi^{-1} \Delta^{-\frac{1}{2}} \left[\Delta d\chi^2 + \xi^{-1} S^2 \left(d\eta - 2\mathcal{A} \right) + \frac{1}{4} \xi^2 C^2 \sum_i \left(h^{(i)} \right)^2 \right] \end{aligned} \tag{2.4.38}$$

$$\begin{aligned} \mathbf{F_5} = 2\, U \epsilon_5 + 3\, S\, C\, \xi^{-1} \star_5 d\xi \wedge d\chi + \frac{C^2}{2\sqrt{2}} \xi^2 \star_5 F_2^{(3)} \wedge \sigma^{(1)} \wedge \sigma^{(2)} \\ - \frac{S\, C}{\sqrt{2}} \xi^2 \star_5 F_2^{(3)} \wedge h^{(3)} \wedge d\chi - 2SC\xi^{-4} \star_5 \mathcal{F}_2 \wedge d\chi \wedge \left(d\eta - 2\mathcal{A} \right), \end{aligned} \tag{2.4.39}$$

the other form fields, the string dilaton and axion vanish. Here, $h^{(i)}$ are the left invariant forms on S^3 ($\sigma^{(i)}$) modified by the $SO(3)$ gauge fields:

$$h^{(i)} = \sigma^{(i)} - 2\sqrt{2}\, A^{(i)}\,. \tag{2.4.40}$$

For constant ξ, we may reparametrize the squashed S^5 as

$$\begin{aligned} W_1 &= \xi \cos\chi \, \cos\frac{\theta}{2} \, e^{\mathrm{i}\frac{\phi+\psi}{2}} \\ W_2 &= \xi \cos\chi \, \sin\frac{\theta}{2} \, e^{\mathrm{i}\frac{\phi-\psi}{2}} \\ W_3 &= \xi^{-1/2} \sin\chi \, e^{\mathrm{i}\eta} \end{aligned} \tag{2.4.41}$$

which, together with the obvious definitions of the gauge covariant differentiation for $W_{1,2}$ and W_3 give the metric of the additional dimensions as

$$ds_5 = -\xi^{-1} \Delta^{-\frac{1}{2}} \left[\, |DW_1|^2 + |DW_2|^2 + |\mathcal{D}W_3|^2 \, \right] \tag{2.4.42}$$

As ξ changes from unity, we can see how the S^5 becomes distorted while maintaining an $SO(3) \times U(1)$ symmetry. Our 5D dilaton is thus a shape modulus for the S^5. Since $\xi \equiv 1$ for AdS_5, it is now transparent how to deal with the degrees of freedom of the probe brane: we simply replace the 'ξ' in (2.4.41) with a radial

[3]Indeed, the uplift of the AdS flows can be generalised in the context of solutions in $D = 10, 11$ dual to $\mathcal{N} = 2$ SCFT's, as studied in [67, 68]. (We thank Jerome Gauntlett for pointing this out.)

[4]We have set $g_1 = g_2/\sqrt{2} = 2$ to match the conventions of [57]

variable $r(\zeta)$, and allow the remaining angular degrees of freedom of the brane to also depend on the brane coordinates ζ^A. We will then expand the action for a slowly moving brane at large r in the asymptotic AdS_5 solution.

We start with the DBI part of the action

$$S_{DBI} \propto -\int d^4\zeta \sqrt{-\det \gamma_{AB}} \tag{2.4.43}$$

where

$$\gamma_{AB} = \frac{\partial X^a}{\partial \zeta^A}\frac{\partial X^b}{\partial \zeta^B} g_{ab} \tag{2.4.44}$$

with $X^\mu = [t, x, r(\zeta), y_1, y_2, \chi(\zeta), \eta(\zeta), \theta(\zeta), \phi(\zeta), \psi(\zeta)]$ being the brane's spacetime coordinates in terms of the intrinsic coordinates ζ, for which we choose the gauge $\zeta^A = (t, x, y_1, y_2)$. Thus

$$\gamma_{AB} = \gamma^0_{AB} - \frac{1}{r^2}\left[D_A W_1 \overline{D_B W_1} + D_A W_2 \overline{D_B W_2} + \mathcal{D}_A W_3 \overline{\mathcal{D}_B W_3} \right] \tag{2.4.45}$$

where $\gamma^0_{AB} = \Delta^{\frac{1}{2}} \cdot \mathrm{diag}\left(e^{2F}, -r^2, -\frac{e^{2h}}{y_2^2}, -\frac{e^{2h}}{y_2^2}\right)$, the $1/r^2$ factor arising because we have replaced ξ with r in (2.4.41). Hence,

$$\sqrt{-\det \gamma_{AB}} \simeq \sqrt{-\det \gamma^0_{ab}} \left(1 - \frac{1}{2r^2}\gamma^{0AB} D_A W_i \overline{D_B W_i}\right) \tag{2.4.46}$$

(where we understand the covariant derivative in the sum to be the one relevant to the particular W_i). Since we are only interested in the leading order behaviour as we change W_i, we only require γ^{0AB} to leading order in W_i, i.e. at the AdS_5 limit:

$$\gamma^{0AB}\big|_{AdS5} = \frac{1}{r^2} \cdot \mathrm{diag}\left(1, -1, -y_2^2 e^{-2h_0}, -y_2^2 e^{-2h_0}\right) \tag{2.4.47}$$

hence

$$S_{DBI} \propto -\int d^4\zeta \, \frac{r\Delta}{y_2^2} e^{F+2h} \left(1 - \frac{1}{2r^4}\sum_i |D_\mu W_i|^2\right) \tag{2.4.48}$$

For the WZ term, note that although the 4-form potential is rather involved for a general flow, we only require the leading order part parallel to the probe brane worldvolume, which can be found by integrating the U function in (2.4.37). Putting this together, we see that

$$S_{\text{eff}} \sim \int d^4\zeta \left\{ -\Delta(\xi,\chi) \cdot r e^{F+2h} \left(1 - \frac{1}{2r^4}\sum_i |D_\mu W_i|^2\right) + 2\int e^{F+d+2h} U(\xi,\chi) dr \right\} \tag{2.4.49}$$

We now expand this action in the asymptotic AdS_5 region, but with one difference to the procedure followed in §2.3.1: we need to consider a linear expansion in the case of *finite* volume of the 2D hyperbolic space, i.e. finite h_0. The full asymptotic solution together with corrected expansion up to r^{-2} order reads

$$\begin{aligned} F &= \ln r \ , & d &= -\frac{e^{-2h_0}}{6r^2} \ , \\ h &= \ln r + h_0 + \frac{e^{-2h_0}}{4r^2} \ , & \xi &= 1 + \frac{\sqrt{2}}{3}\frac{\lambda \ln r}{r^2} + \frac{\sqrt{2}}{3}\frac{\mu}{r^2} \ . \end{aligned} \tag{2.4.50}$$

Substituting these expressions into (2.4.49), and performing the integral for U, we see that all terms proportional to μ and $\lambda \ln r$ cancel leaving

$$S_{\text{eff}} \sim \int d^4\zeta \left\{ \frac{1}{2} e^{2h_0} \sum_i |D_\mu W_i|^2 - \frac{\lambda}{3\sqrt{2}} e^{2h_0} \left(2S^2 - C^2\right) r^2 + \frac{1}{6} r^2 \right\} \tag{2.4.51}$$

It is easy to see that we can identify

$$\left(2S^2 - C^2\right) r^2 = 3\mathcal{O}_2 \ , \quad r^2 = \sum_i |W_i|^2 \tag{2.4.52}$$

and noting the relation between our λ and $\bar{\lambda}$, (2.3.32), as well as the curvature of the 2D hyperbolic space, $R = -2e^{-2h_0}$, we get

$$S_{\text{eff}} \propto \int d^4\zeta \ e^{2h_0} \left\{ \frac{1}{2} \sum_i |D_\mu W_i|^2 - \frac{3}{4}\bar{\lambda} R \mathcal{O}_2 + \frac{1}{12} R \sum_i |W_i|^2 \right\} \tag{2.4.53}$$

which coincides with the expression for the field theory effective action (2.4.34) precisely.

2.4.3 Stability and Lifshitz dual field theories

Having obtained the field theory action, (2.4.35), we now analyse the scalar stability. In order to have stable potential for the $\mathcal{W}_3$ field, we should have

$$\frac{1}{2}\bar{\lambda} - \frac{1}{12} \geq 0 \Rightarrow \bar{\lambda} \geq \frac{1}{6}, \tag{2.4.54}$$

While for the twisted fields $\mathcal{W}_1$ and $\mathcal{W}_2$ we should have

$$\frac{Q^2}{8} - \left(\frac{1}{4}\bar{\lambda} + \frac{1}{12}\right) \geq 0. \tag{2.4.55}$$

For the supersymmetric case, both these bounds are automatically saturated (by our choice of normalization in matching operator sources to bulk modes), reproducing the flat directions of [57].

For AdS_3 solutions we know that in the AdS_3 region $Q^2 = \varphi\sqrt{2} - 1$, and, by numerical analysis we determine $\bar{\lambda}$ as a function of the value of φ in the AdS_3 region. The stability criterion for the $\mathcal{W}_3$ field, $\bar{\lambda} \geq 1/6$, which corresponds to $\varphi \geq \sqrt{2}$. Meanwhile, (2.4.55) provides an upper bound on φ, as $\bar{\lambda}$ increases more rapidly than Q^2 along the family of AdS_3 flows. Numerically, we find that the AdS_3 solutions with

$$\varphi \in \left[\sqrt{2}, \sim 3.26\right] \tag{2.4.56}$$

result from an RG flow from a field theory in the UV where the field theory deformation is not introducing a field theory scalar instability. The corresponding region for the charge Q is

$$Q^2 \in [1, \sim 3.61] \ . \tag{2.4.57}$$

Disappointingly, for the Lifshitz solutions we found numerically that none of the solutions involve flows with $\bar{\lambda} \geq 1/6$. The flows on the untilded branch do approach $\bar{\lambda} \to 1/6$ when $z \to 2$, but $Q \to 0$ in this limit, so even if we are nearly satisfying the stability condition for $\mathcal{W}_3$ in the limit, the condition for $\mathcal{W}_1$ and $\mathcal{W}_2$ is badly violated. Thus, none of our Lifshitz solutions is obtained as an RG flow from a stable UV field theory, and we cannot use these RG flows to define the field theory dual to the IR fixed points.

This UV instability does not necessarily imply that the IR fixed points are ill-defined, just that this approach to constructing them has failed. There are solutions on the Li_3 branch for which we did not have evidence of a supergravity instability which are still candidates for having a dual field theory; but we will have to look elsewhere for a top-down definition of this field theory.

Chapter 3

Vacuum metastability with black holes

In this chapter, based on [70], we will describe tunnelling in quantum field theory with gravity beyond its homogeneous approximation, described in the introduction. In recent work [87] Gregory with collaborators looked at the effect of gravitational inhomogeneities acting as seeds of cosmological phase transitions in de Sitter space (see also earlier works by Hiscock and Berezin [88, 89]). They found that the decay rates were considerably enhanced by the presence of black holes. Following their work, Sasaki and Yeom [90] have investigated the unitarity implications of bubble nucleation in Schwarzschild-Anti de Sitter spacetimes (see also [91] for a discussion of vacuum stability in the early universe). In this chapter we extend the previous results of [87], to cover all possible gravitational nucleation processes.

We follow the approach of Coleman and de Luccia [14], and assume that the nucleation probability for a bubble of the new phase is given schematically by

$$\Gamma = Ae^{-B}, \tag{3.0.1}$$

where B is the action of an imaginary-time solution to the Einstein and scalar field equations, or instanton, which approaches the false vacuum at large distances. However, unlike Coleman and de Luccia, we consider a spherically symmetric bubble on a black hole background. The nucleation process typically requires an instanton that has a conical singularity at the black hole horizon. Analogous instantons were con-

sidered before in [92, 93] and fall within the generalised type introduced by Hawking and Turok [94, 95]. We show that the nucleation probability is well-defined. An alternative interpretation of (3.0.1) and the instanton has been given in [96].

The vacuum decay process is based on a static black hole, in which a bubble nucleates outside the black hole and either completely replaces the black hole with a bubble of true vacuum expanding outwards, or nucleates a static bubble leaving a remnant black hole surrounded by true vacuum. This latter solution is not stable, and small fluctuations will lead it to either expand as with the first situation completing the phase transition, or to collapse back inwards leaving the initial state unchanged. Of course, this description does not explicitly account for any time dependence of the black hole due to Hawking evaporation, however, we can apply the same argument as that employed for black hole particle production, namely, we consider only vacuum decay precesses which have timescales short compared to the evaporation rate. In other words, we have some confidence in our results when the vacuum decay rate exceeds the mass decay rate of the black hole. (The effects of Hawking radiation on tunnelling rates have been investigated in [97, 98]).

The outline of the chapter is as follows. We first review then extend the thin wall instanton method in §3.1, directly calculating the instanton action in the thin wall limit as a function of wall trajectory and black holes masses. In §3.3 we describe the solutions for the instantons and discuss the preferred decay process for a general seed mass black hole (including charge). Finally, in §3.4, we discuss possible extensions to higher dimensions and collider black holes. Note we use units in which $\hbar = c = 1$, and use the reduced Planck mass $M_p^2 = 1/(8\pi G)$.

3.1 Thin-wall bubbles

In this section, we describe how to construct a thin wall instanton, along the lines of Coleman et al. [12–14], but with the difference that we suppose that an inhomogeneity is present. We apply Israel's thin wall techniques [108] to the bubble wall, and describe the inhomogeneity by a black hole.

3.1.1 Constructing the instanton

The physical process of vacuum decay with an inhomogeneity can be represented gravitationally by a Euclidean solution with two 'Schwarzschild' bulks which have different cosmological constants separated by a thin wall with constant tension (for a general proof of this result in the context of braneworlds, see [109, 110]). On each side of the wall the geometry has the form

$$ds^2 = f(r)_\pm d\tau_\pm^2 + \frac{dr^2}{f(r)_\pm} + r^2 d\Omega_2^2, \qquad f_\pm(r) \equiv 1 - \frac{2GM_\pm}{r} - \frac{\Lambda_\pm r^2}{3}, \tag{3.1.2}$$

where $\tau_\pm$ are the different time coordinates on each side of the wall, and the wall, or boundary of each bulk, is parametrised by some trajectory $r = R(\lambda)$ (the angular θ and ϕ coordinates are the same on each side). The Israel junction conditions [108] relate the solution inside the bubble with mass M_- and cosmological constant Λ_-, to the solution outside the bubble with mass M_+ and cosmological constant Λ_+. Since the bubble exterior is in the false vacuum, we have $\Lambda_+ > \Lambda_-$. ($\Lambda_+ < \Lambda_-$ was discussed by Aguirre and Johnson [111, 112], and the case $M_- = 0$ has been discussed by Sasaki and Yeom [90]). In general, the bubble will follow a time-dependent trajectory representing a reflection, or bounce, which could be described by local coordinates on each side of the wall:

$$X_\pm^a = (t_\pm(\lambda), r_\pm(\lambda), \theta, \phi) \tag{3.1.3}$$

we choose to parametrize the wall trajectory by the proper time of a comoving observer, i.e. λ is chosen so that

$$f_\pm \dot{\tau}_\pm^2 + \frac{\dot{R}^2}{f_\pm} = 1, \tag{3.1.4}$$

here dots denote derivatives with respect to λ and $r_+ = r_- = R(\lambda)$ along the wall. We will use normal forms that point towards increasing r:

$$n_\pm = \dot{\tau}_\pm \, dr_\pm - \dot{r} \, d\tau_\pm \tag{3.1.5}$$

and also take $\dot{\tau}_\pm \geq 0$ for orientability (see also [90]). By choosing the intrinsic coordinates on the wall $\xi^A = (\lambda, \theta, \phi)$, we can introduce the induced metric h_{ab}, which the wall inherits from the spacetime

$$ds^2 = -d\lambda^2 + R^2(\lambda) \left[d\theta^2 + \sin^2\theta d\phi^2 \right] \tag{3.1.6}$$

Using (3.1.5) we can construct the extrinsic curvature of each side of the wall:

$$K_{\pm AB} = X^a_{\pm,A} X^b_{\pm,B} \nabla_a n_{\pm b} \,. \tag{3.1.7}$$

Israel junction conditions [108] then provide us the relation between the surface stress tensor of the wall S_{ab} and the geometry of its embedding measured via a jump in the extrinsic curvature across the wall:

$$\Delta K_{ab} - \Delta K h_{ab} = -8\pi G S_{ab} \tag{3.1.8}$$

here $\Delta K_{ab} = K_{+ab} - K_{-ab}$ and analogously for the trace $K = K_{ab} h^{ab}$. By taking the trace one can rewrite (3.1.8):

$$\Delta K_{ab} = -8\pi G \left(S_{ab} - \frac{1}{2} h_{ab} S \right) \tag{3.1.9}$$

and introducing the tension of the wall σ, we have $S_{ab} = \sigma h_{ab}$, and this equation reduces to

$$f_+ \left[R(\lambda) \right] \dot{t}_+ - f_- \left[R(\lambda) \right] \dot{t}_- = -4\pi G \sigma R. \tag{3.1.10}$$

The combination of surface tension and Newton's constant recurs so frequently that for clarity we define

$$\bar{\sigma} = 2\pi G \sigma. \tag{3.1.11}$$

To find solutions to the equations of motion, first note that the junction condition (3.1.10) implies

$$f_\pm \dot{\tau}_\pm = \left(f_\pm - \dot{R}^2 \right)^{1/2} = \frac{f_- - f_+}{4\bar{\sigma} R} \mp \bar{\sigma} R \,. \tag{3.1.12}$$

It is convenient to rewrite this as an equation for $\dot{R}$ using the explicit forms for $f_\pm$

$$\dot{R}^2 = 1 - \left(\bar{\sigma}^2 + \frac{\bar{\Lambda}}{3} + \frac{(\Delta\Lambda)^2}{144\bar{\sigma}^2} \right) R^2 - \frac{2G}{R} \left(\bar{M} + \frac{\Delta M \Delta\Lambda}{24\bar{\sigma}^2} \right) - \frac{(G\Delta M)^2}{4R^4\bar{\sigma}^2}, \tag{3.1.13}$$

where $\Delta M = M_+ - M_-$ and $\bar{M} = (M_+ + M_-)/2$ with similar expressions for Λ.

Although this seems to be a more complex system than that considered in [87], in fact it is possible to rescale the variables so that the analysis is very nearly identical to that in [87]. To begin with, define

$$\ell^2 = \frac{3}{\Delta\Lambda}, \qquad \gamma = \frac{4\bar{\sigma}\ell^2}{1 + 4\bar{\sigma}^2\ell^2}, \qquad \alpha^2 = 1 + \frac{\Lambda_- \gamma^2}{3}, \tag{3.1.14}$$

and rescale the coordinates to $\tilde{R} = \alpha R/\gamma$, $\tilde{\tau} = \alpha\tau/\gamma$, $\tilde{\lambda} = \alpha\lambda/\gamma$. Then writing

$$k_1 = \frac{2\alpha G M_-}{\gamma} + \frac{(1-\alpha)\alpha G \Delta M}{\bar{\sigma}\gamma^2}, \quad k_2 = \frac{\alpha^2 G \Delta M}{2\bar{\sigma}\gamma^2}. \tag{3.1.15}$$

gives a Friedman-like equation for $\tilde{R}(\tilde{\lambda})$:

$$\left(\frac{d\tilde{R}}{d\tilde{\lambda}}\right)^2 = 1 - \left(\tilde{R} + \frac{k_2}{\tilde{R}^2}\right)^2 - \frac{k_1}{\tilde{R}} = -U(\tilde{R}) \tag{3.1.16}$$

together with equations for $\tilde{\tau}_\pm$. These equations with $\alpha = 1$ are precisely the system explored in [87].

The allowed parameter ranges for k_1 and k_2 are limited by requiring existence of a solution to $\dot{\tilde{R}}^2 + U(\tilde{R}) = 0$, where U is defined in (3.1.16), requiring positivity of the black hole masses, and positivity of the arrows of time on each side of the wall:

$$f_+ \frac{d\tilde{\tau}_+}{d\tilde{\lambda}} = \frac{k_2}{\tilde{R}^2} + \frac{\tilde{R}}{\alpha}(1 - 2\bar{\sigma}\gamma) \tag{3.1.17}$$

$$f_- \frac{d\tilde{\tau}_-}{d\tilde{\lambda}} = \frac{k_2}{\tilde{R}^2} + \frac{\tilde{R}}{\alpha} \tag{3.1.18}$$

where

$$\begin{aligned} f_+ &= 1 - \frac{k_1}{\tilde{R}} - \frac{2k_2}{\alpha\tilde{R}}\left(\alpha - (1 - 2\bar{\sigma}\gamma)\right) - \frac{\tilde{R}^2}{\alpha^2}\left[\alpha^2 - (1 - 2\bar{\sigma}\gamma)^2\right] \\ f_- &= 1 - \frac{k_1}{\tilde{R}} + \frac{2k_2}{\alpha\tilde{R}}(1-\alpha) + \frac{\tilde{R}^2}{\alpha^2}(1-\alpha^2)\,. \end{aligned} \tag{3.1.19}$$

The first requirement is algebraically identical to the constraint discussed in [87] (although the expression given there in the appendix was not correct). Simultaneously requiring $U = U' = 0$ and eliminating $\tilde{R}_*$ gives an upper limit $k_1 \leq k_1^*$, the correct expression for which is:

$$\begin{aligned} k_1^* = \frac{2}{9}\Bigg[1 + 81k_2^2 - \left(-1 - 5(27k_2)^2 + \frac{(27k_2)^4}{2} + \frac{27k_2}{2}\left(4 + (27k_2)^2\right)^{3/2}\right)^{1/3} \\ + \left(1 + 5(27k_2)^2 - \frac{(27k_2)^4}{2} + \frac{27k_2}{2}\left(4 + (27k_2)^2\right)^{3/2}\right)^{1/3}\Bigg]^{1/2} - 2k_2 \end{aligned} \tag{3.1.20}$$

To get lower limits for k_1 we have to consider positivity of the black hole masses and the arrows of time on each side of the wall. These now depend on the sign and magnitude of the cosmological constants and are different to [87]. First, note the

relation between the physical quantities and the parameters:

$$\begin{aligned} GM_- &= \frac{\gamma}{2\alpha}\left(k_1 - 2\frac{(1-\alpha)}{\alpha}k_2\right) \\ GM_+ &= \frac{\gamma k_1}{2\alpha} + \frac{k_2\gamma}{\alpha^2}\left(\alpha - 1 + 2\bar{\sigma}\gamma\right) \\ \Lambda_- &= 3\frac{\alpha^2-1}{\gamma^2} \\ \Lambda_+ &= \Lambda_- - 12\bar{\sigma}^2 + 12\frac{\bar{\sigma}}{\gamma} = \frac{3}{\gamma^2}\left(\alpha^2 - (1-2\bar{\sigma}\gamma)^2\right) \end{aligned} \tag{3.1.21}$$

thus

$$\begin{aligned} GM_- \geq 0 \quad &\Rightarrow \qquad k_1 \geq 2(1-\alpha)\frac{k_2}{\alpha} \\ GM_+ \geq 0 \quad &\Rightarrow \qquad k_1 \geq 2(1-\alpha+2\bar{\sigma}\gamma)\frac{k_2}{\alpha} \end{aligned} \tag{3.1.22}$$

Secondly, the requirement of positivity of $\dot{\tilde{\tau}}_\pm$, of which the constraint on $\dot{\tilde{\tau}}_+$ is the stronger:

$$\frac{k_2}{\tilde{R}^2} + \frac{\tilde{R}}{\alpha}(1-2\bar{\sigma}\gamma) \geq 0 \tag{3.1.23}$$

saturated by $\tilde{R}_+^3 = \alpha k_2/(2\bar{\sigma}\gamma - 1)$. Clearly, if $2\bar{\sigma}\gamma > 1$, we must have $k_2 > 0$, and U must be positive with positive gradient at $\tilde{R}_+$. A brief manipulation of $U' > 0$ yields

$$\frac{\alpha^2}{(2\bar{\sigma}\gamma-1)^2} - 2 - \frac{k_1+2k_2}{2k_2}\frac{\alpha}{(2\bar{\sigma}\gamma-1)} \geq 0 \tag{3.1.24}$$

From this, we see that $\Lambda_+ > 0$, $2\bar{\sigma}\gamma \leq 1 + \alpha/2$, and k_1 is bounded below by $k_1^m = 2(1-\alpha)k_2/\alpha$ from (3.1.22).

Now consider $2\bar{\sigma}\gamma < 1/2$, for which $k_2 < 0$ is allowed. A similar argument to [87] gives

$$k_1 \geq k_1^m = \left|\frac{\alpha k_2}{2\bar{\sigma}\gamma - 1}\right|^{1/3} + \frac{k_2}{(1-2\bar{\sigma}\gamma)}\frac{(\alpha - 1 + 2\bar{\sigma}\gamma)^2}{\alpha} \tag{3.1.25}$$

for $k_2 \leq 0$, and once again, $k_1^m = 2(1-\alpha)k_2/\alpha$ for $k_2 > 0$. Note that neither of these bounds requires a particular sign for Λ_-.

Where the sign of Λ_- does make a difference is in the range of allowed k_2. The upper limit on k_2 is determined by $M_- = 0$ for the static bounce, i.e.

$$\alpha k_1^*[k_2] = 2(1-\alpha)k_2 \tag{3.1.26}$$

and a lower bound on k_2 is determined when the range of k_1 for $k_2 < 0$ closes off at negative k_2, which occurs when $U(\tilde{R}_+) = U'(\tilde{R}_+) = 0$:

$$\tilde{R}_+^4 - 3\tilde{R}_+^6 + 3k_2^2 = \tilde{R}_+^4 - \frac{\gamma^2 k_2^2}{(1-2\bar{\sigma}\gamma)^2}\Lambda_+ = 0 \tag{3.1.27}$$

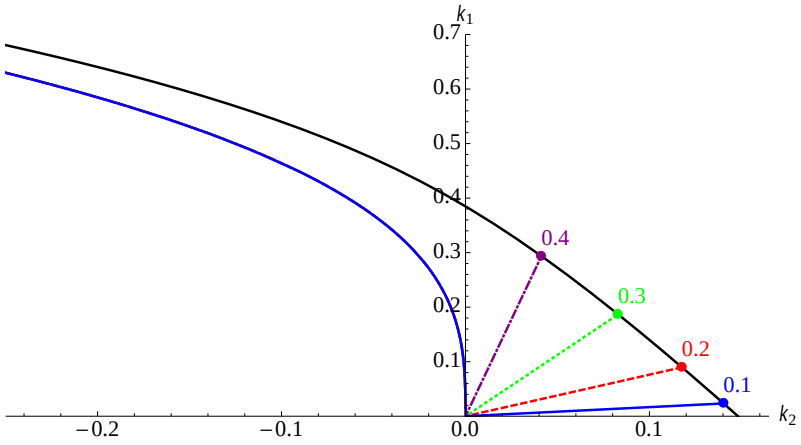

Figure 3.1: The allowed ranges for the parameters k_1 and k_2 with $\Lambda_+ = 0$. The upper bound on k_1 corresponds to stationary wall solutions. The lower bound on k_1 when $k_2 > 0$ is presented for a different values of $\bar{\sigma}\ell = 0.1,\ 0.2,\ 0.3,\ 0.4$ and corresponds to vanishing remnant mass $M_- = 0$. The two limits intersect at a point (k_{1C}, k_{2C}), which depends on the $\bar{\sigma}\ell$ and approaches $(0, 4/27)$ as $\bar{\sigma}\ell \to 0$. The strip of allowed k_1 continues to the left as $|k_2|^{1/3}$.

which is clearly inconsistent for $\Lambda_+ \leq 0$. For $\Lambda_+ > 0$, the range closes off at

$$k_{2,min} = \frac{\alpha^2(2\bar{\sigma}\gamma - 1)}{3\sqrt{3}[\alpha^2 - (1 - 2\bar{\sigma}\gamma)^2]^{3/2}} = \frac{\alpha^2(2\bar{\sigma}\gamma - 1)}{\gamma^3 \Lambda_+^{3/2}} \tag{3.1.28}$$

Note that for $\Lambda_+ < 0$, the range of k_1, while initially narrowing as k_2 becomes negative, eventually opens out, as the linear term in (3.1.25) becomes dominant. Thus large AdS black holes can tunnel to an even larger AdS black hole with a more negative cosmological constant.

An important special case, especially for the application to the Higgs vacuum, is an example with $\Lambda_+ = 0$, for which $\alpha = 1 - 2\bar{\sigma}\gamma$, and many of the expressions above simplify:

$$k_1^m = \begin{cases} (-k_2)^{1/3} & k_2 \leq 0 \\ \frac{2(1-\alpha)}{\alpha} k_2 & k_2 > 0 \end{cases} \tag{3.1.29}$$

and the range of k_2 is plotted in figure 3.1. Note that unlike the figure in [87], where the lower limit for k_1 was dependent on $\bar{\sigma}$ for negative but not positive k_2, in this case it is the lower limits for positive k_2 and not negative that depend on $\bar{\sigma}$.

3.1.2 Computing the action

To compute the action of the bounce, we need to compute the Euclidean action of the thin wall instanton:

$$\begin{aligned} I_E = &- \frac{1}{16\pi G}\int_{\mathcal{M}_+}\sqrt{g}(\mathcal{R}_+ - 2\Lambda_+) - \frac{1}{16\pi G}\int_{\mathcal{M}_-}\sqrt{g}(\mathcal{R}_- - 2\Lambda_-) \\ &+ \frac{1}{8\pi G}\int_{\partial\mathcal{M}_+}\sqrt{h}K_+ - \frac{1}{8\pi G}\int_{\partial\mathcal{M}_-}\sqrt{h}K_- + \int_{\mathcal{W}}\sigma\sqrt{h} \end{aligned} \tag{3.1.30}$$

and subtract the action of the background. In this expression, $\partial\mathcal{M}_\pm$ refers to the boundary induced by the wall – there may also be additional boundary or bulk terms required for renormalisation of the action (see below). Note that we have reversed the sign of the $\partial\mathcal{M}_-$ normal in the Gibbons-Hawking boundary term so that it agrees with the *outward* pointing normal of the Israel prescription. On each side of the wall in the bulk we have $\mathcal{R}_\pm = 4\Lambda_\pm$, and the Israel equations give $K_+ - K_- = -12\pi G\sigma$.

There are three parts to the computation of the action, $\mathcal{M}_-$, $\mathcal{M}_+$, and $\mathcal{W}$.

• $\mathcal{M}_-$

Integrating the bulk term for the "$-$" side of the wall has two contributions, one from the cosmological constant in the bulk volume, and a contribution from any conical deficit at the black hole event horizon, should one exist. A description of how to deal with conical deficits was given in an appendix of [87], essentially the deficit gives a contribution proportional to the horizon area times the deficit angle. Supposing that the periodicity of the Euclidean time coordinate, β, set by the wall solution, may not be the same as the natural horizon periodicity, $\beta_- = 4\pi r_h/(1-\Lambda_- r_h^2)$, this gives a contribution to the action from $\mathcal{M}_-$ of:

$$\begin{aligned} I_{\mathcal{M}_-} &= -\frac{\beta_- - \beta}{\beta_-}\frac{\mathcal{A}_-}{4G} - \frac{1}{4G}\int\frac{2\Lambda_-}{3}(R^3 - r_h^3)d\tau_- \\ &= -\frac{\mathcal{A}_-}{4G} + \frac{\beta}{4G}\left[\frac{\mathcal{A}_-}{\beta_-} + \frac{2\Lambda_- r_h^3}{3} - 2GM_-\right] + \frac{1}{4G}\int d\lambda R^2 f_-'\dot{\tau}_- \end{aligned} \tag{3.1.31}$$

Inserting the value of β_-, and taking into account the value of r_h, the term in square brackets is identically zero, and this contribution to the action does not explicitly depend on the periodicity or indeed any conical deficit angle.

• $\mathcal{M}_+$

The computation of the action of $\mathcal{M}_+$ is a little more involved, as different regularisation prescriptions are needed for the different asymptotics of (A)dS or flat spacetime.

For Schwarzschild de Sitter, the radial coordinate in the static patch has a finite range, and terminates at the cosmological horizon r_c, which has a natural periodicity $\beta_c = -4\pi r_c^2/(2GM_+ - 2\Lambda_+ r_c^3/3)$.

$$\begin{aligned} I_{\mathcal{M}_+} &= -\frac{(\beta_c - \beta)\mathcal{A}_c}{4G\beta_c} - \frac{1}{4G}\int \frac{2\Lambda_+}{3}(r_c^3 - R^3)d\tau_+ \\ &= -\frac{\mathcal{A}_c}{4G} + \frac{\beta}{4G}\left[\frac{\mathcal{A}_c}{\beta_c} - \frac{2\Lambda_+ r_c^3}{3} + 2GM_+\right] - \frac{1}{4G}\int d\lambda R^2 f'_+ \dot{\tau}_+ \end{aligned} \tag{3.1.32}$$

Once again, substituting the values of β_c and r_c demonstrates that the bracketed term vanishes. For future reference, we note the value of the background SDS action at arbitrary periodicity derived in [87]:

$$I_{ESDS} = -\frac{\mathcal{A}_c}{4G} - \frac{\mathcal{A}_+}{4G} \tag{3.1.33}$$

where $\mathcal{A}_+$ is the horizon area of the black hole of mass M_+. Note that this expression is $\beta-$independent as discussed in [87].

For Schwarzschild (and Schwarzschild-AdS) the range of the radial coordinate is now infinite, and we must perform a renormalization procedure. For Schwarzschild, there is no contribution from the bulk integral, and instead we consider an artificial boundary at large r_0, with a subtracted Gibbons-Hawking term so that flat space has zero action [113].

$$I_{\mathcal{M}_+} = \frac{1}{8\pi G}\int_{r=r_0} \sqrt{h}(K - K_0) = \frac{\beta M_+}{2} = \beta M_+ - \frac{1}{4G}\int d\lambda f'_+ R^2 \dot{\tau}_+ \tag{3.1.34}$$

Again for future reference, computing the background Euclidean Schwarzschild action at arbitrary periodicity (with the same background subtraction prescription) yields

$$I_{ESCH} = -\frac{\mathcal{A}_+}{4G} + \beta M_+ \tag{3.1.35}$$

inputting the value of $\beta_{SCH} = 8\pi G M_+$.

For AdS on the other hand, we must subtract off the divergent volume contribution [29] by again introducing a fiducial boundary at r_0, and subtracting a pure

AdS integral, which must have an adjusted time-periodicity so that the boundary manifolds at r_0 agree:

$$\beta_0 = \beta \frac{f_+^{1/2}}{(1-\Lambda_+ r_0^2/3)^{1/2}} \simeq \left(1 + \frac{3GM_+}{r_0^3 \Lambda}\right)\beta. \tag{3.1.36}$$

Thus

$$\begin{aligned} I_{\mathcal{M}_+} &= -\frac{1}{4G}\int d\tau \frac{2\Lambda_+}{3}(r_0^3 - R^3) + \frac{1}{4G}\int d\tau_0 \frac{2\Lambda_+}{3} r_0^3 \\ &= \beta M_+ - \frac{1}{4G}\int d\lambda f_+' R^2 \dot{\tau}_+ \end{aligned} \tag{3.1.37}$$

i.e. an identical result to the Schwarzschild case (3.1.34). Computing the background Euclidean Schwarzschild-AdS action at arbitrary periodicity we get

$$I_{ESADS} = -\frac{\mathcal{A}_+}{4G} + \beta M_+ \tag{3.1.38}$$

again, the same expression as for Schwarzschild, (3.1.35).

• $\mathcal{W}$

Finally, the contribution to the action from the wall has a particularly simple form as the Gibbons-Hawking boundary terms from the wall come in the combination of the Israel junction conditions. We therefore obtain

$$I_{\mathcal{W}} = \pm\frac{1}{8\pi G}\int_{\partial\mathcal{M}_\pm} \sqrt{h}K + \int_{\mathcal{W}} \sigma\sqrt{h} = -\int_{\mathcal{W}} \frac{\sigma}{2}\sqrt{h} = \frac{1}{2G}\int d\lambda\, R\,(f_+\dot{\tau}_+ - f_-\dot{\tau}_-) \tag{3.1.39}$$

having used $f_+\dot{\tau}_+ - f_-\dot{\tau}_- = -2\bar{\sigma}R$.

Putting all of these results together, we find that the action of the instanton solution is

$$I_E = -\frac{\mathcal{A}_-}{4G} + \frac{1}{2G}\int d\lambda\,[(R - 3GM_+)\dot{\tau}_+ - (R - 3GM_-)\dot{\tau}_-] + \begin{cases} \beta M_+ & \Lambda_+ \leq 0 \\ -\dfrac{\mathcal{A}_c}{4G} & \Lambda_+ > 0 \end{cases} \tag{3.1.40}$$

Thus the bounce action, given by subtracting the background Schwarzschild/S(A)dS action is:

$$B = \frac{\mathcal{A}_+}{4G} - \frac{\mathcal{A}_-}{4G} + \frac{1}{4G}\oint d\lambda \left\{\left(2Rf_+ - R^2 f_+'\right)\dot{\tau}_+ - \left(2Rf_- - R^2 f_-'\right)\dot{\tau}_-\right\} \tag{3.1.41}$$

This expression is the central result of this section, and is independent of any choice of periodicity of Euclidean time, and independent of the choices of cosmological constant on each side of the wall. It is in fact even valid when the black hole is charged, as we will consider in section 3.3.3.

3.2 Alternative bounce action calculation

In this section we present an alternative derivation of the general expression for the bounce action using the Hamiltonian approach presented in [87], and extend the result in some cases beyond the thin-wall limit. This approach allows more general inhomogeneous configurations, as long as if they are static.

We will evaluate the Euclidean action for gravity plus a scalar field, with Lagrangian $\mathcal{L}_m$, in an asymptotically AdS or flat spacetime. As in §3.1.2, we take the action on a sequence $\mathcal{M}_r$ of manifolds with boundary $\partial\mathcal{M}_r$ at r_0, and subtract the action of a similar sequence $\overline{\mathcal{M}}_r$ of Euclidean AdS manifolds with the same boundary $\partial\mathcal{M}_r$.

It is instructive to first consider the case where the Euclidean spacetime $\mathcal{M}$ is perfectly regular, with no conical singularities, and has a Killing vector, ∂_τ. We perform a foliation of $\mathcal{M}_r$ with a family of non-intersecting surfaces Σ_τ (assuming the global topology permits), with $0 < \tau < \beta$. The canonical decomposition of such foliations has been investigated by Hawking and Horowitz, [130]. In order to decompose the action, we use their identity

$$\mathcal{R} = {}^3\mathcal{R} - K^2 + K_{ab}^2 - 2\nabla_a(u^a\nabla_b u^b) + 2\nabla_b(u^a\nabla_a u^b), \tag{3.2.42}$$

where the vector u^μ is normal to Σ_τ and ${}^3\mathcal{R}$ is the Ricci-curvature of Σ_τ. The action therefore splits into bulk and boundary parts,

$$\begin{aligned} I_{\mathcal{M}_r} = &-\frac{1}{16\pi G}\int_0^\beta d\tau \int_{\Sigma_\tau} \left({}^3\mathcal{R} - K^2 + K_{ab}^2 + 16\pi G\mathcal{L}_m\right)\sqrt{g} \\ &+ \frac{1}{8\pi G}\int_{\partial\mathcal{M}_r} n_b u^a \nabla_a u^b \sqrt{h}. \end{aligned} \tag{3.2.43}$$

The bulk term expressed in terms of canonical momenta π^{ij} and π becomes

$$\frac{1}{16\pi G}\int_0^\beta d\tau \left[\int_{\Sigma_\tau} \left(\partial_\tau\gamma_{ij}\pi^{ij} + \partial_\tau\phi\,\pi - N\mathcal{H} - N^i\mathcal{H}_i\right)\sqrt{h}\right], \tag{3.2.44}$$

where $\mathcal{H}$ and $\mathcal{H}_i$ are the Hamiltonian and momentum constraints respectively. The field equations imply that $\mathcal{H} = \mathcal{H}_i = 0$, and furthermore the symmetry implies $\partial_\tau\phi = \partial_\tau\gamma_{ij} = 0$. Therefore only the boundary term in (3.2.43) survives.

To evaluate the boundary term, we use the fact that the metric is static and asymptotically AdS, therefore at large r we have

$$ds^2 = f(r)d\tau^2 + f(r)^{-1}dr^2 + r^2 d\Omega^2 \tag{3.2.45}$$

where $f = 1-2GM/r-\Lambda r^2/3$. For this metric $n_b u^a \nabla_a u^b = f^{-1/2} f'/2$, and subtracting the Euclidean AdS action from (3.2.43) we arrive at the following expression

$$I = \lim_{r\to\infty} \left(\frac{\beta r^2 f'}{4G} - \frac{\beta_0 r^2 f_0'}{4G} \right), \tag{3.2.46}$$

where β_0 and f_0' are the time-period and metric function of AdS space, and using (3.1.36) the Euclidean action (3.2.46) becomes,

$$I = \beta M. \tag{3.2.47}$$

If there is a horizon at $r = r_h$, then by properly treating the conical singularity as in [87], we get an additional area term contribution to the action

$$I = \beta M - \frac{1}{4G}\mathcal{A}_h. \tag{3.2.48}$$

This result generalises a previous result of Hawking and Horowitz, who found the same formula for the Euclidean action of static Einstein-matter solutions with $\Lambda = 0$ and no conical singularities [130]. The $\Lambda \to 0$ case can also be obtained using the Gibbons-Hawking subtraction procedure described in §3.1.2. The expression (3.2.48) is of course the same as (3.1.35, 3.1.38), but we have not assumed anywhere for the static case that the bubble is in the thin-wall limit.

Solutions with a moving bubble wall $(\tau(\lambda), R(\lambda))$ break the time-translation symmetry of the full space-time, but the canonical method can still be used if the wall is thin and the geometries on both sides of the bubble wall, $\mathcal{M}_\pm$, individually possess the Killing vector, ∂_τ. Along with the contributions from $\mathcal{M}_\pm$ and the wall, $\mathcal{W}$, we will have an additional contribution from the conical singularity which can be dealt with by the methods of [87]. The action splits into contributions from each of these parts

$$I_{\mathcal{M}_r} = I_- + I_+ + I_{\mathcal{W}} - \frac{\mathcal{A}_-}{4G}, \tag{3.2.49}$$

where $\mathcal{A}_-$ is the area of the black hole horizon in the interior of the bubble. In the thin wall limit $I_{\mathcal{W}} = \int_{\mathcal{W}} \sigma$, and

$$I_\pm = -\frac{1}{16\pi G}\int_{\mathcal{M}_\pm} \mathcal{R}\sqrt{g} - \int_{\mathcal{M}_\pm} \mathcal{L}_m(g,\phi)\sqrt{g} + \frac{1}{8\pi G}\int_{\mathcal{W}} K_\pm \sqrt{h}, \tag{3.2.50}$$

Hence, performing the same decomposition as in the static case we can cancel the bulk contributions and are left only with the boundary terms

$$I_\pm = -\frac{1}{8\pi G}\int_{\mathcal{W}} K_\pm \sqrt{h} + \frac{1}{8\pi G}\int_{\partial\mathcal{M}_\pm} n_{\pm b} u^a \nabla_a u^b \sqrt{h}, \tag{3.2.51}$$

where $\partial\mathcal{M}_+$ now includes the wall and the large distance boundary $\partial\mathcal{M}_r$. Using Israel's junction condition to relate the extrinsic curvatures on each side of the wall to the tension, and inserting the normal to the wall (3.1.5), $n_b u^a \nabla_a u^b = \dot{\tau} f^{-1/2} f'/2$, we reach our final result

$$I = \beta M_+ - \frac{1}{4G}\mathcal{A}_- - \frac{1}{2}\int_{\mathcal{W}} \sigma\sqrt{h} - \frac{1}{16\pi G}\int_{\mathcal{W}} \left(f'_+\dot{\tau}_+ - f'_-\dot{\tau}_-\right)\sqrt{h}, \tag{3.2.52}$$

The expression for the bounce action B which governs the decay rate is obtained from I by subtracting the background action without the bubble, I_0:

$$I_0 = \beta M_+ - \frac{1}{4G}\mathcal{A}_+. \tag{3.2.53}$$

Therefore the tunnelling rate is determined by

$$B = \frac{\mathcal{A}_+}{4G} - \frac{\mathcal{A}_-}{4G} - \frac{1}{2}\int_{\mathcal{W}} \sigma\sqrt{h} - \frac{1}{16\pi G}\int_{\mathcal{W}} \left(f'_+\dot{\tau}_+ - f'_-\dot{\tau}_-\right)\sqrt{h}\,, \tag{3.2.54}$$

which is identical to (3.1.41), after using the relation $f_+\dot{\tau}_+ - f_-\dot{\tau}_- = -2\bar{\sigma}R$ for the wall integral.

3.3 Instanton solutions

In section 3.1.1 we derived the equations of motion for a bubble wall separating a region of true vacuum from the false vacuum, and derived the "master expression" (3.1.41) for the instanton action. In this section we discuss general properties of these solutions, and demonstrate how the action varies as we change the seed black hole mass and the wall tension. Rather than presenting absolute values of the bounce action, it proves useful instead to present a comparator to the 'Coleman de Luccia' action, by which we mean the bounce solution in the absence of any black holes (but with, for now, arbitrary cosmological constants).

3.3.1 Coleman de Luccia

The 'CDL' bubble wall satisfies (3.1.16)-(3.1.18) with $k_1 = k_2 = 0$, which are solved by

$$\begin{aligned} \tilde{R} &= \cos\tilde{\lambda} \\ \tilde{t}_- &= \frac{\alpha}{\sqrt{\alpha^2-1}}\arctan\sqrt{\alpha^2-1}\sin\tilde{\lambda} \quad ; \\ \tilde{t}_+ &= \frac{\alpha}{\sqrt{\alpha^2-(1-2\bar{\sigma}\gamma)^2}}\arctan\frac{\sqrt{\alpha^2-(1-2\bar{\sigma}\gamma)^2}}{(1-2\bar{\sigma}\gamma)}\sin\tilde{\lambda} \end{aligned} \tag{3.3.55}$$

and the action can be computed analytically as

$$B_{CDL} = -\frac{1}{2G}\int R(\dot{\tau}_+ - \dot{\tau}_-) = \frac{\pi}{G}\frac{\bar{\sigma}\gamma^3}{\alpha(\alpha+1)(\alpha+1-2\bar{\sigma}\gamma)} \xrightarrow{\Lambda_+=0} \frac{\pi\ell^2}{G}\frac{16(\bar{\sigma}\ell)^4}{(1-4\bar{\sigma}^2\ell^2)^2} \tag{3.3.56}$$

Note that by analytic continuation, these expressions include arbitrary $\Lambda_\pm$, for which $\alpha < 1$ or $1-2\bar{\sigma}\gamma$ are possible. In this special case the symmetry of the bubble solution has been raised from $O(3)$ to $O(4)$, and the result for the tunnelling rate agrees with explicitly $O(4)$ symmetric methods discussed in the first chapter.

3.3.2 The general instanton

The general bubble wall will have a black hole mass term on each side, and a general instanton will consist of a bubble trajectory between a minimum and maximum value of $\tilde{R}$. For fixed seed mass, M_+, there will be a range of allowed k_1 and k_2 (see (3.1.21)), and a corresponding range of values for the bounce action. By exploring the $\{k_1, k_2\}$ parameter space numerically and plotting the ratio of the bounce action to the CDL action, we can build up a qualitative understanding of the preferred instanton for vacuum decay.

For example, if $\Lambda_+ = 0$, $GM_+ = \gamma k_1/2\alpha$, and $GM_- = GM_+ - \gamma k_2(1-\alpha)/\alpha^2$. Referring to figure 3.1, we see there are two possibilities for the range of k_2, which is now a horizontal line in the k_1 plot: Either the maximal value of k_2 lies on the k_1^m branch with $GM_- = 0$, or on the static branch $k_1^*(k_2)$. The picture is similar for general Λ_+, but the constant GM_+ lines are now at an angle, and interpolate between the k_1^m curve at negative k_2 and either the k_1^m line at positive k_2 or the $k_1^*(k_2)$ curve. The crossover between the two possibilities occurs at $M_+ = M_C$, given

by the algebraic solution to

$$k_1^*(k_2) = \frac{2k_2}{\alpha}(1-\alpha) \tag{3.3.57}$$

when we have a static bubble with $GM_- = 0$. In either case, as k_2 drops, GM_- increases until the lower limit of k_2 is reached at negative k_2 on the $k_1^m(k_2)$ curve. By solving numerically for the wall trajectories we find that the action *increases* as k_2 drops. The preferred instanton therefore is the one with the maximally allowed value of k_2 consistent with the value of GM_+.

This qualitative picture remains true irrespective of the values of $\Lambda_\pm$: for seed mass $M_+ < M_C$, the dominant tunnelling process leaves behind a true vacuum region and removes the black hole. The tunnelling rate is always faster than the vacuum tunnelling rate for these instantons. The bounce action reaches a minimum at $M_+ = M_C$, where the bubble is static. For $M_+ > M_C$ the dominant tunnelling process is a static bubble with a remnant black hole being left behind. As the seed mass increases further, eventually the tunnelling rate becomes lower than the vacuum tunnelling rate. Exploring the instantons for general Λ's, we find that the ratio of B/B_{CDL} changes very little as the Λ's vary. In figure 3.2, we show how this dominant tunneling action varies as the values for the cosmological constants are changed. Since the change in B/B_{CDL} is minimal (and B_{CDL} itself is not varying much), we now restrict our discussion to the $\Lambda_+ = 0$ set-up where $\alpha = 1 - 2\bar{\sigma}\gamma$, and many of the formulae simplify.

Before discussing the general dominant tunneling process, we begin by considering the critical instanton where the static bubble tunnels and removes the seed black hole altogether. Although (3.3.57) in general is a complicated algebraic equation, for small $\bar{\sigma}\ell$ the various parameters can be expanded straightforwardly to give

$$k_{1C} \simeq \frac{64}{27}(\bar{\sigma}\ell)^2 = \frac{4}{9} - 3k_{2C} \quad \Rightarrow \quad \frac{GM_C}{\ell} \simeq \frac{128}{27}(\bar{\sigma}\ell)^3 \tag{3.3.58}$$

From (3.1.41), the action of a static bounce in general is

$$B = \frac{\mathcal{A}_+}{4G} - \frac{\mathcal{A}_-}{4G} = 4\pi G M_+^2 - \pi G \left(\frac{\ell}{G}\right)^{4/3} (\mu_+^{1/3} - \mu_-^{1/3})^2, \tag{3.3.59}$$

where

$$G\mu_\pm = \sqrt{G^2 M_-^2 + \frac{\ell^2}{27}} \pm \frac{GM_-}{\ell} \tag{3.3.60}$$

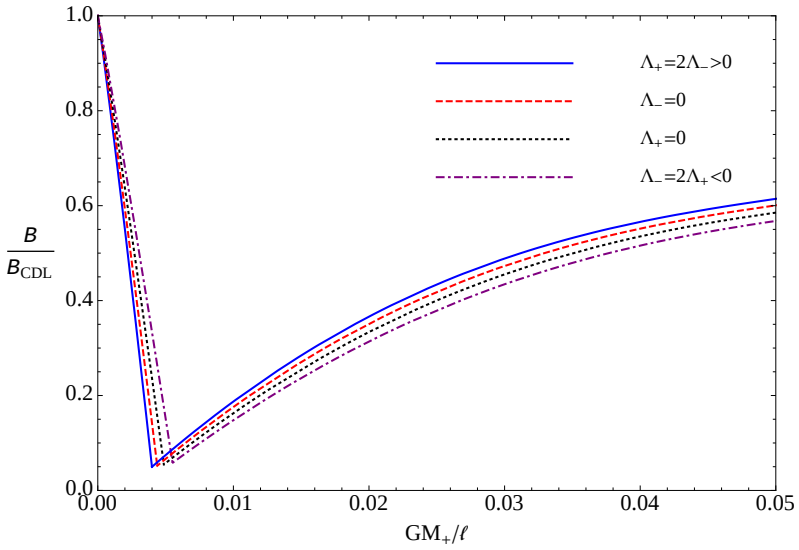

Figure 3.2: A plot of the minimum bounce action as M_+ is varied for $\bar{\sigma}\ell = 0.1$, and varying values of $\Lambda_+ = 6/\ell^2, 3/\ell^2, 0, -3/\ell^2$, $\Lambda_- = 3/\ell^2, 0, -3/\ell^2, -6/\ell^2$ as indicated. The ratio of the bounce action to the CDL value is plotted, but as $\Lambda_\pm$ vary, this value itself changes. For $\bar{\sigma}\ell = 0.1$, $B_{CDL} = 0.101, 0.117, 0.137, 0.165\,\ell^2/L_p^2$ as Λ_+ drops from its maximal to minimal value considered here.

although it must be noted that, for the static bubble M_- is a complicated function of M_+. For the critical bubble, $GM_- = 0$, hence the critical bounce action is

$$B_C = 4\pi G M_C^2 \simeq \frac{\pi\ell^2}{G}\left(\frac{256}{27}\right)^2 (\bar{\sigma}\ell)^6 \simeq \left(\frac{4}{3}\right)^6 (\bar{\sigma}\ell)^2 B_{CDL}\,. \tag{3.3.61}$$

Thus as $\bar{\sigma}\ell \to 0$, the tunnelling action becomes small compared to the CDL action.

One problem with having a small critical mass is of course that the decay rate due to tunnelling may be outstripped by the evaporation rate of the black hole, as we will discuss later, however, what this expansion indicates is that the minimal bounce action for a particular $\bar{\sigma}\ell$ can be extremely small, so that even if we are above the critical black hole mass, the decay rate can still be significant.

Having determined that the dominant tunneling process is either the static bubble or the $GM_- = 0$ branch, we can now compute the dominant bounce action either by numerically solving the time-dependent bubbles with $GM_- = 0$, or computing the static bubble actions with $k_1 = k_1^*$. We used a simple mathematica program to calculate these exponents, and double checked by a totally numerical computation. The results for some sample values of $\bar{\sigma}\ell$ are presented in figure 3.3.

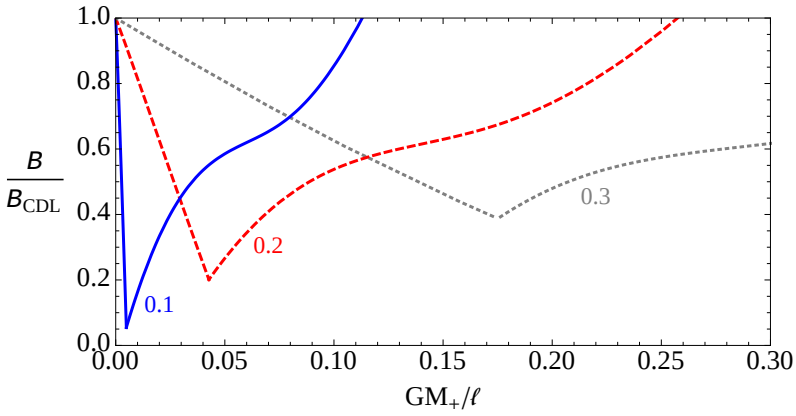

Figure 3.3: The exponent B for the dominant tunnelling process divided by the appropriate vacuum tunnelling value B_{CDL}, for different masses M_+ of the nucleation seed. The surface tension σ and AdS radius ℓ enter in the combination $\bar{\sigma}\ell$.

The general bubble solution for $GM_- = 0$ oscillates between two values $\tilde{R}_{MAX}$ and $\tilde{R}_{MIN}$ where the potential $U(\tilde{R})$ vanishes. This periodic solution in $\tilde{\lambda}$ can only be single-valued in $\mathcal{M}_\pm$ if the manifolds on each side have the same time-periodicity as the bubble wall solution. In general, this will not be the same as the natural periodicity $\Delta\tau_+ = 8\pi GM_+$ of the Euclidean Schwarzschild solution, hence the need to consider general periodicity in the computation of the action in section 3.1.2. For the static solution of course, this is not an issue. The values of $\tilde{R}_{MAX}/\tilde{R}_{MIN}$ are well outside the black hole horizon radius, and move together as GM_+ is increased. Eventually, at GM_C, the two roots of U meet, and the static branch begins.

The static branch is the preferred instanton with nonzero GM_-, i.e. with a black hole remnant, although non-static solutions exist with higher action and remnant mass. Initially, the static bubble shrinks with increasing GM_+, but remains well outside the Schwarzschild radius, however, as we increase GM_+ further, the bubble becomes constrained by the expanding black hole horizon, and becomes stretched just outside $\tilde{R}_{SCH}$. Meanwhile, the remnant black hole mass GM_- increases along the static branch and eventually becomes larger than GM_+, however, because of the negative cosmological constant, the horizon radius, while increasing, does not increase as rapidly as $\tilde{R}_{SCH}$. The static bubble action therefore increases as GM_+ increases, eventually becoming larger than B_{CDL} (see figure 3.3). Figure 3.4 illustrates the behaviour of these minimal/maximal and static values of $\tilde{R}$ as $\tilde{R}_{SCH} = 2GM_+$

varies, the remnant horizon radius is also shown.

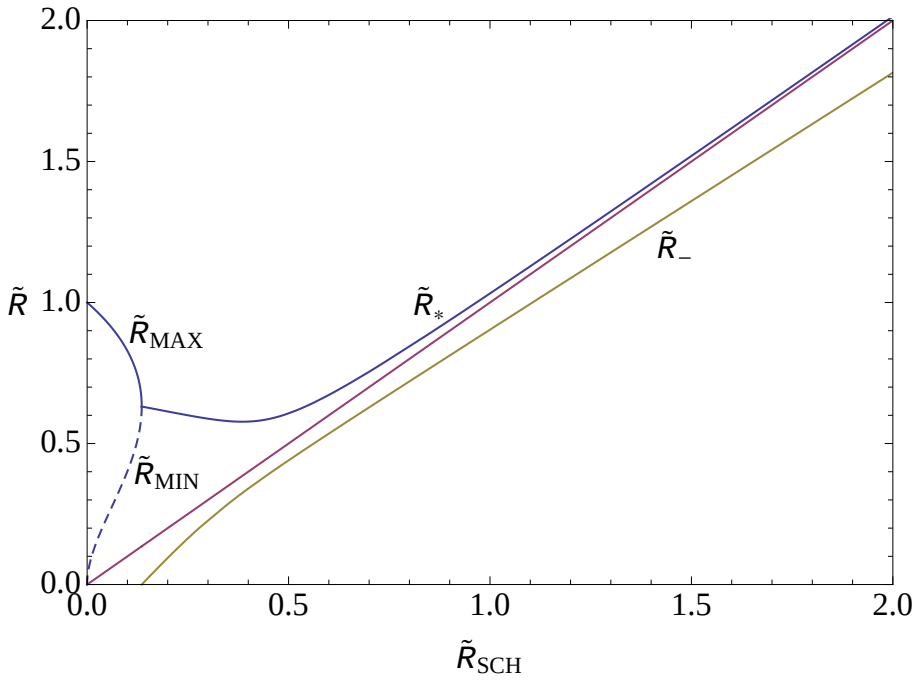

Figure 3.4: A plot of the variation of the bubble wall radius $\tilde{R}$ as GM_+ is increased for $\bar{\sigma}\ell = 0.25$ (chosen to highlight the qualitative features). As $\bar{\sigma}\ell$ drops, the features of the phase diagram remain the same, but 'squash up' towards smaller $\tilde{R}_{SCH}$. The unlabelled red line running from corner to corner represents $\tilde{R}_{SCH}$, the seed black hole horizon radius.

3.3.3 Charged black holes instantons

In this section we briefly comment on an obvious generalisation of our instantons to Einstein-Yang-Mills-Higgs theory. The combination of Einstein gravity with Yang-Mills and Higgs fields admits the possibility of charged black hole solutions [114,115]. Electrically charged black holes can discharge by the emission of charged particles [116], but magnetically charged black holes may be the lightest magnetically charged particles in the theory, in which case a large mass black hole evaporates towards the extremal limit, and the Hawking radiation flux falls to zero.

Magnetically charged black holes may be produced in the early universe [92,93], and form the seeds for vacuum decay of an unstable standard model Higgs field. Uncharged black holes can easily evaporate before they seed a phase transition, but

the charged black holes hang around for a longer time making them better candidates for vacuum decay nucleation sites.

An $SU(2)\times U(1)$ Yang-Mills theory with Higgs field $\mathcal{H}$ in the fundamental $SU(2)$ representation has no flat-space monopole solutions, but it does have Dirac and Yang-Mills black-hole monopoles. The non-abelian monopoles can be constructed from the $SU(2)$ fields W using an ansatz

$$\mathcal{H} = \phi(r)\sigma_r\mathcal{H}_0, \tag{3.3.62}$$

$$W = G^{1/2}\frac{P}{r}\left(\sigma_\phi\, d\theta - \sigma_\theta \sin\theta\, d\phi\right), \tag{3.3.63}$$

where σ_r, σ_θ and σ_ϕ are Pauli matrices projected along the spherical polar coordinate frame and $\mathcal{H}_0$ is constant. (The magnetic charge has been scaled so that an extreme black hole has $P = M$ in the absence of a cosmological constant.)

For a potential which allows decay from flat space to AdS, there are thin-wall bubble solutions with spherical symmetry and constant values of ϕ at the appropriate minima of the potential. The metric coefficients are

$$f_- = 1 - \frac{2GM_-}{r} + \frac{r^2}{\ell^2} + \frac{G^2P^2}{r^2}, \tag{3.3.64}$$

$$f_+ = 1 - \frac{2GM_+}{r} + \frac{G^2P^2}{r^2} \tag{3.3.65}$$

In this case, the bubble wall carries no magnetic charge. Generalised solutions may also be possible in which the interior and exterior have different magnetic charges.

The action for the bubble solutions is given by the same formula, (3.1.41), as in the uncharged case, though with the appropriate expressions for $f_\pm$. The plot of the dependence of the action on GM_+/ℓ is surprisingly similar to the uncharged case at fixed ratio P/M_+, with one small modification. The time-dependent tunneling solutions prior to the switching on of the static bubbles now do not remove the black hole altogether as this would leave a naked singularity. Instead, the bubbles leave behind an extremal remnant, $M_- = M_{ext}(P)$, where

$$GM_{ext}(P) = \frac{\ell}{3\sqrt{6}}\left(2 + \sqrt{1 + \frac{12G^2P^2}{\ell^2}}\right)\sqrt{\sqrt{1 + \frac{12G^2P^2}{\ell^2}} - 1}\,. \tag{3.3.66}$$

The static branch meets this time-dependent branch at a critical mass M_{CP}, where the static bubble now has an extremal black hole in its interior. On the static branch,

the action is, as before, the difference of the areas of the seed and remnant black holes, but as the extremal limit is approached, the horizon radius of the remnant black hole shrinks only as the root of $M_+ - M_{CP}$, whereas the radius of the seed black hole (which is not approaching an extremal limit) depends linearly on $M_+ - M_{CP}$, thus, as we increase M_+ from M_{CP}, the action actually starts to *drop* briefly, before the effect of the increasing horizon area kicks in causing the usual rising of the bounce action. This small dip in the action near the critical point is very hard to see at low P/M_+, but for larger ratios becomes more visible. The dip is however very minor, and the minimum action is well approximated by the value at M_{CP}.

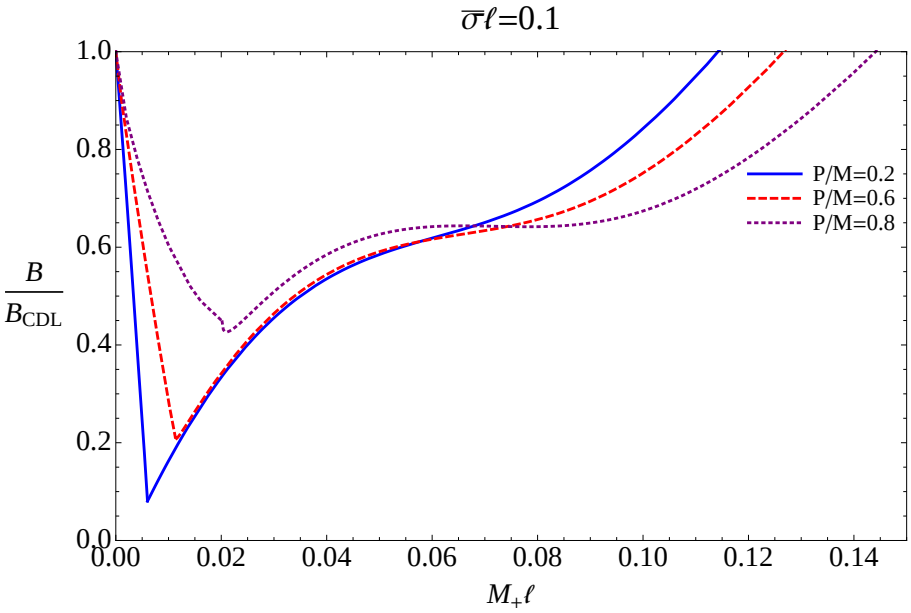

Figure 3.5: The exponent B for the dominant tunnelling process with black-hole monopoles of mass M_+ acting as nucleation seeds.

From figure 3.5 we see the dip is most visible at large ratio P/M, however, perhaps surprisingly, it is also the case that at large P/M the catalytic effect of the black hole is much reduced. We therefore expect that the addition of a monopole charge will not particularly assist with vacuum decay.

3.4 Conclusions

The main aim of this chapter was to demonstrate that black holes can massively speed up the rate of decay of a metastable vacuum by acting as nucleation sites. We have shown that is the case, subject to the limitations of the analysis, some of which we shall address in the next chapter for the particular example of the Higgs potential.

We have simplified the analysis by employing a thin-wall approximation. In this limit, we have showed that when the seed mass is above some (calculable) critical mass, then the seeded nucleation proceeds via a static bubble solution. This gives a good starting point for an analysis of the thick wall bubble nucleation, which is far simpler for static than for non-static field configurations and will be discussed for the particular example of metastable Higgs potential in the next chapter.

Chapter 4

Gravity and the stability of the Higgs vacuum

The recent discovery of the Higgs boson [71, 72] raises the possibility that, even within the standard model of particle physics, the present vacuum state of the universe may not be stable, but only metastable, with another lower energy state at high expectation values of the Higgs field [18, 73–76]. In general, this would not conflict with observation because the lifetime of the present vacuum would be far longer than the age of the universe. Indeed, the possibility that we live in a metastable state was mooted long before the discovery of the Higgs [77–85].

However, as we have demonstrated in the previous chapter, black holes can catalyse vacuum decay, it is therefore important to investigate whether the metastable Higgs vacuum might be ruled out if the seeded nucleation rates for vacuum decay are comparatively large. In this chapter, based on [69] and [70], we will address this issue.

We start by summarizing some of the features of the Higgs potential relevant to the calculation. As with the phenomenological explorations of the Higgs potential, we write the potential in terms of an overall magnitude of the Higgs, ϕ, and approximate the potential with an effective coupling λ_{eff},

$$V(\phi) = \frac{1}{4}\lambda_{\text{eff}}(\phi)\phi^4. \tag{4.0.1}$$

The exact form of λ_{eff} is determined by a renormalisation group computation with

the parameters and masses measured at low-energy. Two-loop calculations of the running coupling [18, 99–101], can be approximated by an expression of the form

$$\lambda_{\text{eff}} \approx \lambda_* + b\left(\ln\frac{\phi}{\phi_*}\right)^2, \tag{4.0.2}$$

where $-0.01 \lesssim \lambda_* \lesssim 0$, $0.1M_p \lesssim \phi_* \lesssim M_p$ and $b \sim 10^{-4}$. The uncertainty on these parameter ranges is due mostly to experimental uncertainties in the Higgs mass and the top quark mass, however the possibility of negative λ_{eff} approaching the Planck scale is quite real. The present-day broken symmetry vacuum may therefore be a metastable state, but quantum tunnelling in the Higgs potential determined by the usual Coleman de Luccia expressions is very slow, and the lifetime of the false vacuum far exceeds the lifetime of the universe.

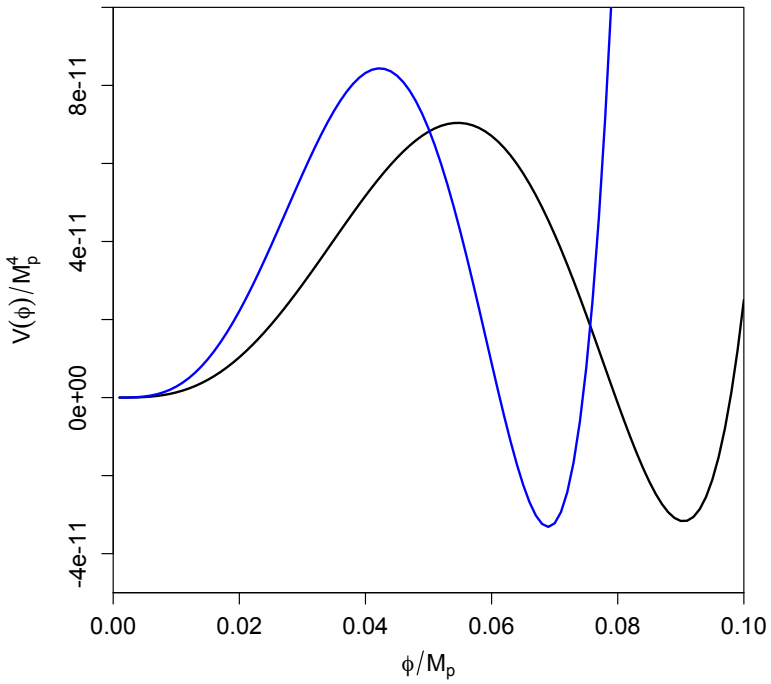

Figure 4.1: The Higgs potential at large values of one of the Higgs field components ϕ. The parameter values for the blue line are $\lambda_* = -0.001$, $\phi_* = 0.5M_p$. The black line shows the effect of adding a ϕ^6 term with coefficient $\lambda_6 = 0.34$.

The observation of negative λ_{eff} of course assumes no corrections from new physics between the TeV scale and the Planck scale. We might expect quantum

gravity, or other effects will have to be taken into account. On dimensional grounds, we can write modifications to the potential of the following form [102–107],

$$V(\phi) = \frac{1}{4}\lambda_{\text{eff}}(\phi)\phi^4 + \frac{1}{4}(\delta\lambda)_{\text{bsm}}\phi^4 + \frac{1}{6}\lambda_6\frac{\phi^6}{M_p^2} + \frac{1}{8}\lambda_8\frac{\phi^8}{M_p^4} + \dots \tag{4.0.3}$$

where $(\delta\lambda)_{\text{bsm}}$ includes corrections from BSM physics, and the polynomial terms represent unknown physics from the Planck scale. If these coefficients are similar in magnitude, then the small size of λ_{eff} at the Planck scale has the consequence that there is an intermediate range of ϕ where the potential is determined predominantly by λ_{eff} and λ_6.

Quantum tunnelling in a corrected potential has been explored by Branchina et al. [104,105]. They considered potentials with $\lambda_* \sim -0.1$, where the potential barrier occurs at $\phi \ll M_p$, and they further enhanced the tunnelling rate by taking $\lambda_6 = -2$. They claimed a greatly enhanced tunnelling rate, with a lifetime much shorter than the age of the universe, however, their discussion did not include gravitational interactions.

4.1 Seeded tunnelling of the Higgs vacuum in a thin-wall limit

In a previous chapter, the vacuum decay process has been described in gravitational terms using the surface tension of the wall, σ, and the AdS radius of the 'true' vacuum, ℓ. In this section we will explore vacuum decay in the Higgs model with high energy corrections as discussed in the introduction. The key features of the potential relevant for quantum tunnelling are the barrier height, the separation between the minima and the energy of the true vacuum (TV). These three parameters can be encoded as follows,

$$g = \phi_{TV}/M_p, \qquad \epsilon = -V(\phi_{TV}), \qquad \zeta = \sup_{0<\phi<\phi_{TV}} V(\phi) \tag{4.1.4}$$

Following our previous discussion we shall restrict attention to potentials which allow thin-wall bubbles. Although we would expect $\zeta \gg \epsilon$ for a thin wall bubble, numerical solutions show that the wall approximation is reasonably accurate even

when $\zeta \sim \epsilon$, therefore we use this lower bound for ζ. The range of Higgs model parameters λ_*, ϕ_* and λ_6 which allow thin-wall bubbles is set by $\zeta > \epsilon > 0$, and by the condition that the true vacuum lies at large ϕ. Thin wall bubbles correspond to rather large values of λ_6, as illustrated in table 4.1. Roughly speaking, as λ_* becomes more negative, the values of λ_6 required for thin-wall become larger, similarly as ϕ_* drops, λ_6 increases. In all cases the pure CDL tunneling action is extremely large (10^{6-7}), but the suppression of the critical tunneling action is also large, and increases as λ_* becomes more negative.

Table 4.1: A selection of parameter values for the modified Higgs potential, including the AdS radius ℓ, the rescaled surface tension $\bar{\sigma}\ell$ and the critical mass M_C for optimal nucleation seeded by a black hole. These parameters lie along the bottom edge of the parameter ranges for thin-wall bubbles. The vacuum tunnelling exponent B_{CDL} is around 4e+06 in each of these examples.

λ_*	ϕ_*/M_p	λ_6	g	ℓ/L_p	$\bar{\sigma}\ell$	M_C/M_p	B_C/B_{CDL}
-0.005	1	500	0.00146	3.17e+8	0.00045	3.5	1.2e-6
-0.005	0.5	2e+03	0.00073	1.27e+9	0.00023	1.8	2.9e-7
-0.007	2	1.98e+03	0.0008	9.33e+8	0.00024	1.5	3.2e-7
-0.007	1	7.93e+03	0.0004	3.79e+9	0.00012	0.8	8.2e-8
-0.007	0.75	1.41e+04	0.0003	6.76e+9	9.1e-05	0.61	4.7e-8
-0.007	0.5	3.17e+04	0.0002	1.51e+10	6e-05	0.39	2e-8
-0.008	1	27e+03	0.00022	1.18e+10	6.9e-05	0.46	2.7e-8
-0.008	3	3e+03	0.00067	1.31e+9	0.00021	1.4	2.4e-7
-0.009	1	85e+03	0.00013	3.43e+10	4.1e-05	0.28	9.4e-9
-0.01	2	63e+03	0.00016	2.55e+10	5.4e-05	0.49	1.7e-8

Following Coleman and De Luccia, we can express the surface tension of the bubble wall in terms of the potential. In order to extend the result to moderate values of ζ/ϵ, we compute the tension using the integral

$$\sigma = \int_0^{\phi_1} d\phi \, (2V)^{1/2} \simeq \kappa g M_p \, \zeta^{1/2}, \tag{4.1.5}$$

where the upper limit of the integral is at $V(\phi_1) = 0$. The constant κ depends on

the details of the potential, but since $\phi_1 < gM_p$ and $V \leq \xi$, it is subject to the constraint $\kappa < \sqrt{2}$. The AdS radius ℓ is related to the vacuum energy density by

$$\ell = \sqrt{3} M_p \epsilon^{-1/2}. \tag{4.1.6}$$

The back-reaction parameter $\bar{\sigma}\ell$ is therefore

$$\bar{\sigma}\ell = \frac{1}{4M_p^2}\sigma\ell = \frac{\sqrt{3}}{4}\kappa g \left(\frac{\zeta}{\epsilon}\right)^{1/2}. \tag{4.1.7}$$

Note that $\bar{\sigma}\ell < 1/2$ puts an upper bound on g. The CDL tunnelling exponent B_{CDL} given in (3.3.56) is

$$B_{CDL} = \frac{27\pi^2\sigma^4}{2\epsilon^3(1-4\bar{\sigma}^2\ell^2)^2} = \frac{27\kappa^4\pi^2}{2}\left(\frac{g^4M_p^4}{\epsilon}\right)\left(\frac{\zeta}{\epsilon}\right)^2(1-4\bar{\sigma}^2\ell^2)^{-2}. \tag{4.1.8}$$

The large size of $B_{\rm CDL}$ in the parameter range covered by table 4.1 guarantees a tunnelling lifetime longer than the age of the universe (for unseeded nucleation).

When the vacuum decay is seeded by a black hole, the most rapid decay process occurs for a seed mass $M_+ = M_C$ given in (3.3.58),

$$M_C \approx \frac{128}{27}\frac{\ell}{G}(\bar{\sigma}\ell)^3 = \frac{16}{3}\pi\kappa^3\left(\frac{g^4M_p^4}{\epsilon}\right)^{1/2}\left(\frac{\zeta}{\epsilon}\right)^{3/2} M_p. \tag{4.1.9}$$

The corresponding exponent in the nucleation rate is $B_C = 0.5(M_C/M_p)^2$. Some values for M_C are shown in table 4.1. If $M_C \gg M_p$, then the exponent B_C is large and the seeded decay rate becomes vanishingly small. On the other hand, if $M_C \lesssim M_p$ then even if we have a seed mass $M_+ \gg M_C$, we can still get significant suppression of the bounce action while remaining well above the Planck mass from tunneling on the static branch, as we see from figure 3.3. Our strategy therefore is to explore the decay seeded by a small mass black hole via the static instanton, which (for convenience) we determine numerically.

A brief consideration of the dependence of the bounce action on M_+ shows that we are exploring seeded tunnelling for very light or primordial black holes [117], with temperatures well above that of the CMB. We must therefore check that the black hole can seed the false vacuum decay before it disappears through Hawking radiation. The vacuum decay rate Γ_D, (3.0.1), contains not only the exponential of the bounce action, but also a pre-factor, A. According to Callan and Coleman

[13], this pre-factor is made up of a factor of $(B/2\pi)^{1/2}$ for each translational zero mode of the instanton and a determinant factor. In our case, there will be a single zero mode representing the time translation symmetry, and rather than evaluate the determinant factor, we use the inverse horizon timescale as a rough estimate $(GM_+)^{-1}$, giving

$$\Gamma_D \approx \sqrt{\frac{B}{2\pi}}\frac{e^{-B}}{GM_+}. \tag{4.1.10}$$

The black hole emits Hawking radiation at a rate depending on fundamental particle masses and spins. The total decay rate for a subset of the standard model was evaluated by Page, [118]. If we set $\Gamma_H = \dot{M}/M$, then

$$\Gamma_H \approx 3.6 \times 10^{-4}(G^2M_+^3)^{-1} \tag{4.1.11}$$

The branching ratio of the tunnelling rate to the evaporation rate for uncharged black holes is therefore

$$\frac{\Gamma_D}{\Gamma_H} \approx 44\frac{M_+^2}{M_p^2}B^{1/2}e^{-B}. \tag{4.1.12}$$

From this expression we can see roughly how the branching ratio will depend on M_+, even though B is, in principle, a complex function of M_+. The static bubble is the difference in areas of the seed and remnant black holes, which we can deduce from figure 3.4 to be roughly linear (there is actually a slightly stronger dependence on M_+, however, what is important is that it is not quadratic), whereas the prefactor is (again, roughly) $M_+^{5/2}$; we therefore expect the plot to be strongly exponentially suppressed at large M_+, but rising as M_+ falls to a maximum around $M_+/M_p = \mathcal{O}(1)$, then dropping again below M_p. The actual value of the maximum will depend on the details of how B depends on M_+, which requires a full calculation.

The branching ratio is plotted as a function of the seed mass M_+ for two indicative sets of parameters taken from table 4.1 in figure 4.2 in order to illustrate the dependence on the parameters in the Higgs potential (or correspondingly on $\bar{\sigma}$ and ℓ). The branching ratio is shown at fixed ϕ_* with varying λ_* and vice versa. The overall picture is that for lower $\bar{\sigma}$ and higher ℓ (or more negative λ_* / higher ϕ_*) the branching ratio is larger, and is consistently higher than unity over a larger range. While Hawking evaporation always dominates at large M_+, the effect of

Hawking radiation is that the black hole loses mass, hence driving it towards increasing branching ratio. A black hole produced in the early universe, for example, starts out with a mass well beyond the right-hand side of the plots, but at some point after evaporation, the vacuum decay rate becomes larger than the Hawking evaporation rate and the black hole seeds the transition to a new vacuum. This can occur for seed masses well above the Planck mass, where we have some confidence in the validity of the vacuum decay calculation. The timescales for Hawking evaporation and vacuum decay will both be less than roughly a million Planck times.

Finally, for the case of a monopole charged black hole, we might expect the branching ratio to be larger due to their reduced Hawking radiation rate: The Hawking flux is proportional to $\mathcal{A}_+ T_+^4$, where $\mathcal{A}_+$ is the event horizon, and T_+ is the Hawking temperature

$$T_+ = \frac{1}{8\pi G M_+} \frac{4\Delta}{(1+\Delta)^2}, \tag{4.1.13}$$

setting $\Delta^2 = 1 - P^2/M_+^2$. The evaporation rate is now

$$\Gamma_H \approx 3.6 \times 10^{-4} (G^2 M_+^3)^{-1} \frac{64\Delta^4}{(1+\Delta)^6} \tag{4.1.14}$$

The branching ratio Γ_D/Γ_H can now be re-computed using this evaporation rate and the vacuum decay rates from the previous section. The result is shown in figure 4.3.

4.2 Higher dimensional instantons

The seeded nucleation calculation presented here requires a black hole, and for large tunneling enhancement, this is expected to be a primordial black hole which is evaporating and nearing the end of its life. There is of course another situation in which a small black hole might occur. A possible alternative solution to the hierarchy problem has been to consider large extra dimensions, [119–122]. In these models, our universe is presumed to be a "brane" living within higher dimensions on which standard model physics is confined. The higher dimensional Planck scale is not hierarchically large, but instead our 4D Planck scale, which is derived via an integration over these extra dimensions, gains its leverage via the "large" internal

volume. In such scenarios black holes can be created in particle collisions [123, 124], leading to considerable interest in the possibility of black holes being produced at the LHC (for a recent review see [125]). There are no known exact solutions for these black hole plus brane systems, and instead the black hole is usually considered to be approximately a higher dimensional Schwarzschild or Myers-Perry [126] solution (see [127, 128] for reviews on the issues and properties of brane black holes). For the Randall-Sundrum braneworld models, where the extra dimension is strongly warped, one could also consider "brane only" solutions, such as the tidal black hole [129].

Calculating the vacuum decay rates for these systems would be challenging, to say the least, not only because of the lack of a true higher dimensional black hole solution, but also because an instanton presumably would have to have a different vacuum only on the brane, and not in the bulk (although the braneworld equivalent of the CDL instantons were constructed in [110,131]). However, some features of our calculation should be present. The tidal black holes, for example, resemble black-hole monopoles, but with negative square monopole charge P^2. The bubble solutions for tidal holes are simple generalisations of the ones we have already discussed (3.3.3).

In this section we briefly outline the simple higher dimensional instanton model. We take a higher dimensional black hole solution with different masses and cosmological constant on each side of the wall, and compute how the branching ratio changes with dimension.

The equations of motion have the same schematic form as (3.1.12)

$$\dot{R}^2 = \bar{\sigma}^2 R^2 - \bar{f} + \frac{(\Delta f)^2}{16\bar{\sigma}^2 R^2} \tag{4.2.15}$$

but with $\bar{\sigma} = 4\pi G\sigma/(D-2)$ [110,131], and f now the higher dimensional Schwarzschild potential:

$$f = 1 - \frac{2\Lambda r^2}{(D-1)(D-2)} - \frac{16\pi G_D M}{(D-2)A_{D-2}r^{D-3}} \tag{4.2.16}$$

where G_D is the higher dimensional Newton constant and $A_{D-2} = 2\pi^{\frac{D+1}{2}}/\Gamma[\frac{D+1}{2}]$.

Defining ℓ, γ and α in a similar fashion:

$$\ell^2 = \frac{(D-1)(D-2)}{2\Delta\Lambda} \quad , \quad \gamma = \frac{4\bar{\sigma}\ell^2}{1+4\bar{\sigma}^2\ell^2} \quad , \quad \alpha^2 = 1 + \frac{2\Lambda_-\gamma^2}{(D-1)(D-2)} \tag{4.2.17}$$

and

$$k_1 = \frac{16\pi G_D}{(D-2)A_{D-2}}\left(\frac{\alpha}{\gamma}\right)^{D-3}\left[M_- + (1-\alpha)\frac{\Delta M}{2\bar{\sigma}\gamma}\right]$$
$$k_2 = \frac{16\pi G_D}{(D-2)A_{D-2}}\left(\frac{\alpha}{\gamma}\right)^{D-2}\frac{\Delta M}{4\bar{\sigma}} \tag{4.2.18}$$

Then setting $\tilde{R} = \alpha R/\gamma$, $\tilde{\lambda} = \alpha\lambda/\gamma$ gives the equation of motion

$$\left(\frac{d\tilde{R}}{d\tilde{\lambda}}\right)^2 = 1 - \tilde{R}^2 - \frac{k_1 + 2k_2}{\tilde{R}^{D-3}} - \frac{k_2^2}{\tilde{R}^{2(D-2)}} \tag{4.2.19}$$

which is of the same form as (3.1.16) albeit with different exponents of $\tilde{R}$. We can use the same procedure as before to find the static solution and the dynamical bubble which removes the black hole. The static action (which is what is needed for the branching ratio) is, as before, the difference in horizon areas:

$$B_D = \frac{A_{D-2}}{4G}\left(r_+^{D-2} - r_-^{D-2}\right) \tag{4.2.20}$$

where $r_\pm$ are determined numerically, and the corresponding tunneling rate is

$$\Gamma_D = \sqrt{\frac{B_D}{2\pi}}\frac{e^{-B_D}}{r_+} \tag{4.2.21}$$

Meanwhile the Hawking temperature of the higher dimensional black hole is [126, 127]

$$T_H = \frac{(D-3)}{4\pi r_+} \tag{4.2.22}$$

To estimate the decay rate of the black hole, we will assume that the main channel is due to emission of particles on the brane [132, 133], leading to

$$\Gamma_H \sim 3.6\times 10^{-4}\frac{64\pi G_D}{A_{D-2}r_+^{D-1}}\frac{(D-3)^4}{(D-2)} \tag{4.2.23}$$

hence dimension dependent branching ratio is

$$\frac{\Gamma_D}{\Gamma_H} \approx 550\frac{M_+ r_+}{(D-3)^4}\sqrt{B_D}e^{-B_D} = \frac{550\sqrt{B_D}e^{-B_D}}{(D-3)^4}\left[\frac{16\pi G_D M_+^{D-2}}{(D-2)A_{D-2}}\right]^{1/(D-3)} \tag{4.2.24}$$

Defining the higher dimensional reduced Planck mass as[1]

$$M_D^{D-2} = \frac{1}{8\pi G_D} \tag{4.2.25}$$

[1]Note that in the literature, see e.g. [127], the non-reduced Planck mass is often used. Due to the dimension dependence of the Planck mass this will introduce various dimension dependent renormalisation factors between our expressions and those assumed there. Although these are of order unity, they do have some impact.

we can track the branching ratio as a function of M_+/M_D and its dependence on D. To illustrate this dimensional dependence, we chose test-case values of $\bar{\sigma}\ell = 0.01$ and $\ell = 0.1$, and plotted Γ_D/Γ_H in figure 4.4.

The figure shows that as the number of extra dimensions increases, the branching ratio decreases, however the exact normalisation of the plot will depend on the confidence of translating modifications of the potential to the new Planck scale and variables. Given the crudeness of this particular model, we leave this, and possible refinements of the decay modelling to future work.

4.3 Seeded tunnelling of the Higgs vacuum via thick bubbles

The main wrinkle in our previous calculations is that the condition for the thin wall approximation requires that the energy at the potential minimum is smaller than the potential barrier height, and scanning through parameter space of the corrected Higgs potential (4.0.3) we find that requiring a thin wall is very constraining: the range of λ_6 for which this occurs is very small, and occurs for large values of the parameter $\lambda_6 \geq 10^3 - 10^5$, depending on λ_*. On the other hand, computing the branching ratio, (4.1.12), for these models shows that tunnelling does indeed dominate. Thus, while our pseudo-analytic discussion is limited in the sense of parameter space, it has provided a proof of principle that black holes could potentially seed vacuum decay.

In order to decide whether this effect is restricted to a niche of parameter space, or is potentially relevant, a full exploration of instantons outside of the thin wall approximation is necessary [134].

We will again concentrate on the static branch for the tunnelling instantons, as we expect that the static bounce solutions will dominate the vacuum decay rate for $M_+ > M_C$. Moreover, as we already saw, in the static regime bounce action calculation simplifies significantly and the general expression (3.1.41) reduce to the 'area difference'. Even if these solutions do not have the lowest action, this would only mean the static instantons constructed would give an upper bound on the

seeded nucleation rate, and our main point about enhancement of the decay rate is made a fortiori.

To construct the instanton, we require an SO(3) invariant geometry with a Schwarzschild-like mass term; our geometry and scalar field therefore depends on a single radial coordinate r. It proves numerically convenient to take the area gauge, and to parametrise the static, spherically symmetric Euclidean metric as:

$$ds^2 = f(r)e^{2\delta(r)}d\tau^2 + \frac{dr^2}{f(r)} + r^2(d\theta^2 + \sin^2\theta d\varphi^2), \tag{4.3.26}$$

where we write f in the form

$$f = 1 - \frac{2G\mu(r)}{r}. \tag{4.3.27}$$

The equations of motion for the bounce solution are therefore

$$f\phi'' + f'\phi' + \frac{2}{r}f\phi' + \delta' f\phi' - V_\phi = 0, \tag{4.3.28}$$

$$\mu' = 4\pi r^2\left(\frac{1}{2}f\phi'^2 + V\right), \tag{4.3.29}$$

$$\delta' = 4\pi G r\phi'^2. \tag{4.3.30}$$

Note that by using (4.3.30) in (4.3.28), we can decouple the equations for μ and ϕ, solve, then infer δ by integration of (4.3.30).

The black hole horizon is defined as usual by the condition $f(r_h) = 0$. It will be convenient to discuss the solutions in terms of a remnant mass parameter $\mu_- = \mu(r_h)$, rather the actual remnant black hole mass, as the vicinity of the horizon we will typically not be in the true AdS vacuum (our Higgs may not have fallen to its minimum) nor will our horizon radius be expressible as a simple ratio of μ_-. Instead, $r_h = 2G\mu_-$ is now a simple ratio of μ_-, and the expressions in our calculations are much clearer. The seed mass M_+ on the other hand is straightforwardly defined as the mass at spatial infinity $r \to \infty$, where the field is in the false vacuum. Finally, since we integrate out from the event horizon, it proves convenient to fix the time co-ordinate gauge there, rather than at asymptotic infinity. This means the $t-$coordinate is no longer the time for an asymptotic observer, however, the action we compute is gauge invariant, hence this is irrelevant.

The boundary conditions are therefore

$$\mu(r_h) = \mu_-,\ \delta(r_h) = 0,\ \text{at } r = r_h, \tag{4.3.31}$$

$$\mu(r) \to M_+,\ \phi(r) \to 0,\ \text{as } r \to \infty. \tag{4.3.32}$$

If we expand Eqs. (4.3.28-4.3.30) about the horizon, we obtain a relation between $\phi'(r_h)$ and $\phi(r_h)$ which fixes an additional boundary condition,

$$\phi'(r_h) = \frac{r_h V_\phi[\phi(r_h)]}{1 - 8\pi G r_h^2 V[\phi(r_h)]}. \tag{4.3.33}$$

This is analogous to the condition $\phi'(0) = 0$ in the $O(4)$ case. The boundary value problem is overdetermined, which in practice means that the remnant mass parameter μ_- is fixed by the value of the seed mass M_+. The solutions can be obtained by a shooting method, integrating from the horizon and trying different initial values of $\phi(r_h)$. The integration leads to the value of the seed mass M_+ for a given remnant mass parameter. From this we can infer the remnant mass for a given seed mass.

As we discussed above an expression for the tunnelling exponent B reduced to the simple 'area difference' formula and also can be expressed in terms of the black hole mass parameters

$$B = \frac{\mathcal{A}_+}{4G} - \frac{\mathcal{A}_-}{4G} = \frac{M_+^2 - \mu_-^2}{2M_p^2}. \tag{4.3.34}$$

For a given scalar field potential V, the numerical relationship between M_+ and μ_- implies that the vacuum decay rate depends on the seed mass M_+ and the potential. The resulting values of the action for a selection of Higgs models is shown in figure 4.5. Note that the semi-classical bubble nucleation argument only applies when the action $B > 1$.

Computing the branching ratio now with these "thick wall" solutions gives figure 4.6. Although black holes produced in the early universe start out with relatively high masses, their temperature is nonetheless above that of the microwave background, and they evaporate down into the range plotted in figure 4.6. At this point, the mass hits a range in which vacuum decay is more probable, i.e. the tunneling half life becomes smaller than the (instantaneous) Hawking lifetime of the black hole. Note that this range is well above the Planck mass, where we have some confidence in the validity of the vacuum decay calculation. Given that this evaporation

timescale is $\sim 10^{-28}$s for a $10^5 M_p$ mass black hole, it is clear that once a primordial black hole nears the end of its life cycle, it *will* seed vacuum decay in these models. Hence with these Higgs potentials, the presence of any primordial black holes will eventually trigger a catastrophic phase transition from our standard model vacuum thus ruling out potentials with parameters in these ranges.

4.4 Conclusions

We have shown that the vacuum decay seeded by black holes greatly exceeds the Hawking evaporation rate for particle physics scale bubbles. This clearly has relevance for the Higgs potential which we consider here. A primordial black hole losing mass by the Hawking process would decay down to a mass around 10-100 times the Planck mass and then seed a vacuum transition. The fact that this has not happened therefore means that either the Higgs parameters are not the the relevant range or there are no primordial black holes in the observable universe.

An overall conclusion is that the lifetime of our universe in a metastable Higgs phase is crucially dependent on the absence of any nucleation seeds, and a primordial black hole could drastically reduce the time it takes to decay onto a different 'standard model'. Instability of the standard model is therefore more problematic than was hitherto supposed. Further exploration of the parameter space, using a wider class of bubble nucleation scenarios, should give us the range of Higgs parameters which lead to a long-lived standard model in the presence of black holes.

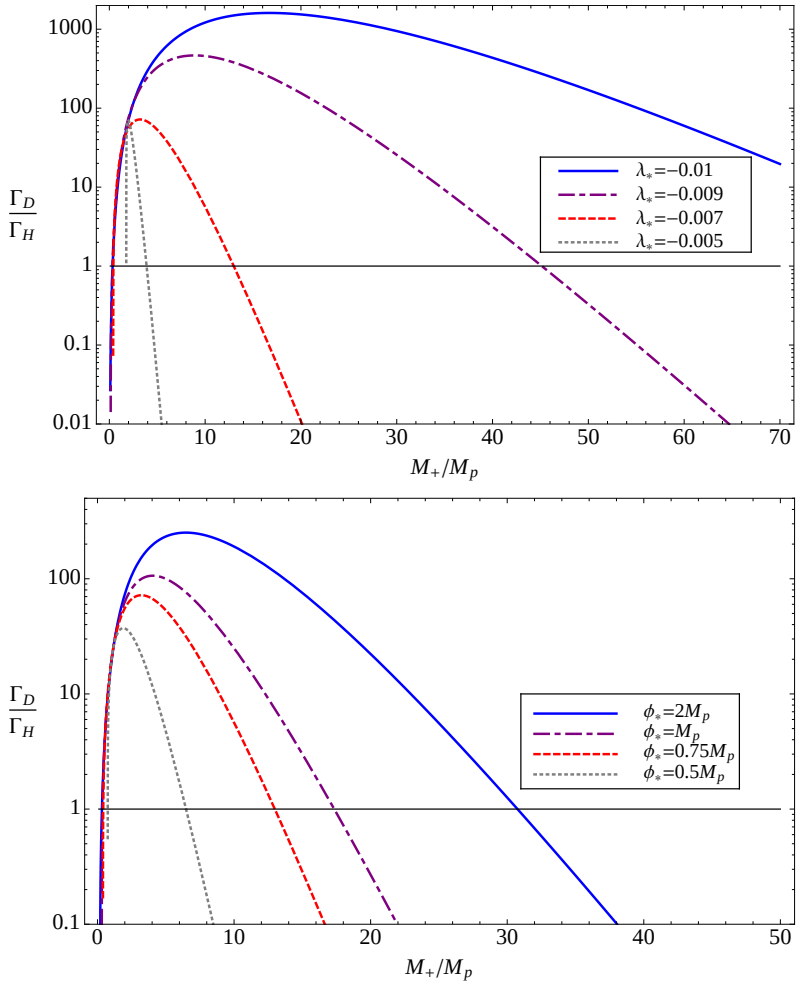

Figure 4.2: The branching ratio of the false vacuum nucleation rate to the Hawking evaporation rate as a function of the seed mass for a selection of Higgs models from table 4.1. The first plot shows the branching ratio for $\phi_* = M_p$ with the labelled values of λ_*, and the second for $\lambda_* = -0.007$ for the labelled values of ϕ_*. The black hole starts out with a mass beyond the right-hand side of the plot and the mass decreases by Hawking evaporation. At some point, the vacuum decay rate becomes larger than the Hawking evaporation rate.

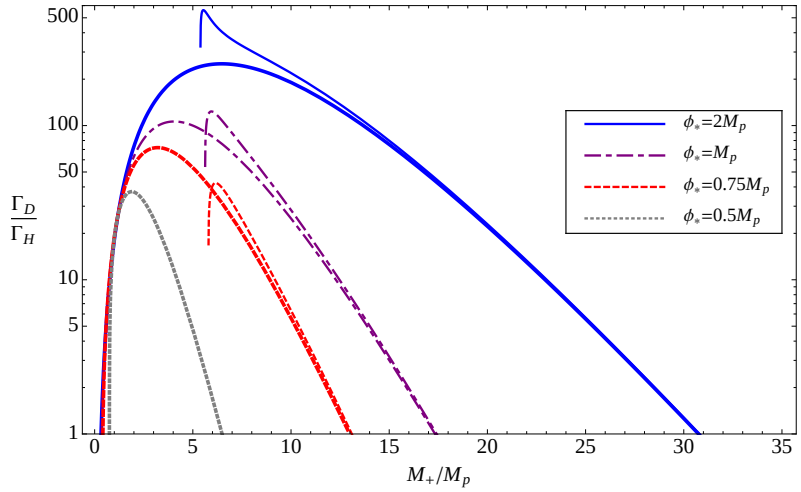

Figure 4.3: The branching ratio of the false vacuum nucleation rate to the Hawking evaporation rate for a monopole charged black hole with $P = 5M_p$, shown as a function of the seed mass for a selection of Higgs models from table 4.1. The plot for the uncharged black hole ($P = 0$) is repeated for comparison. As before, $\lambda_* = -0.007$ for the labelled values of ϕ_*.

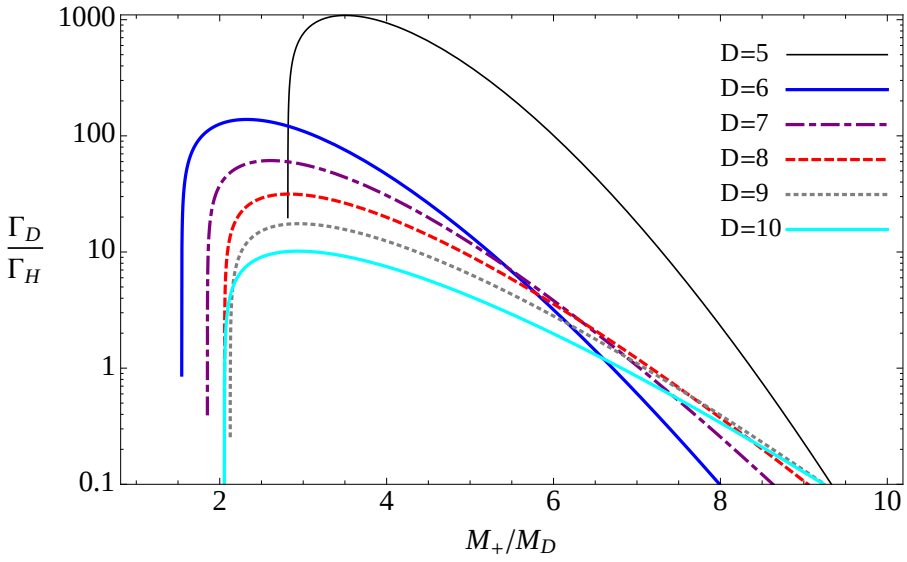

Figure 4.4: The dependence of the branching ratio on the dimensionality of space-time, D. Here, the $D-$dimensional Planck mass is fixed, i.e. $8\pi G_D$ always has the same value.

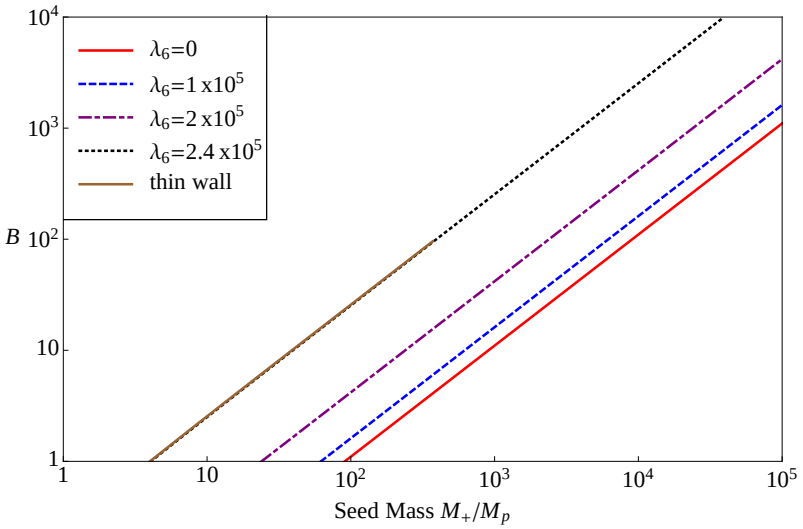

Figure 4.5: The action for a bounce solution. Each plot corresponds to a different value of λ_6 in the Higgs potential (4.0.3), with $\lambda_* = -0.01$ and $b = 1.0 \times 10^{-4}$. The largest value of λ_6 is within the range of the thin wall approximation, and the thin wall result is shown for comparison.

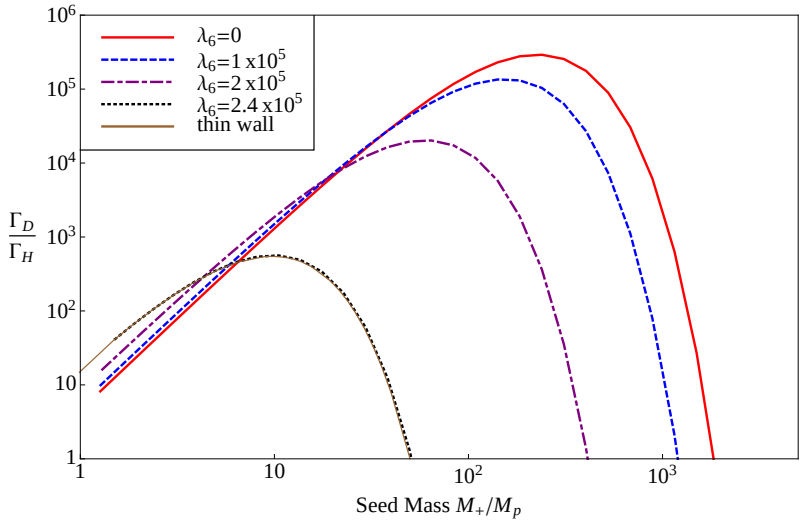

Figure 4.6: The branching ratio of the false vacuum nucleation rate to the Hawking evaporation rate as a function of the seed mass for a selection of Higgs models. Each plot corresponds a different value of λ_6 in (4.0.3), with $\lambda_* = -0.01$.

Chapter 5

Comments and future directions

In the present thesis we have considered two quite distinctive examples of interplay between gravity and field theory. We would like to conclude by several comments on the relation between these examples and possible directions for future work.

The first example was from a modern branch of theoretical physics called holography, for which gravitational calculations play an essential role. It is even probably fair to say that holography is responsible for a rebirth of interest in the exploration of different solutions of gravitational theories, especially in the context of supergravity in (asymptotically) Anti de Sitter spacetime. Exploring the space of such solutions, and relations between them, is especially important if we would like to address questions about applications of holography to condensed matter, or more generally, non-relativistic field theories. We have provided an example of a top-down approach to this problem, and the results, while not entirely successful, look promising. The spontaneous breaking of Lorentz symmetry we have found for the Type IIB system, along with the fact that such supergravity systems contain non-relativistic solutions, gives us hope that we might find a proper sector of supergravity theories where such solutions and corresponding field theories will not suffer from instabilities.

For the second example, the physics of false vacuum decay, it was known for a long time that gravity plays a central role, especially if cosmological implications are discussed. However, by pushing an analogy with condensed matter theory phase transitions we were able to appreciate the role of impurities, which in the gravitational context are most naturally mimicked by black holes. We have performed a

general analysis of the fate of a metastable vacuum in the presence of black holes along with a discussion about the application of our calculations to the problem of stability of the Higgs potential. The fact that we have an example of a metastable potential within the Standard Model (and we are living in a false vacuum state) makes this question especially interesting. Moreover, as we have shown, taking into account impurities could in principle reduce the lifetime of such false vacua significantly, hence this problem surely deserves further investigation. It is important to scan through the space of parameters of the effective Higgs potential more carefully [134], study the effects of possible new physics on the stability of the potential and also explore other sources of impurities, for example, lumps of matter or stars. Finally, as we have mentioned before, further investigation of the application of tunnelling catalysed by black holes in higher dimensional braneworld-type models is also very interesting.

There is also a direction of further investigation, which unifies these two examples in some way. In the context of holography the main focus has recently moved towards quantum information theory aspects of the correspondence, for example calculations of entanglement entropy for different regions on the boundary through the Ryu-Takayanagi prescription [135]. Such calculations could provide useful insights for holographic RG flow solutions in the bulk [136], hence it will be interesting to investigate our constructed solutions from the entanglement entropy perspective. A holographic description of the decay of metastable vacuum has been addressed before [137–139], however all these considerations are far from general and it would be interesting to investigate this further. For example, black holes, play a very important role in holography and, as we highlighted, were not previously included in the false vacuum decay picture. Black holes typically change their mass during the decay process, hence we have different temperatures inside and outside of the bubble, and from a general perspective one could imagine that on the boundary, this corresponds to some non-equilibrium process in a dual field theory. The holographic description of such a process could be quite complicated, however we can address this problem from an entanglement entropy on the boundary point of view and use the holographic prescription for calculation of changes in entanglement entropy on

a boundary due to the bubbles of true vacuum in the bulk.

Bibliography

[1] A. Einstein, *Zur allgemeinen Relativitätstheorie*, Akademie-Vorträge, (1915).

[2] N. Ashby, *Relativity and the Global Positioning System*, Physics Today, vol. **55**, iss. no. 5, p. 41-47.

[3] S. W. Hawking, *Black hole explosions*, Nature **248**, 30 (1974).

[4] J. D. Bekenstein, *Black holes and entropy*, Phys. Rev. D **7**, 2333 (1973).

[5] A. Strominger and C. Vafa, *Microscopic origin of the Bekenstein-Hawking entropy*, Phys. Lett. B **379**, 99 (1996) [hep-th/9601029]].

[6] A. Y. Morozov, *String theory: What is it?*, Sov. Phys. Usp. **35**, 671 (1992) [Usp. Fiz. Nauk **162**, 83 (1992)].

[7] C. Rovelli, *Loop quantum gravity*, Living Rev. Rel. **1**, 1 (1998) [gr-qc/9710008]].

[8] R. D. Sorkin, *Causal sets: Discrete gravity*, [gr-qc/0309009]].

[9] J. Ambjorn, A. Goerlich, J. Jurkiewicz and R. Loll, *Quantum Gravity via Causal Dynamical Triangulations*, [arXiv:1302.2173 [hep-th]].

[10] J. M. Maldacena, *The Large N limit of superconformal field theories and supergravity*, Int. J. Theor. Phys. **38**, 1113 (1999) [hep-th/9711200].

[11] S. Kachru, X. Liu and M. Mulligan, *Gravity duals of Lifshitz-like fixed points*, Phys. Rev. D **78** (2008) 106005 [arXiv:0808.1725 [hep-th]].

[12] S. Coleman, *Fate of the false vacuum: Semiclassical theory*, Phys.Rev. **D15** (1977) 2929–2936.

[13] C. G. Callan and S. Coleman, *Fate of the false vacuum II: First quantum corrections*, Phys.Rev. **D16** (1977) 1762–1768.

[14] S. Coleman and F. De Luccia, *Gravitational effects on and of vacuum decay*, Phys.Rev. **D21** (1980) 3305–3315.

[15] A. D. Linde, *On the Vacuum Instability and the Higgs Meson Mass*, Phys. Lett. B **70**, 306 (1977).

[16] C. D. Froggatt, H. B. Nielsen and Y. Takanishi, *Standard model Higgs boson mass from borderline metastability of the vacuum*, Phys. Rev. D **64**, 113014 (2001) [hep-ph/0104161].

[17] J. Elias-Miro, J. R. Espinosa, G. F. Giudice, G. Isidori, A. Riotto and A. Strumia, *Higgs mass implications on the stability of the electroweak vacuum*, Phys. Lett. B **709**, 222 (2012) [arXiv:1112.3022 [hep-ph]].

[18] G. Degrassi, S. Di Vita, J. Elias-Miro, J. R. Espinosa, G. F. Giudice, G. Isidori and A. Strumia, *Higgs mass and vacuum stability in the Standard Model at NNLO*, JHEP **1208** (2012) 098, [arXiv:1205.6497 [hep-ph]].

[19] S. S. Gubser, I. R. Klebanov and A. M. Polyakov, *Gauge theory correlators from noncritical string theory*, Phys. Lett. B **428**, 105 (1998) [hep-th/9802109].

[20] J. H. Schwarz, *Off-mass-shell dual amplitudes without ghosts*, Nucl. Phys. B **65**, 131 (1973).

[21] E. Corrigan and D. B. Fairlie, *Off-Shell States in Dual Resonance Theory*, Nucl. Phys. B **91**, 527 (1975).

[22] C. V. Johnson, *D-brane primer*, Phys. Lett. B **428**, 105 (1998) [hep-th/0007170].

[23] J. Polchinski, *Dirichlet Branes and Ramond-Ramond charges*, Phys. Rev. Lett. **75**, 4724 (1995) [hep-th/9510017].

[24] G. T. Horowitz and A. Strominger, *Black strings and P-branes*, Nucl. Phys. B **360**, 197 (1991).

[25] O. Aharony, S. S. Gubser, J. M. Maldacena, H. Ooguri and Y. Oz, *Large N field theories, string theory and gravity*, Phys. Rept. **323**, 183 (2000) [hep-th/9905111].

[26] G. T. Horowitz and J. Polchinski, *Gauge/gravity duality*, in Oriti, D. (ed.): Approaches to quantum gravity, 169-186 (2006) [gr-qc/0602037]].

[27] V. E. Hubeny, *The AdS/CFT Correspondence*, Class. Quant. Grav. **32**, no. 12, 124010 (2015) [arXiv:1501.00007 [hep-th]].

[28] S. Weinberg and E. Witten, *Limits on Massless Particles*, Phys. Lett. B **96**, 59 (1980).

[29] E. Witten, *Anti-de Sitter space and holography*, Adv. Theor. Math. Phys. **2**, 253 (1998) [hep-th/9802150]].

[30] P. Breitenlohner and D. Z. Freedman, *Stability in Gauged Extended Supergravity*, Annals Phys. **144** (1982) 249.

[31] P. Burda, R. Gregory and S. Ross, *Lifshitz flows in IIB and dual field theories*, JHEP **1411**, 073 (2014) [arXiv:1408.3271 [hep-th]].

[32] S. Sachdev, *Condensed Matter and AdS/CFT*, Lect. Notes Phys. **828**, 273 (2011) [arXiv:1002.2947 [hep-th]].

[33] J. McGreevy, *Holographic duality with a view toward many-body physics*, Adv. High Energy Phys. **2010**, 723105 (2010) [arXiv:0909.0518 [hep-th]].

[34] S. A. Hartnoll, *Lectures on holographic methods for condensed matter physics*, Class. Quant. Grav. **26**, 224002 (2009) [arXiv:0903.3246 [hep-th]].

[35] M. Taylor, *Non-relativistic holography*, arXiv:0812.0530 [hep-th].

[36] K. Balasubramanian and K. Narayan, *Lifshitz spacetimes from AdS null and cosmological solutions*, JHEP **1008** (2010) 014 [arXiv:1005.3291 [hep-th]].

[37] A. Donos and J. P. Gauntlett, *Lifshitz Solutions of D=10 and D=11 supergravity*, JHEP **1012** (2010) 002 [arXiv:1008.2062 [hep-th]].

[38] D. Cassani and A. F. Faedo, *Constructing Lifshitz solutions from AdS*, JHEP **1105** (2011) 013 [arXiv:1102.5344 [hep-th]].

[39] P. Dey and S. Roy, *From AdS to Schrödinger/Lifshitz dual space-times without or with hyperscaling violation*, JHEP **1311**, 113 (2013) [arXiv:1306.1071 [hep-th]].

[40] R. Gregory, S. L. Parameswaran, G. Tasinato and I. Zavala, *Lifshitz solutions in supergravity and string theory*, JHEP **1012** (2010) 047 [arXiv:1009.3445 [hep-th]].

[41] H. Singh, *Special limits and non-relativistic solutions*, JHEP **1012** (2010) 061 [arXiv:1009.0651 [hep-th]].

[42] H. Singh, *Lifshitz/Schródinger Dp-branes and dynamical exponents*, JHEP **1207** (2012) 082 [arXiv:1202.6533 [hep-th]].

[43] A. Donos, J. P. Gauntlett, N. Kim and O. Varela, *Wrapped M5-branes, consistent truncations and AdS/CMT*, JHEP **1012**, 003 (2010) [arXiv:1009.3805 [hep-th]].

[44] H. Braviner, R. Gregory and S. F. Ross, *Flows involving Lifshitz solutions*, Class. Quant. Grav. **28** (2011) 225028 [arXiv:1108.3067 [hep-th]].

[45] H. Singh, *Holographic flows to IR Lifshitz spacetimes*, JHEP **1104** (2011) 118 [arXiv:1011.6221 [hep-th]].

[46] G. Bertoldi, B. A. Burrington and A. W. Peet, *Thermal behavior of charged dilatonic black branes in AdS and UV completions of Lifshitz-like geometries*, Phys. Rev. D **82** (2010) 106013 [arXiv:1007.1464 [hep-th]].

[47] S. S. Gubser and A. Nellore, *Ground states of holographic superconductors*, Phys. Rev. D **80** (2009) 105007 [arXiv:0908.1972 [hep-th]].

[48] K. Goldstein, N. Iizuka, S. Kachru, S. Prakash, S. P. Trivedi and A. Westphal, *Holography of Dyonic Dilaton Black Branes*, JHEP **1010** (2010) 027 [arXiv:1007.2490 [hep-th]].

[49] S. A. Hartnoll and A. Tavanfar, *Electron stars for holographic metallic criticality*, Phys. Rev. D **83** (2011) 046003 [arXiv:1008.2828 [hep-th]].

[50] J. T. Liu and Z. Zhao, *Holographic Lifshitz flows and the null energy condition*, [arXiv:1206.1047 [hep-th]].

[51] H. Singh, *Lifshitz to AdS flow with interpolating p-brane solutions*, JHEP **1308** (2013) 097 [arXiv:1305.3784 [hep-th]].

[52] S. Kachru, N. Kundu, A. Saha, R. Samanta and S. P. Trivedi, *Interpolating from Bianchi Attractors to Lifshitz and AdS Spacetimes*, JHEP **1403** (2014) 074 [arXiv:1310.5740 [hep-th]].

[53] P. Dey and S. Roy, *Interpolating solution from AdS_5 to hyperscaling violating Lifshitz space-time*, [arXiv:1406.5992 [hep-th]].

[54] K. Uzawa and K. Yoshida, *Dynamical Lifshitz-type solutions and aging phenomena*, Phys. Rev. D **87**, no. 10, 106003 (2013) [arXiv:1302.5224 [hep-th]].

[55] Y. Korovin, K. Skenderis and M. Taylor, *Lifshitz from AdS at finite temperature and top down models*, JHEP **1311**, 127 (2013) [arXiv:1306.3344 [hep-th]].

[56] Y. Korovin, K. Skenderis and M. Taylor, *Lifshitz as a deformation of Anti-de Sitter*, JHEP **1308**, 026 (2013) [arXiv:1304.7776 [hep-th]].

[57] J. M. Maldacena and C. Nunez, *Supergravity description of field theories on curved manifolds and a no go theorem*, Int. J. Mod. Phys. A **16** (2001) 822 [hep-th/0007018].

[58] N. Seiberg and E. Witten, *The D1 / D5 system and singular CFT*, JHEP **9904** (1999) 017 [hep-th/9903224].

[59] E. Witten and S. -T. Yau, *Connectedness of the boundary in the AdS / CFT correspondence*, Adv. Theor. Math. Phys. **3** (1999) 1635 [hep-th/9910245].

[60] L. J. Romans, *Gauged $N = 4$ Supergravities in Five-dimensions and Their Magnetovac Backgrounds*, Nucl. Phys. B **267** (1986) 433.

[61] H. Lu, C. N. Pope and T. A. Tran, *Five-dimensional N=4, SU(2) x U(1) gauged supergravity from type IIB*, Phys. Lett. B **475**, 261 (2000) [hep-th/9909203].

[62] L. Girardello, M. Petrini, M. Porrati and A. Zaffaroni, *Novel local CFT and exact results on perturbations of N=4 superYang Mills from AdS dynamics*, JHEP **9812** (1998) 022 [hep-th/9810126].

[63] D. Z. Freedman, S. S. Gubser, K. Pilch and N. P. Warner, *Renormalization group flows from holography supersymmetry and a c theorem*, Adv. Theor. Math. Phys. **3** (1999) 363 [hep-th/9904017].

[64] A. J. Amsel, G. T. Horowitz, D. Marolf and M. M. Roberts, *No Dynamics in the Extremal Kerr Throat*, JHEP **0909** (2009) 044 [arXiv:0906.2376 [hep-th]].

[65] F. Benini and N. Bobev, *Exact two-dimensional superconformal R-symmetry and c-extremization*, Phys. Rev. Lett. **110** (2013) 6, 061601 [arXiv:1211.4030 [hep-th]].

[66] F. Benini and N. Bobev, *Two-dimensional SCFTs from wrapped branes and c-extremization*, JHEP **1306** (2013) 005 [arXiv:1302.4451 [hep-th]].

[67] J. P. Gauntlett and O. Varela, *Consistent Kaluza-Klein reductions for general supersymmetric AdS solutions*, Phys. Rev. D **76**, 126007 (2007) [arXiv:0707.2315 [hep-th]].

[68] J. P. Gauntlett and O. Varela, *D=5 SU(2) x U(1) Gauged Supergravity from D=11 Supergravity*, JHEP **0802**, 083 (2008) [arXiv:0712.3560 [hep-th]].

[69] P. Burda, R. Gregory and I. Moss, *Gravity and the stability of the Higgs vacuum*, Phys. Rev. Lett. **115**, 071303 (2015) [arXiv:1501.04937 [hep-th]].

[70] P. Burda, R. Gregory and I. Moss, *Vacuum metastability with black holes*, JHEP **1508**, 114 (2015) [arXiv:1503.07331 [hep-th]].

[71] G. Aad *et al.* [ATLAS Collaboration], *Combined search for the Standard Model Higgs boson using up to 4.9 fb^{-1} of pp collision data at $\sqrt{s} = 7$ TeV with the ATLAS detector at the LHC,* Phys.Lett. **B710**, 49 (2012) [arXiv:1202.1408 [hep-ex]].

[72] S. Chatrchyan *et al.* [CMS Collaboration], *Combined results of searches for the standard model Higgs boson in pp collisions at $\sqrt{s} = 7$ TeV,* Phys.Lett. **B710**, 26 (2012) [arXiv:1202.1488 [hep-ex]].

[73] A. Gorsky, A. Mironov, A. Morozov and T. N. Tomaras, *Is the Standard Model saved asymptotically by conformal symmetry?*, JETP **120** (2015) 399-409, [Zh.Eksp.Teor.Fiz. **147** (2015) 399-409] [arXiv:1409.0492 [hep-ph]].

[74] F. Bezrukov and M. Shaposhnikov, *Why should we care about the top quark Yukawa coupling?*, Zh.Eksp.Teor.Fiz. **147** (2015) 389, [arXiv:1411.1923 [hep-ph]].

[75] J. Ellis, *Discrete Glimpses of the Physics Landscape after the Higgs Discovery*, [arXiv:1501.05418 [hep-ph]].

[76] K. Blum, R. T. D'Agnolo and J. Fan, *Vacuum stability bounds on Higgs coupling deviations*, [arXiv:1502.01045 [hep-ph]].

[77] I. V. Krive and A. D. Linde, *On the Vacuum Stability Problem in Gauge Theories*, Nucl.Phys. **B432** (1976) 265.

[78] N. Cabibbo, L. Maiani, G. Parisi and R. Petronzio, *Bounds on the Fermions and Higgs Boson Masses in Grand Unified Theories*, Nucl. Phys. **B158** (1979) 295.

[79] M. S. Turner and F. Wilczek, *Is our vacuum metastable*, Nature **D79** (1982) 633.

[80] M. Lindner, M. Sher and H. W. Zaglauer, *Probing Vacuum Stability Bounds at the Fermilab Collider,* Phys. Lett. B **228**, 139 (1989).

[81] M. Sher, *Electroweak Higgs Potentials and Vacuum Stability,* Phys. Rept. **179**, 273 (1989).

[82] G. Isidori, G. Ridolfi and A. Strumia, *On the metastability of the standard model vacuum,* Nucl. Phys. B **609**, 387 (2001) [hep-ph/0104016].

[83] J. R. Espinosa, G. F. Giudice and A. Riotto, *Cosmological implications of the Higgs mass measurement,* JCAP **0805**, 002 (2008) [arXiv:0710.2484 [hep-ph]].

[84] G. Isidori, V. S. Rychkov, A. Strumia and N. Tetradis, *Gravitational corrections to standard model vacuum decay*, Phys. Rev. **D77** (2008) 025034, [arXiv:0712.0242 [hep-ph]].

[85] J. Elias-Miro, J. R. Espinosa, G. F. Giudice, G. Isidori, A. Riotto and A. Strumia, *Higgs mass implications on the stability of the electroweak vacuum,* Phys. Lett. B **709**, 222 (2012) [arXiv:1112.3022 [hep-ph]].

[86] I. Y. Kobzarev, L. B. Okun and M. B. Voloshin, *Bubbles in Metastable Vacuum*, Sov.J.Nucl.Phys. **20** (1975) 644, [Yad.Fiz. **20** (1974) 1229].

[87] R. Gregory, I. G. Moss and B. Withers, *Black holes as bubble nucleation sites*, JHEP **1403** (2014) 081, [arXiv:1401.0017 [hep-th]].

[88] W. A. Hiscock, *Can black holes nucleate vacuum phase transitions?*, Phys.Rev. **D35** (1987) 1161–1170.

[89] V. Berezin, V. Kuzmin, and I. Tkachev, *O(3) invariant tunneling in general relativity*, Phys.Lett. **B207** (1988) 397.

[90] M. Sasaki and D. h. Yeom, *Thin-shell bubbles and information loss problem in anti de Sitter background*, JHEP **1412** (2014) 155, [arXiv:1404.1565 [hep-th]].

[91] A. Shkerin and S. Sibiryakov, *On stability of electroweak vacuum during inflation*, [arXiv:1503.02586 [hep-ph]].

[92] F. Mellor and I. Moss, *Black Holes and Quantum Wormholes*, Phys.Lett. **B222** (1989) 361.

[93] F. Mellor and I. Moss, *Black Holes and Gravitational Instantons*, Class.Quant.Grav. **6** (1989) 1379.

[94] S. Hawking and N. Turok, *Open inflation without false vacua*, Phys.Lett. **B425** (1998) 25–32, [hep-th/9802030].

[95] N. Turok and S. Hawking, *Open inflation, the four form and the cosmological constant*, Phys.Lett. **B432** (1998) 271–278, [hep-th/9803156].

[96] A. R. Brown and E. J. Weinberg, *Thermal derivation of the Coleman-De Luccia tunneling prescription*, Phys.Rev. **D76** (2007) 064003, [arXiv:0706.1573 [hep-th]].

[97] I. G. Moss, *Black-hole bubbles*, Phys.Rev. **D32** (1985) 1333–1344.

[98] C. Cheung and S. Leichenauer, *Limits on New Physics from Black Holes*, Phys.Rev. **D89** (2014) 104035, [arXiv:1309.0530 [hep-ph]].

[99] C. Ford, D. R. T. Jones, P. W. Stephenson and M. B. Einhorn, *The Effective potential and the renormalization group,* Nucl. Phys. B **395**, 17 (1993) [hep-lat/9210033].

[100] K. G. Chetyrkin and M. F. Zoller, *Three-loop beta-functions for top-Yukawa and the Higgs self-interaction in the Standard Model,* JHEP **1206**, 033 (2012) [arXiv:1205.2892 [hep-ph]].

[101] F. Bezrukov, M. Y. Kalmykov, B. A. Kniehl and M. Shaposhnikov, *Higgs Boson Mass and New Physics*, JHEP **1210** (2012) 140, [arXiv:1205.2893 [hep-ph]].

[102] B. Bergerhoff, M. Lindner and M. Weiser, *Dynamics of metastable vacua in the early universe*, Phys.Lett. **B469** (1999) 61, [hep-ph/9909261].

[103] E. Greenwood, E. Halstead, R. Poltis and D. Stojkovic, *Dark energy, the electroweak vacua and collider phenomenology*, Phys.Rev. **D79** (2009) 103003, [arXiv:0810.5343 [hep-ph]].

[104] V. Branchina and E. Messina, *Stability, Higgs Boson Mass and New Physics*, Phys.Rev.Lett. **111** (2013) 241801, [arXiv:1307.5193 [hep-ph]].

[105] V. Branchina, E. Messina and M. Sher, *The lifetime of the electroweak vacuum and sensitivity to Planck scale physics*, Phys.Rev. **D91** (2015) 013003, [arXiv:1408.5302 [hep-ph]].

[106] A. Eichhorn, H. Gies, J. Jaeckel, T. Plehn, M. Scherer, R. Sondenheimer, *The Higgs Mass and the Scale of New Physics*, [arXiv:1501.02812 [hep-ph]].

[107] F. Loebbert and J. Plefka, *Quantum Gravitational Contributions to the Standard Model Effective Potential and Vacuum Stability*, [arXiv:1502.03093 [hep-ph]].

[108] W. Israel, *Singular hypersurfaces and thin shells in general relativity*, Nuovo Cimento Soc. Ital. Phys. **B44** (1966) 4349.

[109] P. Bowcock, C. Charmousis and R. Gregory, *General brane cosmologies and their global spacetime structure*, Class.Quant.Grav. **17** (2000) 4745, [hep-th/0007177].

[110] R. Gregory and A. Padilla, *Nested brane worlds and strong brane gravity*, Phys. Rev. D **65** (2002) 084013 [hep-th/0104262].

[111] A. Aguirre and M. C. Johnson, *Dynamics and instability of false vacuum bubbles*, Phys.Rev. **D72** (2005) 103525, [gr-qc/0508093].

[112] A. Aguirre and M. C. Johnson, *Two tunnels to inflation*, Phys.Rev. **D73** (2006) 123529, [gr-qc/0512034].

[113] G. W. Gibbons and S. W. Hawking, *Action Integrals and Partition Functions in Quantum Gravity*, Phys.Rev.D **15** (1977) 2752.

[114] F. A. Bais and R. J. Russell, *Magnetic-monopole solution of non-Abelian gauge theory in curved spacetime*, Phys. Rev. **D11** (1975) 2692–2695

[115] Y. M. Cho and F. G. O. Freund, *Gravitating 't hooft monopoles*, Phys. Rev. **D12** (1975) 1588–1589

[116] G. W. Gibbons, *Vacuum Polarization and the Spontaneous Loss of Charge by Black Holes*, Commun.Math.Phys. **44** (1975) 245.

[117] B. J. Carr and S. W. Hawking, *Black holes in the early Universe*, Mon. Not. Roy. Astron. Soc. **168**, 399 (1974).

[118] D. N. Page, *Particle emission rates from a black hole*, Phys.Rev. **D13** (1976) 198-206.

[119] N. Arkani-Hamed, S. Dimopoulos and G. R. Dvali, *The Hierarchy problem and new dimensions at a millimeter*, Phys.Lett. **B429**, 263 (1998) 263–272, [hep-ph/9803315].

[120] I. Antoniadis, N. Arkani-Hamed, S. Dimopoulos and G. R. Dvali, *New dimensions at a millimeter to a Fermi and superstrings at a TeV*, Phys. Lett. B **436**, 257 (1998) [hep-ph/9804398].

[121] L. Randall and R. Sundrum, *A Large mass hierarchy from a small extra dimension*, Phys.Rev.Lett.**83**, 3370 (1999) 3370–3373, [hep-ph/9905221].

[122] L. Randall and R. Sundrum, *An Alternative to compactification*, Phys. Rev. Lett. **83**, 4690 (1999) [hep-th/9906064].

[123] S. Dimopoulos and G. L. Landsberg, *Black holes at the LHC*, Phys.Rev.Lett. **87** (2001) 161602. [hep-ph/0106295].

[124] S. B. Giddings and S. D. Thomas, *High-energy colliders as black hole factories: The End of short distance physics*, Phys. Rev. D **65**, 056010 (2002) [hep-ph/0106219].

[125] P. Kanti and E. Winstanley, *Hawking Radiation from Higher-Dimensional Black Holes*, Fundam.Theor.Phys. **178** (2015) 229 [hep-th/1402.3952].

[126] R. C. Myers and M. J. Perry, *Black Holes in Higher Dimensional Space-Times*, Annals Phys. **172** (1986) 304.

[127] P. Kanti, *Black holes in theories with large extra dimensions: A Review*, Int.J.Mod.Phys.A**19**, 4899 (2004) 4899-4951, [hep-ph/0402168].

[128] R. Gregory, *Braneworld black holes*, Lect. Notes Phys. **769** (2009) 259, [arXiv:0804.2595 [hep-th]].

[129] N. Dadhich, R. Maartens, P. Papadopoulos and V. Rezania, *Black holes on the brane*, Phys. Lett. B **487**, 1 (2000) [hep-th/0003061].

[130] S. Hawking and G. T. Horowitz, *The Gravitational Hamiltonian, action, entropy and surface terms*, Class.Quant.Grav. **13** (1996) 1487–1498, [gr-qc/9501014].

[131] R. Gregory and A. Padilla, *Brane world instantons*, Class.Quant.Grav. **19** (2002) 279, [hep-th/0107108].

[132] R. Emparan, G. T. Horowitz and R. C. Myers, *Black holes radiate mainly on the brane*, Phys. Rev. Lett. **85**, 499 (2000) [hep-th/0003118].

[133] C. M. Harris and P. Kanti, *Hawking radiation from a (4+n)-dimensional black hole: Exact results for the Schwarzschild phase*, JHEP **0310**, 014 (2003) [hep-ph/0309054].

[134] P. Burda, R. Gregory and I. Moss, in preparation

[135] S. Ryu and T. Takayanagi, *Holographic derivation of entanglement entropy from AdS/CFT*, Phys. Rev. Lett. **96**, 181602 (2006) [hep-th/0603001].

[136] S. Cremonini and X. Dong, *Constraints on renormalization group flows from holographic entanglement entropy*, Phys. Rev. D **89**, no. 6, 065041 (2014) [arXiv:1311.3307 [hep-th]].

[137] J. L. F. Barbon and E. Rabinovici, *Holography of AdS vacuum bubbles*, JHEP **1004**, 123 (2010) [arXiv:1003.4966 [hep-th]].

[138] B. Freivogel, V. E. Hubeny, A. Maloney, R. C. Myers, M. Rangamani and S. Shenker, *Inflation in AdS/CFT*, JHEP **0603**, 007 (2006) [hep-th/0510046].

[139] T. Nishioka and T. Takayanagi, *AdS Bubbles, Entropy and Closed String Tachyons*, JHEP **0701**, 090 (2007) [hep-th/0611035].